Comenius University in Bratislava
Faculty of Mathematics, Physics and Informatics

Collision-free Low Degree Bézier Path with Regular Quadratic Obstacles

Dissertation Thesis

Bratislava 2015 RNDr. Barbora Pokorná

Comenius University in Bratislava
Faculty of Mathematics, Physics
and Informatics

Collision-free Low Degree Bézier Path with Regular Quadratic Obstacles

Dissertation Thesis

Branch of study:	Geometry and Topology
Study programme:	9.1.7. Geometry and Topology
Department:	Department of Algebra, Geometry and Didactics of Mathematics
Supervisor:	doc. RNDr. Pavel Chalmovianský, PhD.

Bratislava 2015

RNDr. Barbora Pokorná

Univerzita Komenského v Bratislave
Fakulta matematiky, fyziky a informatiky

ZADANIE ZÁVEREČNEJ PRÁCE

Meno a priezvisko študenta: RNDr. Barbora Pokorná
Študijný program: geometria a topológia (Jednoodborové štúdium, doktorandské III. st., denná forma)
Študijný odbor: 9.1.7. geometria a topológia
Typ záverečnej práce: dizertačná
Jazyk záverečnej práce: anglický
Sekundárny jazyk: slovenský

Názov: Collision-free Low Degree Bézier Path with Regular Quadratic Obstacles
Bezkolízna po častiach Bézierova cesta nízkeho stupňa medzi prekážkami z regulárnych kužeľosečiek

Literatúra: S. Basu, R. Pollack, and M.-F. Roy. Algorithms in real algebraic geometry, volume 10 of Algorithms and Computation in Mathematics. Springer-Verlag, Berlin, second edition, 2006.

L. González-Vega, T. Recio, H. Lombardi, and M.-F. Roy. Sturm- Habicht sequences, determinants and real roots of univariate polynomials. In Quantifier elimination and cylindrical algebraic decomposition (Linz, 1993), Texts Monogr. Symbol. Comput., pages 300–316. Springer, Vienna, 1998.

S. M. LaValle. Planning Algorithms. Cambridge University Press, Cambridge, U.K., 2006.

Cieľ: Identifikuje sa množina kvadratických/kubických kriviek s pevnými koncovými bodmi, ktoré sa nepretínajú s danými prekážkami. Hranice prekážok sa reprezentujú regulárnymi kvadratickými krivkami. Podmienky sa formulujú synteticky aj výpočtovo a nájde sa algoritmus na výpočet splajnu, ktorý obchádza všetky prekážky.

Anotácia: Práca sa zaoberá nájdením a opisom množiny všetkých kriviek určitého stupňa s fixnými koncovými bodmi a obchádzajúcimi prekážku s regulárnou kvadratickou hranicou. Výsledok sa aplikuje na množinu prekážok a počíta sa splajn s vopred určeným rádom spojitosti. V práci sa použijú moderné metódy počítania koreňov na intervale spolu s využitím teórie kužeľosečiek a kriviek reprezentovaných v Bézierovom tvare.

Školiteľ: doc. RNDr. Eduard Boďa, CSc.
Školiteľ: doc. RNDr. Pavel Chalmoviansky, PhD.
Katedra: FMFI.KAGDM - Katedra algebry, geometrie a didaktiky matematiky
Vedúci katedry: prof. RNDr. Pavol Zlatoš, PhD.

Spôsob sprístupnenia elektronickej verzie práce:
bez obmedzenia

69804809

Univerzita Komenského v Bratislave
Fakulta matematiky, fyziky a informatiky

Dátum zadania: 15.10.2010

Dátum schválenia: 15.10.2010

prof. RNDr. Július Korbaš, CSc.
garant študijného programu

....

študent školiteľ

Comenius University in Bratislava
Faculty of Mathematics, Physics and Informatics

69804809

THESIS ASSIGNMENT

Name and Surname: RNDr. Barbora Pokorná
Study programme: Geometry and Topology (Single degree study, Ph.D. III. deg., full time form)
Field of Study: 9.1.7. Geometry And Topology
Type of Thesis: Dissertation thesis
Language of Thesis: English
Secondary language: Slovak

Title: Collision-free Low Degree Bézier Path with Regular Quadratic Obstacles

Literature: S. Basu, R. Pollack, and M.-F. Roy. Algorithms in real algebraic geometry, volume 10 of Algorithms and Computation in Mathematics. Springer-Verlag, Berlin, second edition, 2006.

L. González-Vega, T. Recio, H. Lombardi, and M.-F. Roy. Sturm- Habicht sequences, determinants and real roots of univariate polynomials. In Quantifier elimination and cylindrical algebraic decomposition (Linz, 1993), Texts Monogr. Symbol. Comput., pages 300–316. Springer, Vienna, 1998.

S. M. LaValle. Planning Algorithms. Cambridge University Press, Cambridge, U.K., 2006.

Aim: A set of quadratic-cubic curves with fixed endpoints, which are not intersecting given obstacles. The boundaries of obstacles are represented with quadratic curves. The conditions are formulated in synthetic and computational way and an algorithm for computing spline avoiding obstacles is formed.

Annotation: The work deals with determining and description of a set of all curves of certain degree with fixed endpoints which avoid an obstacle bounded by a regular conic section. The result is applied on a set of obstacles and computes a spline with a predefined order of continuity. The modern methods of counting roots on an interval, conic section theory and representation of curves in Bézier form are used in the work.

Tutor: doc. RNDr. Eduard Boďa, CSc.
Tutor: doc. RNDr. Pavel Chalmovianský, PhD.
Department: FMFI.KAGDM - Department of Algebra, Geometry and Didactics of Mathematics
Head of department: prof. RNDr. Pavol Zlatoš, PhD.

Assigned: 15.10.2010

Approved: 15.10.2010 prof. RNDr. Július Korbaš, CSc.
Guarantor of Study Programme

69804809

Comenius University in Bratislava
Faculty of Mathematics, Physics and Informatics

....

Student Tutor

Acknowledgements

I would like to thank to doc. RNDr. Pavel Chalmovianský, PhD. for all his help, time, support and priceless advices he has given me throughout my studies, the research and also the writing period of this thesis.

Bratislava, April 2015

. . . .
Barbora Pokorná

Declaration

I herewith declare that I produced this dissertation thesis without the prohibited assistance of third parties and without making use of aids other than those specified; notions taken over directly or indirectly from other sources that have not been identified as such.

This document has not previously been presented in identical or similar form to any other Slovak or foreign examination board.

This research was conducted under the supervision of doc. RNDr. Pavel Chalmovianský, PhD. at Faculty of Mathematics, Physics and Informatics, Comenius University in Bratislava, Slovakia from 2010 to 2015.

Bratislava, April 2015

. . . .
Barbora Pokorná

Abstrakt

V práci sa zaoberáme klasifikáciou vzájomnej polohy Bézierovej krivky a regulárnej kvadriky v trojrozmernom euklidovskom priestore. Pre daný prvý a posledný riadiaci vrchol hľadáme množinu všetkých kvadratických Bézierových kriviek, ktoré nemajú s regulárnou kvadrikou žiadne spoločné body. Tento systém Bézierových kriviek je reprezentovaný pomocou vhodných stredných riadiacich vrcholov. Priestorový problém sme previedli na problém rovinný, kde je regulárna kvadrika reprezentovaná kužeľosečkou. Následne sme určili množinu vhodných stredných riadiacich vrcholov pre každý typ kužeľosečky zvlášť. Kľúčovou úlohou bolo nájdenie hranice tejto množiny. Táto hranica je tvorená strednými riadiacimi vrcholmi takých Bézierových kriviek, ktoré sa iba dotýkajú danej kužeľosečky. Aplikovaním postupu na danú množinu bodov sme našli kvadratický splajn, ktorý interpoluje dané body a je bezkolízny vzhľadom na danú množinu regulárnych kvadrík. Uvažujeme zvlášť C^0 a C^1-spojitý prípad. Ďalej sa zaoberáme rovinnými kubickými Bézierovými krivkami s danými koncovými bodmi a jedným zo stredných riadiacich vrcholov. Určili sme množinu všetkých takýchto kriviek, ktoré sú bezkolízne vzhľadom na danú singulárnu kužeľosečku. V prípade regulárnych kužeľosečiek sme určili nutné geometrické podmienky bezkolíznosti. Naše výsledky sa dajú využiť pri hľadaní bezkolíznych ciest pre virtuálne roboty. Pričom prekážky sú reprezentované regulárnymi kvadrikami, prípadne sú kvadriky obaľujúcim objektom prekážok. Ďalšie využitie môžeme nájsť pri hľadaní bodovo priestoru-podobných kriviek v Minkowského priestore.

Kľúčové slová: Bézierová krivka · regulárna kvadrika · bezkolízna cesta · kvadratický splajn

Abstract

We classify mutual position of a quadratic Bézier curve and a regular quadric in three dimensional Euclidean space. For given its first and last control point, we find the set of all quadratic Bézier curves having no common point with a regular quadric. This system of such quadratic Bézier curves is represented by the set of their admissible middle control points. The spatial problem is reduced to a planar problem where the regular quadric is represented by a conic section. Then, the set of all middle control points is found for each type of conic section separately. The key issue is to find the boundary of this set. It is formed from the middle control points of the Bézier curves touching the given conic section. Applying the method on a given sequence of points, we find quadratic interpolation spline, collision-free with respect to the given set of quadrics. We distinguish C^0 and C^1-continuous cases. Then, we consider planar cubic Bézier curves with given first and last control point and one of the middle control points. We find the set of all such curves, which are collision-free with respect to the given singular conic section. In the case of regular conic sections, we determine the sufficient geometrical conditions for curves to be collision-free. Our results are applicable in collision-free paths computation for virtual agents where the obstacles are represented or bounded by regular quadrics. Another application can be found in searching for pointwise space-like curves in Minkowski space.

Keywords: Bézier curve · regular quadric · collision-free path · quadratic spline

Contents

Introduction

Bézier curves were discovered by Paul de Casteljau in 1959, who worked for French automobile manufacturer Citroën. He used the de Casteljau's algorithm to evaluate Bézier curves. However, he can not published his early work and the curves were publicized and popularized in 1962 by Pierre Bézier. He used the Bernstein polynomials as basis and did not use control points but their first difference vectors as the coefficients. These curves play an important role in geometric modeling, Computer Aided Geometric Design (CAGD) and computer graphics systems due to their properties.

Path planning (as a part of motion planning) is a major topic in robotics. It involves finding a collision-free strategy from the current location, or configuration, to a desired goal location, or configuration. It is a purely geometric process that is only concerned with finding a collision-free path regardless of the feasibility of the path. Many topics that serve as the basis for path planning include exact roadmap methods, graph theory, geometric algorithms, sampling-based algorithms, potential fields, etc.

Theory of Minkowski space served as a mathematical equipment since it has practical applications also in geometric modelling and CAGD. The Bézier curves were also considered in Minkowski space as space-like curves. Their properties like space-like conditions, regularity, curvature, torsion are known.

We decide to study a mutual position of Bézier curve and regular quadric in three dimensional Euclidean space. The gained knowledge are applicable in path planning where a path is represented by the Bézier curve and the obstacles represented by quadrics. We start with quadratic curves and splines, later we extend the propositions for cubic curves because of their better properties. Another application can be found in searching for pointwise space-like curves in Minkowski space where the light-cone is regular quadric.

The structure of the work is as follows. In the first chapter, we summarize some useful notations and facts from Euclidean geometry, Bézier curves, quadrics, searching of collision-free path, Bézier space-like curves in Minkowski space and finding real solutions of the polynomials. We choose the facts appropriate for our work. We define the main goals of the work and the partial goals necessary for achieving the main goals in the second chapter. In the third chapter, we find the quadratic collision-free Bézier path with respect to the regular quadric. The generalization for avoiding more quadrics and finding the collision-free quadratic spline is described in the fourth chapter. In fifth chapter, we shown some properties of cubic collision-free Bézier paths with respect to regular quadric. The results and their applications are presented in the sixth chapter.

1

Theoretical background

In this chapter, we present basic definitions, relations and all concepts required later in the text. At first, we mention an Euclidean space as the basic space where we work and a regular quadrics, which we use later for representing the obstacles. Then, we say about Bézier curves and splines, which are used to represent a collision-free path. A brief introduction to motion planning with basic definition of the problem of collision-free path finding is following. Minkowski space is mentioned for another application of our results. At the end, we show the relations between discriminant, number of sign changes and number of real roots of real polynomial function in an interval for future use in computations.

1.1 Euclidean space with quadratic form

Let $\mathbb{E}^3$ be three dimensional vector Euclidean space formed by vectors $\boldsymbol{x} = (x_1, x_2, x_3)$ with scalar product $\langle \cdot\,, \cdot \rangle \colon \mathbb{E}^3 \times \mathbb{E}^3 \to \mathbb{R}$. Let $M_{3,3}(\mathbb{R})$ be the set of 3×3 matrices with real coefficients. A quadratic form is the map $q \colon \mathbb{E}^3 \to \mathbb{R}$, where $q(\boldsymbol{x}) = \boldsymbol{x}\boldsymbol{Q}\boldsymbol{x}^\top$ for the symmetric $\boldsymbol{Q} \in M_{3,3}(\mathbb{R})$. We talk about *regular quadratic form* if the matrix $\boldsymbol{Q}$ is diagonal with entries $\lambda_{1,2,3} \in \{-1, 1\}$ in a certain basis of $\mathbb{E}^3$. The unique symmetric bilinear form giving rise to q is denoted by P and called the *polar form* of q. We have $q(\boldsymbol{x}) = P(\boldsymbol{x}, \boldsymbol{x})$, $P(\boldsymbol{x}, \boldsymbol{y}) = \boldsymbol{x}\boldsymbol{Q}\boldsymbol{y}^\top$.

By a standard construction, we get three dimensional affine Euclidean space $\mathbb{R}^3$ with a Cartesian coordinate system $\langle O, e_1, e_2, e_3 \rangle$ formed by points $X = [x_1, x_2, x_3]$. Let $M_{4,4}(\mathbb{R})$ be the set of 4×4 matrices with real coefficients. Let $\boldsymbol{Q_\kappa} \in M_{4,4}(\mathbb{R})$ be regular and symmetric. An image of a *regular quadric* κ is the set of points $\{[x_1, x_2, x_3] \in \mathbb{R}^3 \colon (x_1\ x_2\ x_3\ 1)\boldsymbol{Q_\kappa}(x_1\ x_2\ x_3\ 1)^\top = 0\}$. The matrices 4×4 and extended coordinates $(X, 1) = (x_1, x_2, x_3, 1)$ are used to express an arbitrary translation and rotation of the quadric by one matrix. Moreover, projective properties are formulated in a more natural way. The used properties of affine and projective quadrics are in [Ber87b]. Similarly as in an associated vector space, we can define $P(X, Y) = (X, 1)\boldsymbol{Q_\kappa}(Y, 1)^\top$. Let the point $Y \in \mathbb{R}^3$ be fixed. We call the set $Y^\perp = \{X \in \mathbb{R}^3 \colon P(X, Y) = 0\}$ the *polar (hyperplane)* of Y. We say that X and Y are conjugate with respect to the polar form P, and we denote this fact by $X \perp Y$. For the *self-polar* point Y holds $P(Y, Y) = 0$ (a quadric is the set of all self-polar points with respect to the given polar form).

Let $\mathbb{R}^2$ be an affine Euclidean plane formed by points $X = [x, y]$. Let $\boldsymbol{Q_K} \in M_{3,3}(\mathbb{R})$ be a symmetric matrix. The algebraic curve of degree 2 called *conic section* is the set $K = \{[x, y] \in \mathbb{R}^2 \colon f(x, y) = 0 \text{ for } f(x, y) = (x\ y\ 1)\boldsymbol{Q_K}(x\ y\ 1)^\top\}$. In appropriate cases, we consider the equation of the conic section instead of K due to the fact that the field $\mathbb{R}$ is not algebraically closed. The conic section is the set of self-polar points with respect to polar form determined by the matrix $\boldsymbol{Q_K}$. For the point Y, the $Y^\perp$ is the polar line determined by equation $(Y, 1)\boldsymbol{Q_K}(X, 1)^\top = 0$. The polar line of such a point Y that $P(Y, Y) > 0$ splits the conic section K into some arcs. If $Y^\perp \cap K = \{T_1, T_2\}$ then we denote the arc $\overset{\frown}{T_1T_2} = \{X \in K \colon P(Y, X) > 0\}$.

The study of conic sections founded Greek mathematicians in the fourth century B.C., it is believed that the first definition is due to Menaechmus. A lot of properties of the conic sections was discovered by Apollonius of Perga. By considering a conic as a section of a circular cone, he characterized the points of the conic by their distances from two lines. He deduced a wealth of geometric properties, despite of working entirely in geometric terms without algebraic notation. Among other things, he founded the study of the polar of a point. Pappus of Alexandria discovered the importance of the concept of a focus of a conic. In the first half of the 1600s, Girard Desargues reshaped the study of conics by introducing points at infinity and projections between planes. Later, Charles Brianchon deduced his theorem on hexagons circumscribed about conics and he resolved longstanding problems about determining conics specified by five pieces of information. Building on Brianchon's work, Jean-Victor Poncelet and Jacob Steiner developed duality as a general principle of projective geometry. Julius Plücker clarified the logical basis of the duality principle when he justified the principle analytically in 1830. More about conics and their properties can be found in [Bix06]. More about the conics expressed in parametric Bernstein form can be found in [Far99].

The determinant $\Delta = \det(\boldsymbol{Q_K})$ is called the *determinant of the conic section.* If $\boldsymbol{Q_K} = (q_{ij})$, the determinant $\delta = \det\left(\begin{smallmatrix} q_{11} & q_{12} \\ q_{21} & q_{22} \end{smallmatrix}\right)$ is called the *discriminant of the conic section.* If $\Delta \neq 0$, the conic section is regular. In the case if $\delta = 0$ then the conic section is a parabola, if $\delta < 0$, it is an hyperbola and if $\delta > 0$, it is an ellipse. A conic section is a circle if $\delta > 0$ and $q_{22}\Delta < 0$. If $\Delta = 0$, the conic is a degenerate parabola (two coinciding lines), a degenerate ellipse (a point ellipse), or a degenerate hyperbola (two different intersecting lines). The terms hyperbola, ellipse and parabola is believed to have been coined by Apollonius of Perga in his work Conics, see [BM11]. The words are derived from Greek and they mean "excessive", "deficient" and "comparable". They may refer to the eccentricity of these curves, which is greater than one for hyperbola, less than one for ellipse and exactly one for parabola.

We assign to each family of parallel lines a unique point at infinity, at which "all of such lines meet". All the points at infinity define the line at infinity l^∞. The *extended Euclidean plane*, denoted by $\overline{\mathbb{R}^2}$, is obtained as $\overline{\mathbb{R}^2} = \mathbb{R}^2 \cup l^\infty$. More about this construction can be found e. g. in [Ber87a]. In the extended Euclidean plane, it is necessary to homogenize the equation of conic section by replacing $(x, y, 1)$ with (x, y, z). We obtain the conic section $\overline{K} = \{[x, y, z] \in \overline{\mathbb{R}^2} \colon (x\ y\ z)\boldsymbol{Q_K}(x\ y\ z)^\top = 0\}$ in homogeneous coordinates. For more on plane algebraic curves we refer to the book [Kun05]. From each point $X \in \mathbb{R}^2$ lying outside the regular conic section K (i.e. $P(X, X) > 0$), one can construct two tangent lines to $\overline{K} \subset \overline{\mathbb{R}^2}$. The corresponding points of contact may be either *affine* or *at infinity.* In the case of point of the contact at infinity, the conic section $K \subset \mathbb{R}^2$ is a hyperbola and the projective tangent line is called asymptote a in affine space. We denote its point of contact with K at infinity by a^∞. We denote the set of all tangent lines to K by T_K. Hence, $T_K = \{\ell \subset \mathbb{R}^2 :$ each point $X \in \ell$ satisfies $0 = \langle \nabla f(X_0), X - X_0 \rangle \mid X_0 \in K \cap \ell\}$. We denote by $\nabla f(x_0, y_0)$ the gradient $\left(\frac{\partial f}{\partial x}(x_0, y_0), \frac{\partial f}{\partial y}(x_0, y_0)\right)$ of K at the point $[x_0, y_0] \in K$. Clearly, at a regular point, it is the normal vector of the corresponding tangent line.

1.2 Bézier curves and splines

As we mentioned in the introduction, the Bézier curves were discovered by Paul de Casteljau and Pierre Bézier. Paul de Casteljau adopted the use of Bernstein polynomials for his curve and surface definitions from the very beginning, together with what is now known as the de Casteljau algorithm. The using of control polygons was never used before. Instead of defining a curve through points on it, a control polygon utilizes points near it. If we want to change the curve, we change the control polygon and the curve follows in a very intuitive way. De Casteljau's work was kept a secret by Citröen for a long time. W. Boehm was the first to give de Casteljau recognition for his work in the research community. He found out about de Casteljau's technical reports and coined the term "de Casteljau algorithm". In another vehicle manufacturer, Rénault, Pierre Bézier headed the design department and also realized the need for computer representations of mechanical parts, during the early 1960s. Bézier's initial idea was to represent a "basic curve" as the intersection of two elliptic cylinders. The two cylinders were defined inside a parallelepiped. Affine transformations of this parallelepiped would then result in affine transformations of the curve. Later, Bézier moved to polynomial formulations of this initial concept and also extended it to higher degrees. The result turned out to be identical to de Casteljau's curves, only the mathematics involved was different. In 1972, A. R. Forrest published [For72], where he pointed out that Bézier curve can be defined in terms of control points with help of Bernstein polynomials. More about the history of curves and surfaces in CAGD can be found in [FHK02].

Definition 1.1 (Bézier curve). *Bézier curve* of degree n in the space $\mathbb{R}^d, d \in \mathbb{N}, d \geq 2$ is a polynomial map $b\colon [0,1] \to \mathbb{R}^d$ given by $b(t) = \sum_{i=0}^{n} B_i^n(t)\, V_i$. The

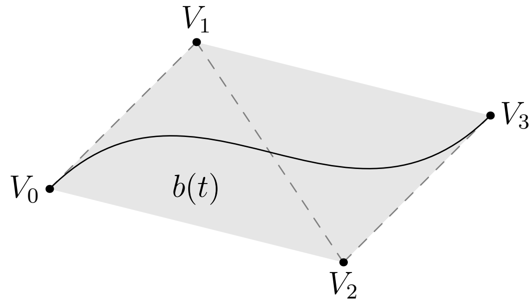

Figure 1.1: The Bézier curve $b(t)$ always passes through the first and the last control point and lies within the convex hull of its control points $V_i \in \mathbb{R}^2$.

points $V_i \in \mathbb{R}^d$ are called *control points*, the functions $B_i^n(t) = \binom{n}{i}(1-t)^{n-i}t^i$ for $i \in \{0, \ldots, n\}$ are Bernstein polynomials of degree n (fig. 1.1).

The Bézier curve interpolates its first and last control point. It lies within the convex hull of the control points. The variation diminishing property of Bézier curves means that the number of intersection points of any straight line with a Bézier curve is at most the number of intersection points of the same straight line with the control polygon of the curve. The construction of Bézier curves is invariant under affine transformations, but not invariant under all projective transformations. More about the properties of Bézier curves can be found e. g. in [HL93, PBP02, Mar05]. Some useful properties of convex curves are mentioned in [Küh06]. The generalizations of Bézier curves to higher dimensions are the Bézier surfaces, which Pierre Bézier used to design automobile bodies.

A *spline* is a piecewise polynomial function with sufficiently high degree of smoothness at the places where the polynomial pieces connect. Splines are very useful for modelling arbitrary functions, and are used extensively in computer graphics. The word "spline" originally meant a thin wood or metal slat used as flexible ruler to draw curves. The strips provided an interpolation of the key points using lead weights called "ducks" into smooth curves. I. J. Schoenberg was the first who used this term in connection with smooth, piecewise polynomial approximation in 1946 in [Sch88]. More about splines as B-spline, β-spline, Hermite spline interpolation and Catmull-Rom splines in the context of computer graphics can be found in [BBB87]. A *Bézier spline* (also *composite Bézier curve*)

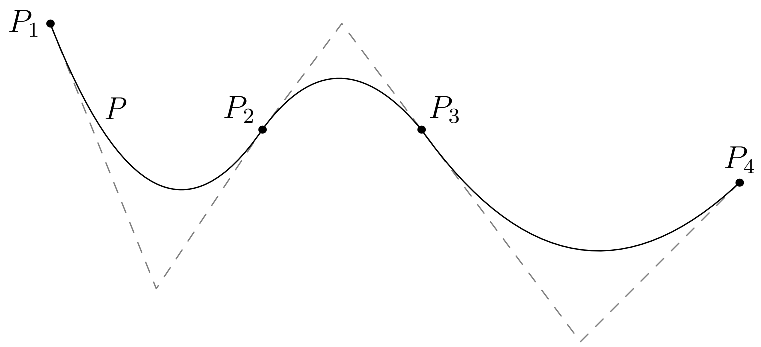

Figure 1.2: An example of quadratic Bézier spline P for the set of points $\{P_1, P_2, P_3, P_4\}$ in $\mathbb{R}^2$.

is a sequence of Bézier curves that share common end points and then are patched together ensuring the continuity of the final curve.

Definition 1.2 (Bézier spline)**.** Let $\{P_1, \dots, P_m\} \subset \mathbb{R}^d, m \in \mathbb{N}$ be the given set of points. *Bézier spline* of degree n in the union of the Bézier curves $b_1, \dots, b_{m-1}$, where $b_i(t)$ is a Bézier curve of degree n with $b_i(0) = P_i, b_i(1) = P_{i+1}$ (fig. 1.2).

Such curve is not necessarily differentiable while additional smoothness requirements at the points of connection are not given. There are two types of smoothness that are considered, functional and geometric. These involve different notions of continuity. Functional continuity involves orders of continuity with respect to the parameter of the curve, while geometric continuity involves continuity with respect to the arc-length parameter of the curve. Useful relations from differential geometry can be found in [dC76, BG88]. The conditions of C^k continuity for C^{k-1}-continuous spline are given by the set of equations $b_i^{(k)}(1) = b_{i+1}^{(k)}(0)$ for $i = 1, \dots, m-2$. Specifically, if $\{B_0, \dots, B_n\}$, $\{B'_0, \dots, B'_n\}$ are the sets of control points of the Bézier curves b_i, b_{i+1} respectively, then

$$\text{for } C^0 \text{ continuity: } B_n = B'_0,$$
$$\text{for } C^1 \text{ continuity: } n(B_n - B_{n-1}) = n(B'_1 - B'_0).$$

For example, the C^2 continuity yields curvature continuity, which is very important for car-like vehicles [FS04]. The curvature being related to the front wheels' orientation. If a real car were to track precisely a path with discontinuous curvature, it would have to stop at each curvature discontinuity so as to reorient its front wheels. Curvature continuity is therefore a desirable property. The derivative of the curvature is related to the steering velocity of the car. So, it is also desirable that the derivative of the curvature be upper-bounded so as to ensure that such paths can be followed with a given speed (proportional to the curvature derivative limit). The most commonly used are cubic splines, because they have relatively low degree and compared with quadratic curves they are not necessarily planar. More about C^2-continuous cubic spline curves and their properties can be found in [Far08].

1.3 Motion planning

Motion planning is a fundamental research area in robotics. It refer to motions of a robot in a two or three dimensional world that contains obstacles. The robot could model an actual robot, or any other collection of moving bodies, such as humans or flexible molecules. A motion plan involves determining what motions are appropriate for the robot so that it reaches a goal state without colliding into obstacles.

We demonstrate the searching of collision-free path on so-called *The Piano Mover's Problem* according [LaV06]. The space, where robot moves and performs the tasks, is called workspace W. This space is two or three dimensional Euclidean space. It contains the set of obstacles $\mathcal{O}$ and the robot $\mathcal{A}$. However, it is necessary to consider other attributes of a robot except the location, the rotation for example. The state space for motion planning is a set of all possible transformations that may be applied to the robot. This will be referred to as the configuration space C, based on the work of Lozano-Pérez [LP83]. The dimension of the configuration space corresponds to the number of degrees of freedom of the robot. Using the configuration space, motion planning will be viewed as a kind of search in a high-dimensional configuration space that contains implicitly represented obstacles. The robot can be only represented by a configuration q with the same dimensions as C. Within the configuration space, we distinguish two regions $C_{free} \cup C_{obs} = C$. Free space C_{free} is the space of all configurations of a robot, which have no collision with any obstacle. Obstacle space C_{obs} represents such configurations of C that a robot has a collision with some obstacle. A configuration, $q_I \in C_{free}$ designated as the initial configuration, and a configuration $q_G \in C_{free}$ designated as the goal configuration. A complete algorithm must compute a (continuous finite length) path $P \subset C_{free}$ represented by a map $\tau\colon [0,1] \to C_{free}$, such that $\tau(0) = q_I$ and $\tau(1) = q_G$, or correctly report that such a path does not exist.

For example, let the robot be a solid three-dimensional shape that can translate and rotate. The workspace W is three-dimensional Euclidean space $\mathbb{R}^3$, but configuration space C is the special Euclidean group $SE(3) = \mathbb{R}^3 \times SO(3)$. The configuration requires six parameters (three for translation, and three for Euler angles). The work space and configuration space for a triangular translating robot is shown in the fig. 1.3.

The method of reduced visibility graph [Nil69] published in 1969 by Nielsson may perhaps be the first example of a motion planning algorithm. The progress of computers has the major influence to development of planning algorithms. Large number of algorithms have been invented yet. We present the basic division according to [LaV06]. There are two alternatives how to transform the continuous model into a discrete one. The first approach is *combinatorial motion planning*, which means that from the input model the algorithms build a discrete representation that *exactly* represents the original problem. This leads to *complete* planning approaches, which are guaranteed to find a solution when it exists, or correctly report failure if one does not exist. The second one is *sampling-based motion planning*, which refers to algorithms that use collision detection methods to sample the configuration space and conduct discrete searches that utilize these samples. In this case, completeness is sacrificed and is often replaced with a weaker notion, such as *probabilistic completeness*. Each methodology has its strengths and weaknesses. Combinatorial methods can solve virtually any motion planning problem, and in some restricted cases, very elegant solutions may be efficiently constructed in practice. However, for the majority of industrial-grade motion planning problems, the running times and implementation difficulties of

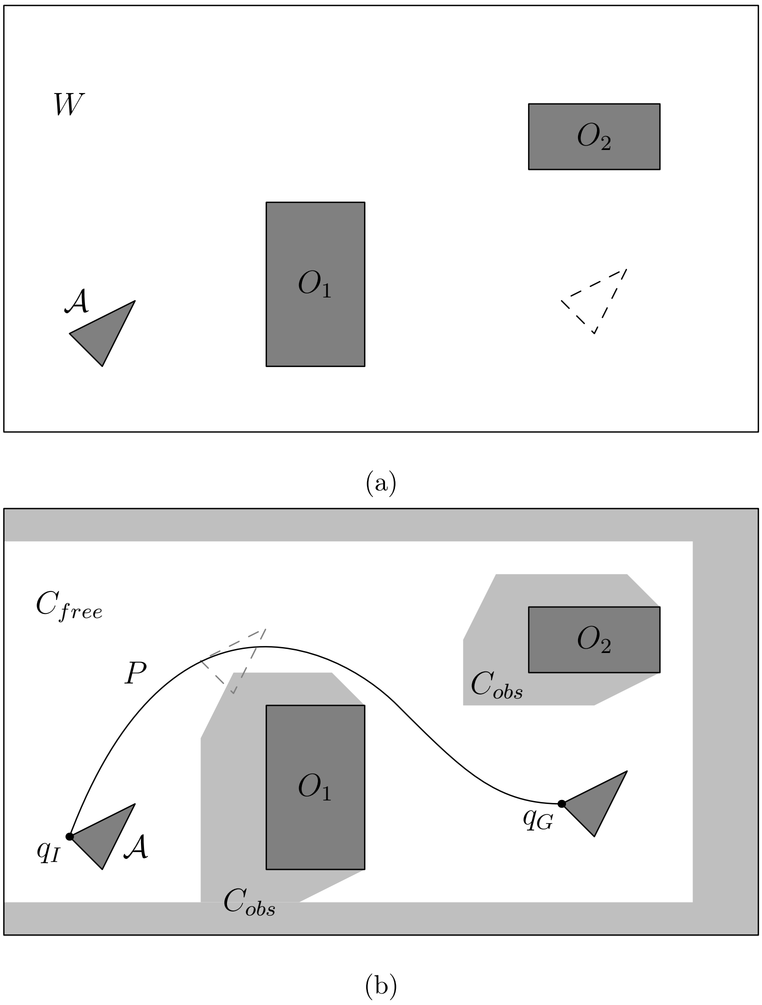

Figure 1.3: (a) Workspace $W = \mathbb{R}^2$ contains a triangular translating robot $\mathcal{A}$ and the set of obstacles $\mathcal{O} = \{O_1, O_2\}$. We want to move a robot to the goal position (dashed line) while avoiding the obstacles. (b) Configuration space C for a triangular translating robot $\mathcal{A}$. The space C_{free} (white) represents all configurations of a robot, which have no collision with any obstacle. Within the C_{obs} we distinguish by color the objects $\mathcal{O}$ (dark gray) and configurations where the robot would touch an object or leave the workspace (light gray). A collision-free path P is represented by a sequence of consecutively connected configurations connecting initial and goal configurations q_I, q_G.

these algorithms make them unappealing. Sampling-based algorithms have fulfilled much of this need in recent years by solving challenging problems in several settings, such as automobile assembly, humanoid robot planning, and conformational analysis in drug design. Although the completeness guarantees are weaker, the efficiency and ease of implementation of these methods have bolstered interest in applying motion planning algorithms to a wide variety of applications.

Early efforts to develop deterministic planning techniques showed that it is computationally demanding even for simple systems. Exact roadmap methods such as visibility graphs, Voronoi diagrams, Delaunay triangulation and adaptive roadmaps attempt to capture the connectivity of the robot search space. Cell decomposition methods use the subdivision of the workspace into small cells. Search algorithms such as Dijkstra and A^* find an optimal solution in a connectivity graph, whereas D^* and AD^* are tailored to dynamic graphs. The overview of algorithms and progress during 70s and 80s can be found in [Lat91].

Sampling based planning is by no means a novel concept in robotics, the overview can be found in [ES14]. It was proposed to overcome the complexity of deterministic robot planning algorithms for a robot with six degrees of freedom. The work [BL91] started a new generation of motion planning algorithms that use the random computations to solve otherwise rather difficult problems. Perhaps the most commonly used algorithms are Probabilistic roadmap method [KL94, KSLO96] and Rapidly-exploring random trees [LaV98]. The intuitive implementation of both methods, and the quality of the solutions, lead to their widespread adoption in robotics and many other fields.

A major drawback of sampling based planning methods is their widely regarded suboptimal paths. This is as a result of the arbitrary approach used in sampling and heuristics that are employed to speed up the search. Whereas some methods attempt to guide to improve the path quality during the search process, the lot of algorithms proceed to smooth and modify the path after planning is complete. The post processing consists of removing the redundant nodes and smoothing the path, see fig. 1.4.

An efficient algorithm [GO07] removes redundant nodes in one dimension at a time and provides some clearance by moving the path towards the medial axis. Smoothing techniques rely on using a curve to interpolate or fit the given way

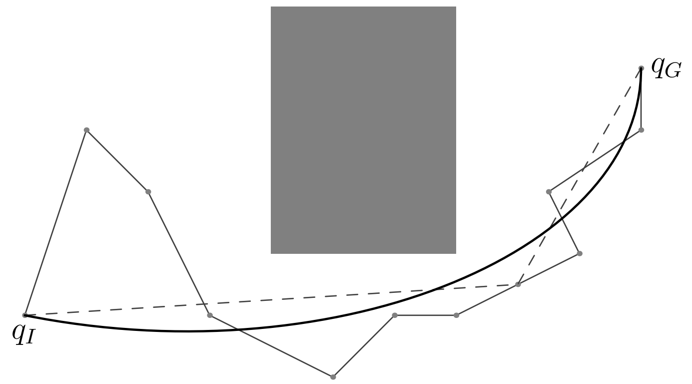

Figure 1.4: An illustration of post processing according [ES14]. The original path is highly suboptimal (grey thin line). Redundant nodes are removed and the rest are connected to provide a shortcut path (grey dashed line). Smoothing techniques are then employed to fit a curve through the short path (black thick line).

points. These methods use smooth curves like cubic polynomials [TMea06], quintic polynomials [UAea09, PPP02], Bézier curves [YS10, YS08, JKV09, YJS13] and Clothoids [KH97]. The works [PZM11, PZM12] use cubic B-splines to generate trajectories which are C^2-continuous almost everywhere, except on a few isolated points. An study shows that Bézier and B-splines are well suited for robotic planning and B-splines were shown to be more effective in replanning situations in dynamic environments. Regardless of the effectiveness of these approaches, post processing does not regulate the impractical attempts to expand nodes towards suboptimal regions. It only proceeds to optimize the path at a later stage. Planning time is wasted in both the search and the optimization stages. A more efficient strategy would be to explicitly consider path quality during planning.

1.4 Minkowski space

Pseudo-Euclidean space, denoted by $\mathbb{R}^n_p$, $n \in \mathbb{N}$, $p \in \mathbb{N}_0$ is an $n-$dimensional real vector space with a regular quadratic form $q\colon \mathbb{R}^n \to \mathbb{R}$, where $q(x_1, \ldots, x_n) = \sum_{i=1}^{n-p} x_i^2 - \sum_{j=n-p+1}^{n} x_j^2$ in certain basis. For $p = 1$, we call it *Minkowski space*, for $p = 0$, we get Euclidean space. Probably, the most popular pseudo-Euclidean space is $\mathbb{R}^4_1$ called *Minkowski space-time* which describes the special theory of relativity, more in [Nab12].

Using the quadratic form, we classify the vectors in the pseudo-Euclidean space. We call the vector $\boldsymbol{x} \in \mathbb{R}^n_p$ *space-like* if $q(\boldsymbol{x}) > 0$, *time-like* if $q(\boldsymbol{x}) < 0$ and *light-like* if $q(\boldsymbol{x}) = 0$. All the vectors in $q^{-1}(0)$ are also called *isotropic* and they form a cone Q. The set of all light-like vectors forms the *isotropic cone* Q of the corresponding quadratic form. If a subspace $F \subset \mathbb{R}^n_p$ consists of isotropic vectors, it is called *isotropic subspace*. We say that the coordinate axes $x_1, \ldots, x_{n-p}$ are space-like and the axes $x_{n-p+1}, \ldots, x_n$ are time-like.

Although we consider a real vector space, we get by a standard construction an affine space with a *pseudo-Cartesian* coordinate system $S(O, x_1, \ldots, x_n)$, where the axes $x_1, \ldots, x_n$ are pseudo-orthogonal and O is the origin. A point $X \in \mathbb{R}^n_p$ is space-like (time-like, light-like respectively) if its position vector $\boldsymbol{x} = X - O$ is such. There are two possible ways, how to define space-like curve (time-like and light-like respectively). A differentiable curve $p\colon I \to \mathbb{R}^n_p$ is called *space-like* if the tangent vector $\dot{p}(t)$ is space-like for each $t \in I$. A curve $p\colon I \to \mathbb{R}^n_p$ is called *pointwise space-like* if it contains only space-like points, i.e. position vector $\boldsymbol{x}$ of the point $X = p(t)$ is space-like for every $t \in I$.

Some properties of the curves, which we know from the Euclidean geometry, changes in pseudo-Euclidean geometry. Specially, those that depend on the scalar product. For example in the differential geometry, the Frenet formulas are much more complicated and it is necessary to distinguish a type of curve. The expression for space-like curves in $\mathbb{R}^4_1$ can be found in [YT08] and for time-like curves in [YÖT09]. Applications of Minkowski $\mathbb{R}^3_1$ space in CAGD are given in [Far08]. The conditions of space-like property, regularity, curvature, torsion and other properties of Bézier curves in $\mathbb{R}^3_1$ are proved in the paper [Geo08]. The properties of space-like Bézier surfaces in $\mathbb{R}^3_1$ have been also studied in [Geo09]. In the [UMY11], the first fundamental form coefficients are derived in terms of coordinates of control points of the surface and then, the conditions of the time-like case and the space-like case for Bézier surfaces are shown.

1.5 Number of real roots of real polynomial function in an interval

For counting the number of real roots of real polynomial function in an interval, the theorems below are useful. The following text is based on the works [GVT97, SB11, BT07]. Let $\mathbb{K}$ be an ordered field and $\mathbb{F}$ a real-closed field with $\mathbb{K} \subseteq \mathbb{F}$ (e.g. $\mathbb{K} = \mathbb{R}, \mathbb{F} = \mathbb{C}$). We denote the set of all polynomials in $\mathbb{K}[x]$ with degree at most d by P_d. The set P_d is $(d+1)$-dimensional vector space over $\mathbb{K}$.

Definition 1.3. Let $\{a_0, a_1, \ldots, a_n\}$ be a sequence of non zero elements in $\mathbb{F}$. We define $\mathbf{V}(\{a_0, a_1, \ldots, a_n\})$ as the number of sign variations in the sequence $\{a_0, a_1, \ldots, a_n\}$, that is the cardinality of $\{i \colon a_i a_{i+1} < 0\}$. If $\{a_0, a_1, \ldots, a_n\}$ is a sequence of real elements, then $\mathbf{V}(\{a_0, a_1, \ldots, a_n\})$ is the number of sign variations in the sequence, which we obtain from $\{a_0, a_1, \ldots, a_n\}$ omitting all zeros.

Theorem 1.1 (Budan-Fourier)**.** Let $f(x) = \sum_{i=0}^{n} a_i x^i \in P_n$, $n > 0$ and $a_n \neq 0$. Let $\alpha < \beta$ and $f(\alpha)f(\beta) \neq 0$ and let $\mathbf{V}(x) = \mathbf{V}(\{f(x), f'(x), \ldots, f^{(n)}(x)\})$. Then, the number (including multiplicity) of real roots of the equation $f(x) = 0$ lying in the interval $\langle \alpha, \beta \rangle$ is equal to or is smaller, by an even number, than $\mathbf{V}(\alpha) - \mathbf{V}(\beta)$.

In the search of the roots of the polynomial function it is important to know, when the two polynomials have a common root in some extension of the field $\mathbb{K}$. One of the theorems in linear algebra says, that two polynomials f, g from $\mathbb{K}[x]$ are commensurable iff there exist non-zero polynomials u, v from $\mathbb{K}[x]$ such that $\deg u < \deg g, \deg v < \deg f$ and $uf + vg = 0$. So if we note $f = \sum_{i=0}^{n} a_i x^i$ and $g = \sum_{i=0}^{m} b_i x^i$, we look for non-zero polynomials $u = \sum_{i=0}^{m-1} c_i x^i$ and $v = \sum_{i=0}^{n-1} d_i x^i$ such that $uf + vg = 0$.

Simplifying the expression, we obtain

$$\begin{aligned} uf + vg = &\sum_{i=0}^{m-1} c_i x^i \sum_{i=0}^{n} a_i x^i + \sum_{i=0}^{n-1} d_i x^i \sum_{i=0}^{m} b_i x^i = \\ &= x^{m+n-1}(a_n c_{m-1} + b_m d_{n-1}) + \\ &+ x^{m+n-2}(a_{n-1}c_{m-1} + a_n c_{m-2} + b_{m-1}d_{n-1} + b_m d_{n-2}) + \\ &+ \ldots + x^0(a_0 c_0 + b_0 d_0). \end{aligned}$$

Hence, $uf + vg = 0$ iff

$$\begin{pmatrix} a_n & 0 & \ldots & 0 & b_m & 0 & \ldots & 0 \\ a_{n-1} & a_n & & \vdots & b_{m-1} & b_m & & 0 \\ \vdots & a_{n-1} & & 0 & \vdots & b_{m-1} & & \vdots \\ \vdots & \vdots & & a_n & \vdots & \vdots & & \vdots \\ a_0 & \vdots & & a_{n-1} & b_0 & \vdots & & 0 \\ 0 & a_0 & & \vdots & 0 & b_0 & & b_m \\ \vdots & 0 & & \vdots & \vdots & 0 & & b_{m-1} \\ \vdots & \vdots & & \vdots & \vdots & \vdots & & \vdots \\ 0 & 0 & & a_0 & 0 & 0 & & b_0 \end{pmatrix} \cdot \begin{pmatrix} c_{m-1} \\ c_{m-2} \\ \vdots \\ \vdots \\ c_0 \\ d_{n-1} \\ d_{n-2} \\ \vdots \\ \vdots \\ d_0 \end{pmatrix} = \begin{pmatrix} 0 \\ 0 \\ \vdots \\ \vdots \\ \vdots \\ \vdots \\ \vdots \\ \vdots \\ 0 \end{pmatrix}.$$

The coefficients of the polynomials u, v are a (nontrivial) solution of this homogeneous system of linear equations. Let us denote the left matrix by $\boldsymbol{M}$. This system has nontrivial solution iff $\det \boldsymbol{M} = 0$ (and thanks to properties of transpose matrix iff $\det \boldsymbol{M}^\top = 0$).

Definition 1.4 (Resultant, subresultant)**.** Let $f = \sum_{i=0}^{n} a_i x^i$, $g = \sum_{i=0}^{m} b_i x^i$ be two non constant polynomials from $\mathbb{K}[x]$. The *Sylvester matrix* $\boldsymbol{M}(f, g)$ is the rectangular matrix of size $m+n$ on $\mathbb{K}$ defined as

$$\boldsymbol{M}(f,g) = \begin{pmatrix} a_n & a_{n-1} & \dots & \dots & \dots & a_0 & 0 & \dots & \dots & 0 \\ 0 & a_n & a_{n-1} & \dots & \dots & \dots & a_0 & 0 & \dots & 0 \\ 0 & 0 & a_n & a_{n-1} & \dots & \dots & \dots & a_0 & \dots & 0 \\ \vdots & & & & & & & & & \\ 0 & 0 & \dots & 0 & a_n & a_{n-1} & \dots & \dots & \dots & a_0 \\ b_m & b_{m-1} & \dots & \dots & \dots & b_0 & 0 & \dots & \dots & 0 \\ 0 & b_m & b_{m-1} & \dots & \dots & \dots & b_0 & 0 & \dots & 0 \\ 0 & 0 & b_m & b_{m-1} & \dots & \dots & \dots & b_0 & \dots & 0 \\ \vdots & & & & & & & & & \\ 0 & 0 & \dots & \dots & \dots & 0 & b_m & b_{m-1} & \dots & b_0 \end{pmatrix}.$$

The determinant of this matrix is called *resultant* of the polynomials f, g and is denoted as

$$\mathbf{res}(f,g) = \det \boldsymbol{M}(f,g).$$

Let $\boldsymbol{M}_{i,j}(f,g)$ be a matrix created from the matrix $\boldsymbol{M}(f,g)$ by removing the last j rows from the upper part, the last j rows from the lower part and the last $2j+1$ columns except $(m+n-i-j)$-th column, where $0 \le j \le \min\{n,m\}$ and $0 \le i \le j$. Then, the j-th *subresultant* is

$$\mathbf{Sres}_j(f,g) = \sum_{i=0}^{j} \det(\boldsymbol{M}_{i,j}(f,g)) \cdot x^i \ .$$

More about the resultants and subresultants can be found in [BPR06]. We mention few statements.

The resultants are useful in detecting of multiplicity of the roots. The polynomial $f \in \mathbb{K}[x]$ have the root of multiplicity at least 2 in $\mathbb{F}$ iff $\mathbf{res}(f,f') = 0$. The resultants also have a strong relationship with the greatest common divisor of polynomials. The two polynomials f, g from $\mathbb{K}[x]$ are commensurable in some extension of the field $\mathbb{K}$ iff $\mathbf{res}(f,g) = 0$.

The subresultants theory is a generalization of this property that allows to characterize generically the greatest common divisor of two polynomials. The relation between resultant and subresultant is $\mathbf{res}(f,g) = \mathbf{Sres}_0(f,g)$. The j-th subresultant $\mathbf{Sres}_j(f,g)$ of two polynomials is a polynomial of degree at most j. Let $LC_j(f,g) = LC(\mathbf{Sres}_j(f,g))$ be the leading coefficient of the subresultant $\mathbf{Sres}_j(f,g)$. They have the property that the greatest common divisor of f and g has a degree d if and only if $LC_0(f,g) = \cdots = LC_{d-1}(f,g) = 0, LC_d(f,g) \neq 0$. In this case, $\mathbf{Sres}_d(f,g)$ is the greatest common divisor of f, g and $\mathbf{Sres}_0(f,g) = \cdots = \mathbf{Sres}_{d-1}(f,g) = 0$.

There exists another view on the resultants and the Sylvester's criterion. Let us consider the map $\omega : (u,v) \to uf + vg$, where $\deg u < m, \deg v < n$. Then we have a map of the spaces $\omega : P_{m-1} \oplus P_{n-1} \to P_{m+n-1}$. Both spaces $P_{m-1} \oplus P_{n-1}$ and P_{m+n-1} are vector spaces of the dimension $m+n$ and the map ω is linear map. Let us choose the bases of both spaces. In the space P_{m+n-1}, we choose a standard monomial basis $x^{m+n-1}, x^{m+n-2}, \ldots, x, 1$. In the space $P_{m-1} \oplus P_{n-1}$ we choose a combination of standard bases of subspaces $(x^{m-1}, 0), (x^{m-2}, 0), \ldots, (x, 0), (1, 0), (0, x^{n-1}), \ldots, (0, x), (0, 1)$. Then the matrix of the map ω is Sylvester matrix of the polynomials f, g. The ω is surjective map iff its matrix is regular, i.e. $\mathbf{res}(f,g) \neq 0$.

Definition 1.5. Let f be a polynomial in $\mathbb{K}[x]$ with $p = \deg f$. If we write

$$\delta_k = (-1)^{\frac{k(k+1)}{2}}$$

for every integer k, the Sturm-Habicht sequence associated to f is defined as the sequence of polynomials $\{\mathbf{StHa}_j(f)\}_{j=0,\ldots,p}$ where $\mathbf{StHa}_p(f) = f$, $\mathbf{StHa}_{p-1}(f) = f'$ and for every $j \in \{0, \ldots, p-2\}$:

$$\mathbf{StHa}_j(f) = \delta_{p-j-1} \mathbf{Sres}_j(f, f')$$

where $\mathbf{Sres}_j(f, f')$ denotes the subresultant of index j for f and f'. For every j in $\{0, \ldots, p\}$ the principal j-th Sturm-Habicht coefficient, $\mathbf{stha}_j(f)$, is defined as the leading coefficient of x^j in $\mathbf{StHa}_j(f)$.

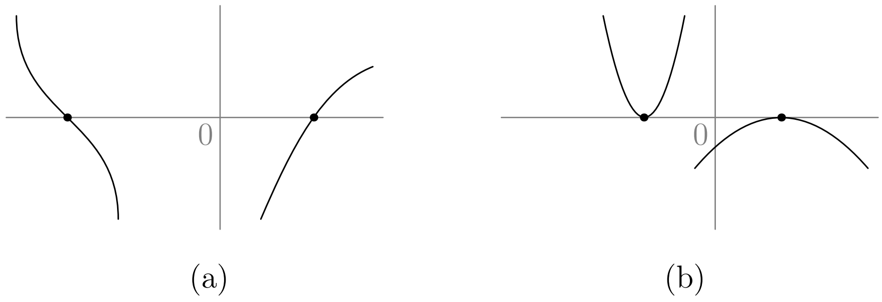

Figure 1.5: (a) The groups of sign variations $[+, 0, -], [-, 0, +]$ represent the simple roots.

(b) The groups of sign variations $[+, 0, 0, +], [-, 0, 0, -]$ represent the multiple roots.

Definition 1.6. Let f be a polynomial in $\mathbb{K}[x]$ and $\alpha \in \mathbb{F}$ with $f(\alpha) \neq 0$. We define the integer number $\mathbf{W}_{\mathrm{StHa}}(f; \alpha)$ in the following way. Firstly, we construct a sequence of polynomials $\{g_0, \ldots, g_s\}$ in $\mathbb{K}[x]$ obtained by deleting the polynomials identically 0 from $\{\mathbf{StHa}_j(f)\}_{j=0,\ldots,p}$. Then, $\mathbf{W}_{\mathrm{StHa}}(f; \alpha)$ is the number of sign variations in the sequence $\{g_0(\alpha), \ldots, g_s(\alpha)\}$ using the following rules for the groups of 0's (see fig. 1.5). We count 1 sign variation for the groups $[-, 0, +], [+, 0, -], [+, 0, 0, -]$ and $[-, 0, 0, +]$. We count 2 sign variations for the groups $[+, 0, 0, +]$ and $[-, 0, 0, -]$.

The *Sturm-Habicht Sequence Theorem* (see [GVRLR98]) implies that it is not possible to find more than two consecutive zeros in the sequence $g_0(\alpha), \ldots, g_s(\alpha)$ and that the sign sequences $[+, 0, +], [-, 0, -]$ can not appear.

Definition 1.7. Let f be a polynomial in $\mathbb{K}[x]$ and $\alpha, \beta \in \mathbb{F}$ with $\alpha < \beta$. We define $\mathbf{W}_{\mathrm{StHa}}(f; \alpha, \beta) = \mathbf{W}_{\mathrm{StHa}}(f; \alpha) - \mathbf{W}_{\mathrm{StHa}}(f; \beta)$.

The next theorem shows how to use the Sturm-Habicht sequence of f and the function $\mathbf{W}_{\mathrm{StHa}}$ to compute the number of real roots of f inside an open interval.

Theorem 1.2. Let f be a polynomial in $\mathbb{K}[x]$ and $\alpha, \beta \in \mathbb{F}$ with $\alpha < \beta$ and $f(\alpha)f(\beta) \neq 0$. Then $\mathbf{W}_{\mathrm{StHa}}(f; \alpha, \beta) = \#(\{\gamma \in (\alpha, \beta) : f(\gamma) = 0\})$.

# of real roots	# of sign changes $V(0) - V(1)$	sign of Δ	corresponding figure
0	0 or 2	$\Delta < 0$ $\Delta = 0$ $\Delta > 0$	fig. 1.6(a) fig. 1.6(b) fig. 1.6(c)
1	1 or 3	$\Delta < 0$ $\Delta = 0$ $\Delta > 0$	fig. 1.6(d) fig. 1.6(e) fig. 1.6(f)
1	2	$\Delta = 0$	fig. 1.6(g)
2	2	$\Delta > 0$	fig. 1.6(h)
2	3	$\Delta = 0$	fig. 1.6(i)
3	3	$\Delta > 0$	fig. 1.6(j)

Table 1.1: The number of real solutions within the interval $\langle 0, 1\rangle$ of a cubic function distinguished by sign changes and sign of Δ.

There also exists a theorem on computation of the total number of real roots (in $\mathbb{F}$) of a polynomial in $\mathbb{K}[x]$ using the Sturm-Habicht sequence (see [GVT97]).

Another indicator of the number of real roots is the *discriminant* $\Delta = \mathbf{res}(f, f')$ *of the function* f. The general cubic equation with real coefficients has the form $p(x) = a_3x^3 + a_2x^2 + a_1x + a_0$ with $a_3 \neq 0$ and all $a_i \in \mathbb{R}$. This equation has three roots, but not all real necessarily. We can distinguish several possible cases using the discriminant $\Delta = \mathbf{res}(p, p')$. We compute $\Delta = 18a_3a_2a_1a_0 - 4a_2^3a_0 + a_2^2a_1^2 - 4a_3a_1^3 - 27a_3^2a_0^2$. If $\Delta > 0$, then the equation has three distinct real roots. If $\Delta = 0$, then the equation has a multiple root and all its roots are real. If $\Delta < 0$, then the equation has one real root and two non-real complex conjugate roots.

Let us focus on the real solutions within interval $\langle 0, 1\rangle$ due to later application. The table 1.1 showing the dependency between number of different real roots, the number of sign changes according to theorem 1.1 and the sign of discriminant Δ.

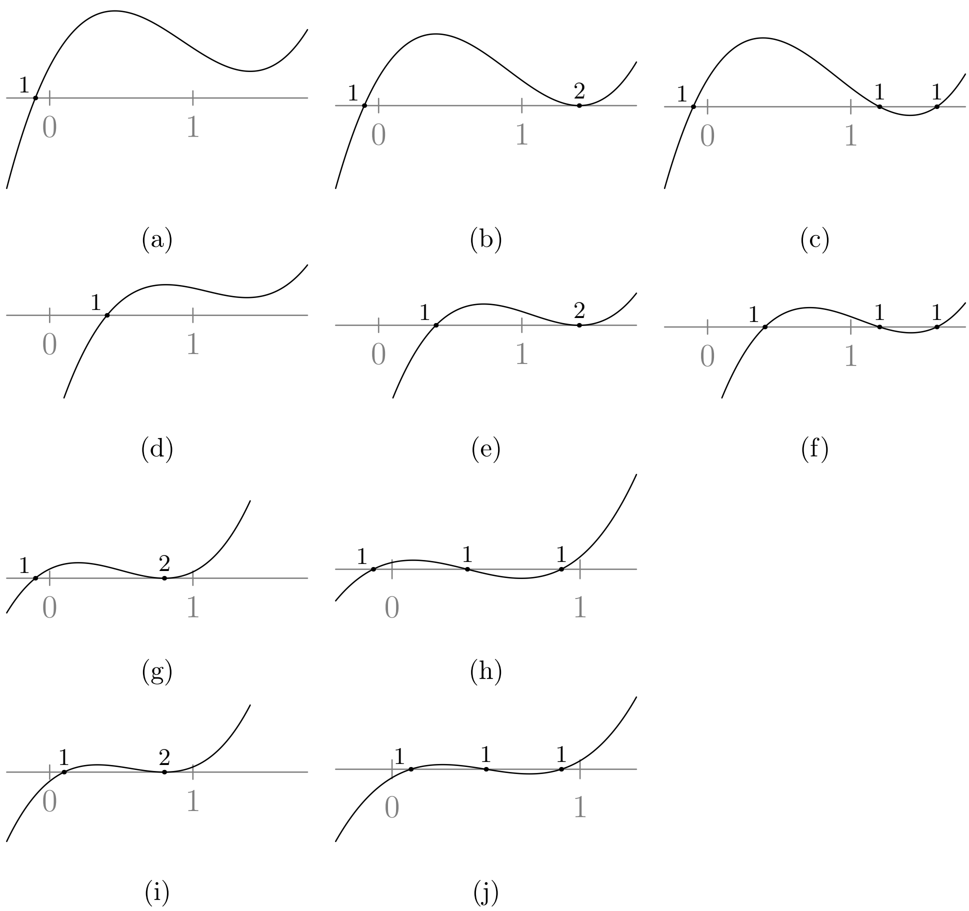

Figure 1.6: The figure shows all possible placements of the real roots of a cubic function up to symmetry ($x \to 1 - x, x \to -f(x)$). The small number over each root is its multiplicity.

(a–c) The cubic function has no real roots within $\langle 0, 1 \rangle$.

(d–g) There is one real root of cubic function in the interval $\langle 0, 1 \rangle$. Its multiplicity may be 1 or 2.

(h–i) The cubic function has two different real roots within $\langle 0, 1 \rangle$. They may be both simple roots or one simple root and one multiple root.

(j) Finally, there may exist three different roots of the cubic function and they are all simple.

2

Goals

We formulate three main goals.

1. Let $\mathbb{R}^3$ be the three dimensional Euclidean space with obstacle represented by regular quadric κ. Let the point A be the start and the point B be the finish. We find all quadratic Bézier paths starting at A and ending at B representing collision-free path with respect to an obstacle κ.

2. The extension of the problem is the existence of more obstacles. Let $O = \{O_1, \dots, O_m\}$ be the set of obstacles represented by regular quadrics. Let $P = \{P_1, \dots, P_n\}$ be a given set of points such that $n \geq 2$, where P_1 is the start of the path and P_n is the end of the path. We want to find the conditions for C^0, resp. C^1 piecewise quadratic spline representing collision-free path with respect to obstacles O. Moreover, the spline have to start at P_1, pass through the points $P_2, \dots, P_{n-1}$ and end at the point P_n.

3. The observations from the quadratic paths are applied on the collision-free paths represented by planar cubic Bézier curves. So, we want to formulate some theorems and hypothesis about collision-free cubic path with respect to an obstacle κ.

For filling these main goals, we define the following partial goals. It is appropriate to represent the set of all collision-free paths by the set of corresponding middle control points $V(A, B)$, because the starting and the last control point do not change in the goal 1. We reduce the spatial problem of $\mathbb{R}^3$ into the plane ρ, where the section of κ is a conic section K. Then, we study the touching situation between conic section K and quadratic Bézier curves with A and B as first and last control points respectively. We find the possible points of contact on K and using the admissible map σ the corresponding middle control points C in ρ. We must show that such middle control points create the boundary ∂V of the set $V(A, B)$.

The partial tasks for the second goal: We use the observations of the properties of the set $V(A, B)$ for one obstacle κ to evading more obstacles simultaneously. Connection of the segments $b_{P_{i-1}P_iP_{i+1}}$ensures the C^0 continuity. The conditions of C^1-continuity for middle control points we derive form the properties of derivatives at the points of connection $P_i, i = 2, \ldots, n-1$.

The partial tasks for the third goal: We consider the paths representing by planar cubic curves b_{ACBF} with fixed control point F. At first, we determine the equation of the map σ for cubic Bézier curves. We derive some theorems and hypotheses about the shape of the set of admissible points of contact from the prescription of this map.

3

Quadratic collision-free Bézier path

This chapter deals with collision-free path planning, where the final path is represented by quadratic Bézier curve and an obstacle is represented by regular quadric. After reducing of the situation into a plane of the path, the touching situations between conic section and Bézier curve are studied.

3.1 Collision-free situation in a plane

Let us consider the Euclidean space $\mathbb{R}^3$, let $\langle O, e_1, e_2, e_3 \rangle$ be an affine coordinate system, with a regular quadric κ represented by the matrix $\boldsymbol{Q_\kappa}$. Let the points $A = [a_1, a_2, a_3]$ and $B = [b_1, b_2, b_3]$ be fixed and $\boldsymbol{a} = A - O, \boldsymbol{b} = B - O$ are their position vectors. Assuming the quadric is an enclosing volume of some obstacle and the points A, B are start and end position of a robot we require $q(\boldsymbol{a}) > 0$ and $q(\boldsymbol{b}) > 0$, i.e. A, B lie outside the quadric κ. We look for all collision-free (relative to quadric) paths supply by quadratic Bézier curves from the point A to the point B. In other words, we look for the set of all such points C that the Bézier curve $b_{ACB}\,(t)$ lie out of quadric. Thus, for all points $X \in b_{ACB}\,(t)$ and their position vectors $\boldsymbol{x}$ the inequality $q(\boldsymbol{x}) > 0$ holds. In applications, $A \neq B$ yields, however we solved also the case $A = B$ for the sake of completeness.

A generic quadratic Bézier curve is a part of a parabola, so it lies in the affine plane $\rho \subset \mathbb{R}^3$. Since the given points $A, B \in \rho$, the construction of the plane

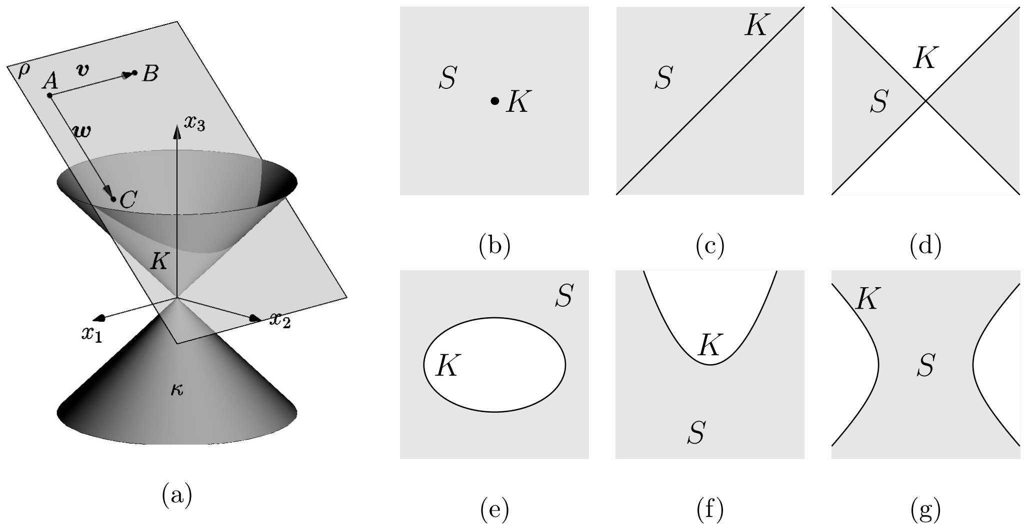

Figure 3.1: (a) Plane ρ spans points A, B, C. In case of their non-collinearity, they generate ρ as affine hull. The conic section K is the intersection of the quadric κ and the plane ρ. (b–g) Let $K \subset \rho$ be the conic section (point, double line, pair of lines, ellipse, parabola, hyperbola). The set S consists of all points lying out of quadric in the plane ρ.

ρ may have several degrees of freedom depending on their positions. Using the equation $\rho = \{X \in \mathbb{R}^3;\, X = A + t\boldsymbol{v} + s\boldsymbol{w}, \text{ for } t, s \in \mathbb{R}\}$, the degree of freedom is represented by the $\dim[\boldsymbol{v}, \boldsymbol{w}]$. If $A \neq B$, the degree of freedom is 1. As the position of the point C changes, the plane ρ accordingly contains the axis $\overleftrightarrow{AB}$, so we can choose as $\boldsymbol{v} = B - A$ and the choice of the vector $\boldsymbol{w}$ is free. If $A = B$, the degree of freedom is 2 and the choice of both vectors $\boldsymbol{v}, \boldsymbol{w}$ is free (up to linear dependency).

In any case, the intersection of the quadric κ and the plane ρ is a conic section K (see fig. 3.1(a)). The figures 3.1(b–g) show all cases how the set S of all points X that $q(\boldsymbol{x}) > 0$ in the possible types of plane ρ looks like. The collision-free Bézier curve $b_{ACB}\,(t) \subset S$. We present a solution in the plane ρ for each type of conic section $K \neq \emptyset$ separately and the planar results can be put together to form the spatial result.

As we shall see later, it is useful to consider ρ as an extended Euclidean plane. However, the control points $A, B, C \notin l^{\infty}$. Let $\langle O, x, y\rangle_{\rho}$ be any Cartesian coordinate system in the plane ρ. Let $A = [a_x, a_y]$, $B = [b_x, b_y]$ and $C = [c_x, c_y]$ be the local affine coordinates of the control points in $\langle O, x, y\rangle_{\rho}$.

Definition 3.1 (Set of admissible solutions)**.** Let $V_{\rho}(A, B)$ be a set of points $C \in \rho$ such that the curve b_{ACB} is collision-free with respect to K. Then, we say that $V_{\rho}(A, B)$ is a *set of admissible solutions* in the plane ρ with respect to A, B. If no confusion arises, we say the set of admissible solutions.

Definition 3.2. By $V_{\rho}^{v}(A, B)$, we denote the set of points $C \in \rho$ such that $b_{ACB} \cap K = M$, where $X \in M$ is a point of contact of order 2 between $b_{ACB}(t)$ and K. We denote the set of points $C \in \rho$ such that b_{ACB} and K have transversal intersection by $V_{\rho}^{t}(A, B)$.

The set M contains at most two such points, since two componentwise different quadratic curves may have at most two common points of contact of order 2 (see e.g. Bézout theorem, [Kun05]).

For the given points A, B, the union of disjoint sets $V_{\rho}(A, B) \cup V_{\rho}^{v}(A, B) \cup V_{\rho}^{t}(A, B)$ gives the whole plane ρ. At first, we study the set $V_{\rho}^{v}(A, B)$. It is natural due to the continuity, because "boundary" between the situation that two curves have no common points and the situation that one curve intersects the other curve is, that they touch each other. If the Bézier curve touches the conic section, they have the common tangent line. The following lemma offers an alternative definition of quadratic Bézier curve by its tangent.

Lemma 3.1 (Alternative definition of quadratic Bézier curve by its tangent)**.**

(a) Let the points $A, B, T \in \mathbb{R}^2$ be non-collinear and ℓ_T be a line such that segment $AB \cap \ell_T = \emptyset$, $T \in \ell_T$. Then, the quadratic Bézier curve $b(t)$ with the end points A, B, containing the point T and with the tangent line ℓ_T at the point T exists and is uniquely determined.

(b) Let the points $A, B, T \in \mathbb{R}^2$ be different collinear, $T \notin AB$ and ℓ_T be a line such that $\ell_T \neq \overleftrightarrow{AB}$, $T \in \ell_T$. Then, the quadratic Bézier curve $b(t)$ with the end points A, B, containing the point T and with the tangent line ℓ_T at the point T, exists and is uniquely determined.

(c) Let the points $A, B, T \in \mathbb{R}^2$ be different collinear, $T \notin AB$ and ℓ_T be a line such that $\ell_T = \overleftrightarrow{AB}$, $T \in \ell_T$. Then, there are infinite number of quadratic Bézier curve $b(t)$ with the end points A, B, containing the point T and with the tangent line ℓ_T at the point T. The admissible middle control points C form a half-line (subset of the line $\overleftrightarrow{AB}$).

(d) Let the points $A, B, T \in \mathbb{R}^2$ be different collinear, $T \in AB$ and $\ell_T = \overleftrightarrow{AB}$. Then, there are infinite number of quadratic Bézier curve $b(t)$ with the end points A, B, containing the point T and with the tangent line ℓ_T at the point T. The admissible middle control points C form the line $\overleftrightarrow{AB}$.

(e) Let the points $A, B, T \in \mathbb{R}^2$ and $A = B \neq T$. Let ℓ_T be a line such that $\ell_T = \overleftrightarrow{AT}$, $T \in \ell_T$. Then, there are infinity number of quadratic Bézier curve $b(t)$ with the end points A, B, containing the point T and with the tangent line ℓ_T at the point T. The admissible middle control points C form a half-line $\overrightarrow{C_S X} \subset \overleftrightarrow{AT}$, where $C_S = 2T - A$ and $X = A + (2 + \epsilon)(T - A)$, $\epsilon > 0$.

(f) Let the points $A, B, T \in \mathbb{R}^2$ and $A = B$. Let ℓ_T be a line such that $\ell_T \neq \overleftrightarrow{AT}$, $T \in \ell_T$. Then, the quadratic Bézier curve $b(t)$ with the end points A, B, containing the point T and with the tangent line ℓ_T at the point T, exists and is uniquely determined.

Proof. (a) Let the vector $\boldsymbol{\ell} = (l_x, l_y) \neq (0, 0)$ be the direction vector of the tangent line ℓ_T and $A = [a_x, a_y], B = [b_x, b_y], T = [t_x, t_y]$. Let the vector $\boldsymbol{n_\ell} = (-l_y, l_x)$.

We define the map τ such that $\tau(A, B, T, \boldsymbol{\ell}) = C$ returns the middle control point of the Bézier curve $b\,(t)$.

$$\tau(A, B, T, \boldsymbol{\ell}) = C = \frac{T - B_0^2(t_0)A - B_2^2(t_0)B}{B_1^2(t_0)} \;, \tag{3.1}$$

where $t_0 \in (0, 1)$ is a solution of the equation

$$0 = \alpha t^2 + 2\beta t + \gamma \tag{3.2}$$

with

$$\begin{aligned} \alpha &= l_x(b_y - a_y) - l_y(b_x - a_x) \;, \\ \beta &= l_x(a_y - t_y) - l_y(a_x - t_x) \;, \\ \gamma &= -\beta \;. \end{aligned}$$

The Bézier curve $b_{ACB}\,(t)$ with its control points A, C, B in this order satisfies the requirements of the theorem. For proving the existence of b_{ACB}, we use the affine transformation mapping the three independent points A, B, T to the points $A = [-1, 0],\ B = [1, 0],\ T = [0, 1]$. We obtain the coefficients $\alpha = -2l_y,\ \beta = -l_x + l_y,\ \gamma = l_x - l_y$ in quadratic equation (3.2). The discriminant of the equation (3.2) is $D = (2\beta)^2 - 4\alpha\gamma = 4(l_x - l_y)(l_x + l_y)$. The discriminant $D \neq 0$, because the equality $D = 0$ leads to $l_x = \pm l_y$ and $t_0 = 0,\ T = A$ or $t_0 = 1,\ T = B$, which is a contradiction with the initial conditions. On the other hand, the initial condition that segment $AB \cap \ell_T = \emptyset$ guarantees $D > 0$. If the vector (l_x, l_y) belongs to I. or VIII. octant, both brackets $(l_x - l_y),\ (l_x + l_y)$ are positive. If the vector (l_x, l_y) belongs to IV. or V. octant, both brackets are negative (see fig. 3.2).

(b) We can use the formula (3.1) for finding the point C. For proving the existence of b_{ACB}, we change the coordinate system to obtain $A = [0, 0],\ B = [1, 0],\ T = [t_x, 0]$. We obtain the coefficients $\alpha = -l_y,\ \beta = l_y t_x,\ \gamma = -l_y t_x$ in quadratic equation for t. The discriminant $D = 4l_y^2 t_x(t_x - 1)$. The point $T \notin AB$, then $t_x,\ (t_x - 1)$ has the same sign and $l_y \neq 0$. Hence, $D > 0$.

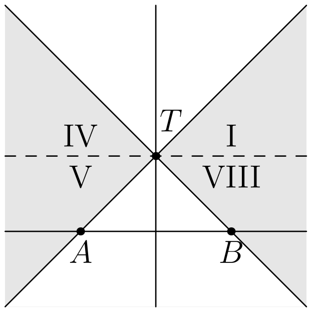

Figure 3.2: Let ℓ_T be a line such that segment $AB \cap \ell_T = \emptyset$, $T \in \ell_T$ (hence it lies in the area determined by octants I, IV, V, VIII). Then, the quadratic Bézier curve $b\,(t)$ with the end points A, B, containing the point T and with the tangent line ℓ_T at the point T, exists and is uniquely determined.

(c) and (e) All admissible points C satisfy: $C \in \overrightarrow{C_S X} \subset \overleftrightarrow{AB}$, where $A, B \notin \overrightarrow{C_S X}$ and C_S is such that the derivative $\dot{b}_{AC_SB}(t_0) = 0$ for $T = b_{AC_SB}(t_0)$. For the special case $A = B$, the point $C_S = A + 2(T - A)$.

(d) All the points $C \in \overleftrightarrow{AB}$ satisfy the requirements.

(f) The middle control point $C = A + 2(T - A)$. $\square$

3.2 Exterior and interior points of contact

For the given points A, B and the conic section K, not every tangent line of K define the quadratic Bézier curve which has no transversal intersections with K. In this section, we show which subset of T_K contains such lines.

Definition 3.3 (Set of points of contact)**.** We say that the set $D \subset K$ is the *set of points of contact* between K and the set of all b_{ACB} if for any point $X \in D$ there is a point C such that $C \in V^v_\rho(A, B)$ and $X \in b_{ACB} \cap K$.

Definition 3.4 (Double contact)**.** We say that b_{ACB} has *double contact*, if it has exactly two points of contact of order 2 with K (i.e. the set M contains exactly

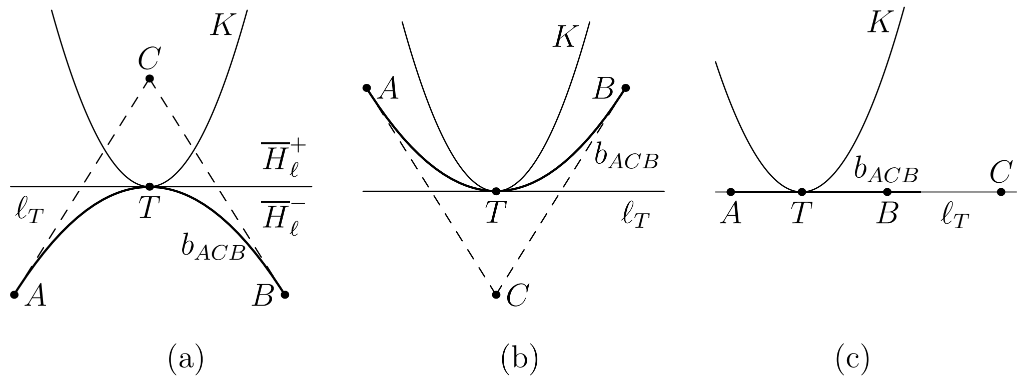

Figure 3.3: Separation of the conic section K and the Bézier curve $b_{ACB}(t)$ by the tangent line ℓ_T – (a) exterior point of contact T, (b) interior point of contact T, (c) exterior point of contact T.

two points). We denote the middle control point of such Bézier curve by C_u. If K is a regular conic section, we denote the touching points by the letters $U_i, i = 1, 2$ (see fig. 3.8). If K is a singular conic section, we denote the touching points by the symbol S_i, for $i = p, r$ (see fig. 3.9(b)).

When we obtain K as a connected component of a regular conic section, it may be an ellipse, a parabola or one component of a hyperbola. Since the connected component of regular conic section is convex, the tangent line is a supporting line of the component. In the case of singular conic section, the connected component may be a point or a line.

Let ℓ_T be a tangent line to a connected component K of a conic section (regular or singular) at the point $T \in K$. It divides the plane ρ into two half-planes $\overline{H}_\ell^+, \overline{H}_\ell^-$ such that $K \subset \overline{H}_\ell^+$. We say, that ℓ_T *separates* the connected component K of the conic section and the arbitrary set of points $\mathcal{O}$, if they lie in the opposite half-planes with respect to the tangent ℓ_T, i.e. $K \subset \overline{H}_\ell^+$ and $\mathcal{O} \subset \overline{H}_\ell^-$ (see fig. 3.3 for $\mathcal{O} = b_{ACB}(t)$). Additionally, in the case of hyperbola the asymptotes separate similarly K and $\mathcal{O}$, but the corresponding touching point is infinite. We denote the set of all separating tangent lines and asymptotes by $T_{sep}(\mathcal{O}, K)$. We denote by $S(\mathcal{O}, K) \subset K$ the maximal open set of all *affine* points of contact of K and separating tangent lines.

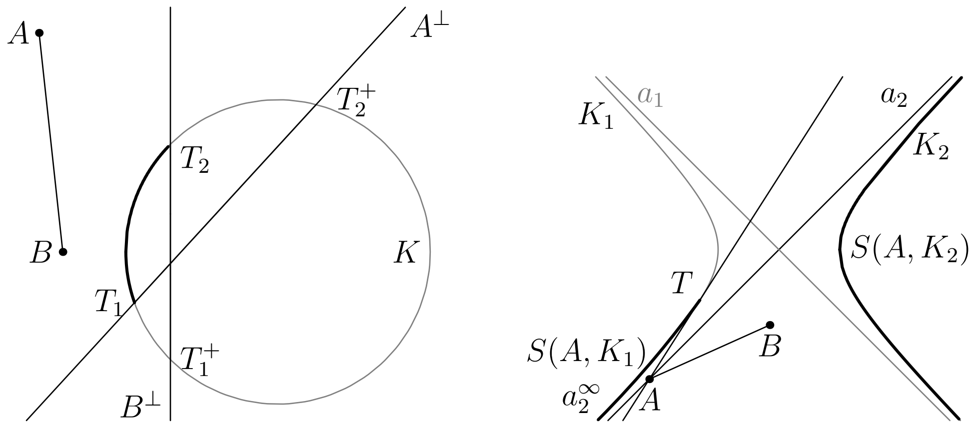

(a) (b)

Figure 3.4: (a) The set of all tangent lines of K, which separate the point A and K, is determined by arc $\widehat{T_1T_2^+}= S(A, K)$. Similarly, the arc $\widehat{T_1^+T_2}= S(B, K)$. The arc $\widehat{T_1T_2}$ determines all tangent lines $T_{sep}(AB, K)$. We obtain it as intersecion of the sets $\overline{S}(A, K) \cap \overline{S}(B, K)$. (b) We have the set $S(A, K_1) = \{X \in K_1 \colon A\boldsymbol{Q_K}X^{\top} > 0\} = \widehat{Ta_2^{\infty}}$. All tangent lines of connected component K_2 separate this component and the point A. Hence, we have the set $S(A, K_2) = K_2$.

Definition 3.5 (Exterior (interior) point of contact)**.** We say that the curve b_{ACB} *touches* a connected component of the regular conic section K from *outside (inside)*, if their common tangent is (is not) separating (see fig. 3.3). Then, the point of contact is called *exterior (interior) point of contact.* The set of all exterior (interior) points of contact is denoted D_{ext} (D_{in}).

Note, the set $\mathcal{O}$ may contain the point T. The set of points of contact $D = D_{ext} \cup D_{in}$. Now, we describe the set of points of contact D for every type of conic section. First, we consider the regular conic sections, then we analyse the singular conic sections.

The polar line of the point A determined by the equation $A\boldsymbol{Q_K}X^{\top} = 0$ splits the conic section K to some arcs. Let K be a regular conic section different from hyperbola. The condition that the point A is separated from K, the point $T \in \{X \in K \colon A\boldsymbol{Q_K}X^{\top} \geq 0\}$. So, the open set $S(A, K) = \{X \in$

$K\colon A\boldsymbol{Q_K}X^\top > 0\}$ (see fig. 3.4(a)). Now, let K_1, K_2 be the connected components of a hyperbola K. We consider each of them separately and we get $S(A, K_1) = \{X \in K_1\colon A\boldsymbol{Q_K}X^\top > 0\}$ and $S(A, K_2)$ (see also fig. 3.4(b)).

Let K be a connected component of a regular conic section. Let $\ell_T \in T_K$ and the point $T \in K$ be its point of contact. The tangent line $\ell_T \in T_{sep}(AB, K)$ if and only if $T \in \overline{S}(A, K) \cap \overline{S}(B, K) = \{X \in K\colon A\boldsymbol{Q_K}X^\top \geq 0 \wedge B\boldsymbol{Q_K}X^\top \geq 0\}$ (see fig. 3.4(a)).

We denote the set of all $X \in K$ such that the corresponding tangent line ℓ_X to K at X contains both control points A, B by D_{AB}. The set $D_{AB} = \{X \in K\colon A\boldsymbol{Q_K}X^\top = 0 \wedge B\boldsymbol{Q_K}X^\top = 0\}$.

Theorem 3.1 (Set of exterior points of contact)**.** Let K be a regular connected component of conic section. The set of exterior points of contact $D_{ext} \neq \emptyset$ if and only if the segment $AB \cap K = \emptyset$ or $AB \cap K = \{T\}$.

The set $D_{ext} = \{X \in K\colon A\boldsymbol{Q_K}X^\top > 0 \wedge B\boldsymbol{Q_K}X^\top > 0\} \cup D_{AB}$.

Proof. Sufficient condition. Let $AB \cap K = \{X_1, X_2\}$. Let ℓ be any tangent line to K. In order that the line ℓ separates AB and K (up to the point of contact if it exists), they must lie in the different half-planes with respect to ℓ (up to the point of contact). But the points $X_1, X_2 \in K$ lie in the same half-plane as AB. Hence, $\overline{S}(A, K) \cap \overline{S}(B, K) = \emptyset$ and there is no separating tangent line $\ell_T \in T_{sep}(AB, K)$. So, there exists no separating tangent line for any Bézier curve b_{ACB}. Consequently, the set $D_{ext} = \emptyset$.

Necessary condition. We discuss each case separately. Mainly, we use the fact that the quadratic Bézier curve is a convex curve, each of its tangent line defines a supporting half-plane to the curve. If $\ell_T \in T_{sep}(A, K)$ and $\ell_T \in T_{sep}(B, K)$, then $\ell_T \in T_{sep}(b_{ACB}, K)$. So, for every $T \in \overline{S}(A, K) \cap \overline{S}(B, K)$ holds that $\ell_T \in T_{sep}(b_{ACB}, K)$. At the end, we decide if endpoints T_1, T_2 of the intersection $\overline{S}(A, K) \cap \overline{S}(B, K)$ belong to the set D_{ext}. It is shown they do not in general. But if one of the triplets of points A, B, T_1 and A, B, T_2 is collinear, without loss of generality A, B, T_1, then the point $T_1 \in D_{AB}$. But $T_1 \in D_{ext}$ too, because the corresponding Bézier curve is a segment tangent to K. Hence, the set $D_{ext} = \{S(A,K) \cap S(B,K)\} \cup \{T_1\} \neq \emptyset$. $\square$

Note, there might be two continuous arcs D^1_{ext}, D^2_{ext}, one on each connected component K_1, K_2 of the hyperbola K. Then, $D_{ext} = D^1_{ext} \cup D^2_{ext}$.

Note 1. We denote the set of all $T \in D_{ext}$ such that the corresponding tangent line ℓ_T to K at T contains both control points A, B by D_{AB}. Such points have different behavior (see note 2).

Now, we show the structure of the interior points of contact.

Lemma 3.2. If $T \in D_{in} \subset D$ is an interior point of contact of the Bézier curve $b(t)$ and the conic section K, then there exists the triangle $\triangle ABC$ such that $T \in \triangle ABC$ and the sides AC, CB have no common point with the conic section K.

Proof. Let the Bézier curve b_{ACB} be determined by the end points A, B and the tangent line ℓ_T at the point $T \in K \cap b_{ACB}$. Then, the triangle $\triangle ABC$ determined by the control points of the Bézier curve satisfies the requirements of the lemma. The point $T \in \triangle ABC$ because the Bézier curve is completely contained in the convex hull of its control points. The sides AC, CB have no common point with the conic section K because they are separated from K by the curve b_{ACB}. $\square$

The line $\overleftrightarrow{AB}$ divides the plane ρ into two half-planes, the open half-plane ρ_-, and the closed half-plane $\overline{\rho_+}$. Let us sort the tangent lines from A and B to K, that are not in $T_{sep}(AB, K)$, into pairs. If there are only two tangent lines not in $T_{sep}(AB, K)$, we denote them ℓ^+_1, ℓ^+_2 (see fig. 3.5(a)). If there are four tangent lines not in $T_{sep}(AB, K)$, we determine two pairs ℓ^+_1, ℓ^+_2 and ℓ^-_1, ℓ^-_2 such that the corresponding points of contact $T^\pm_i = \ell^\pm_i \cap K, i = 1, 2$ lie in the same half-plane $T^+_i \in \overline{\rho_+}$ and $T^-_i \in \rho_-, i = 1, 2$. If $\ell^+_1 \cap \ell^+_2 = P^+ \in \overline{\rho_+}$. We say the tangents ℓ^+_1, ℓ^+_2 *converge*. If $P^+ \in \rho_-$ or P^+ is a point at infinity, we say they *diverge* (see fig. 3.5(b)).

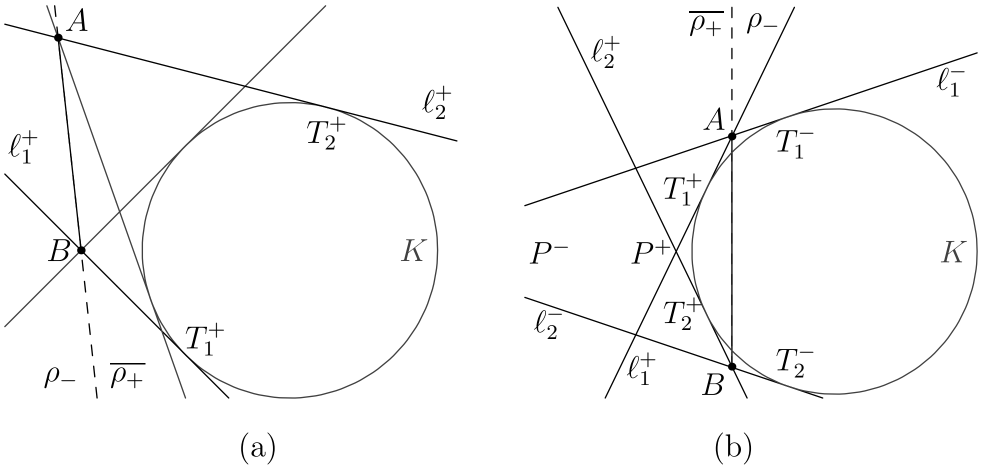

Figure 3.5: (a) There are only two tangent lines not in $T_{sep}(AB, K)$. The corresponding points of contact $T_1^+, T_2^+ \in \overline{\rho_+}$, so we denote the tangent lines ℓ_1^+, ℓ_2^+. They diverge, because their intersection lies in the half-plane ρ_-. (b) If there are four tangent lines not in $T_{sep}(AB, K)$, we determine two pairs ℓ_1^+, ℓ_2^+ and ℓ_1^-, ℓ_2^- according to corresponding points of contact. The pair ℓ_1^+, ℓ_2^+ converge, because their intersection $P^+ \in \overline{\rho_+}$. However, the pair ℓ_1^-, ℓ_2^- diverge.

Theorem 3.2 (Set of interior points of contact)**.** Let K be a regular connected conic section. The set of interior points of contact $D_{in}^+ \neq \emptyset$ ($D_{in}^- \neq \emptyset$) iff the pair of tangents ℓ_1^+, ℓ_2^+ (ℓ_1^-, ℓ_2^-) converges.

Moreover, let $\ell_1^+, \ell_2^+ \notin T_{sep}(AB, K)$ be a pair of converging tangent lines and $P^+ = \ell_1^+ \cap \ell_2^+ \in \rho_+$. If there exists a point $C_u \in \rho_+$ such that curve b_{AC_uB} has double contact (at the points U_1, U_2), then the set $D_{in}^+ = \{X \in K \cap \rho_+ \colon A\boldsymbol{Q_K}X^\top < 0 \wedge B\boldsymbol{Q_K}X^\top < 0\} \setminus \{\overset{\frown}{U_1U_2}\}$ (see fig. 3.8). Else, the set $D_{in}^+ = \{X \in K \cap \rho_+ \colon A\boldsymbol{Q_K}X^\top < 0 \wedge B\boldsymbol{Q_K}X^\top < 0\}$. A similar statement holds for a pair of tangent lines converging in the half-plane ρ_- and D_{in}^-.

Proof. Necessary condition. If the mentioned pair of tangent lines diverges, then there exists no triangle $\triangle ABC$ from the lemma 3.2.
Sufficient condition of the existence $D_{in}^+ \neq \emptyset$. Let the pair of tangent lines ℓ_1^+, ℓ_2^+

converges in the half-plane ρ_+, i. e. $P^+ \in \rho_+$. We consider the parallel line v_a, resp. v_b containing the point A, resp. B, and have no common points with K in the half-plane ρ_+. Let $C_{mid} = \frac{1}{2}A + \frac{1}{2}B$ be. Let the line v_{mid} be parallel to the lines v_a, v_b and $C_{mid} \in v_{mid}$. Let $C_1 \in v_{mid}$ be an arbitrary point such that the Bézier curve $b_{AC_1B} \cap K = \emptyset$. It exists, because the $K \cap \rho_+$ is bounded within $\triangle AP^+B$. The Bézier curve $b_{AC_{mid}B} \cap K = \{X_1, X_2\}$. Hence, the segment $C_{mid}C_1$ contains such point C_0 that the corresponding Bézier curve touches the conic section K at the point $\{T\} = b_{AC_0B} \cap K$. The set D_{in} is non-empty and contains at least this point T. The proof for the set D_{in}^- can be done in a similar way.

Now, we indicate how to get the expression of the set D_{in}^+. Let us construct the curve $\Gamma(X) = \tau(A, B, X, \boldsymbol{\ell_X})$, where $X \in \{X \in K \cap \rho_+ \colon A\boldsymbol{Q_K}X^\top < 0 \wedge B\boldsymbol{Q_K}X^\top < 0\} = \overset{\frown}{T_1T_2}$ and $\boldsymbol{\ell_X}$ is the direction vector of the tangent line ℓ_X to the conic section K at the point X. The curve Γ is connected, because the continuous map τ maps the connected arc $\overset{\frown}{T_1T_2}$ onto one connected curve. Let $s\colon (0,1) \to \overset{\frown}{T_1T_2}$ be any regular parameterization of the arc $\overset{\frown}{T_1T_2}$ such that for $t \to 0$ be $s(t) \to T_1$ and for $t \to 1$ be $s(t) \to T_2$. The parameterization s also parametrizes the curve Γ via its preimage. If $t \to 0, s(t) \to T_1$, then $\Gamma(X) \to \ell_1^\infty$ and if $t \to 1, s(t) \to T_2$, then $\Gamma(X) \to \ell_2^\infty$, where ℓ_1, ℓ_2 are the tangents lines to K at the points T_1, T_2. It is important, that Bézier curves $b_{A\ell_1^\infty B}$ and $b_{A\ell_2^\infty B}$ have no transversal intersection with K (they are pairs of half-lines parallel with ℓ_1, ℓ_2). Then, we study a self-intersections of the curve $\Gamma(X)$. It can be proved the curve Γ has at most one self-intersection.

If Γ has one self-intersection $C_u = \Gamma(U_1)$, there exists another point $U_2 \in \overset{\frown}{T_1T_2}$ such that $C_u = \Gamma(U_2)$ and the Bézier curve b_{AC_uB} has double contact with K (see fig. 3.6(b)). Let the parameters for U_1, resp. U_2 be $s_1 < s_2$. Now, we prove the existence of two special Bézier curves lying in $\overline{\rho}_{AB}^+$ – the curve $b_{AC_{2T}B}$ having two transversal intersections with K and the curve $b_{AC_{4T}B}$ having four transversal

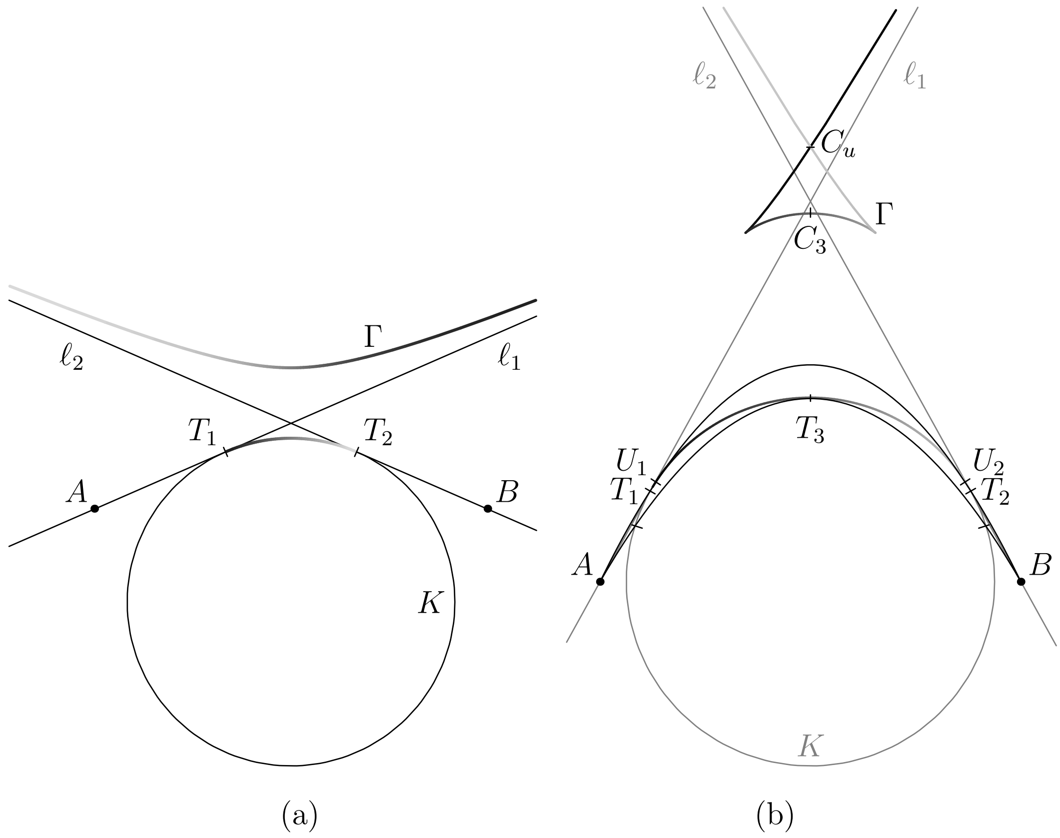

Figure 3.6: (a) The curve Γ has no self-intersection, so the set $D_{in} = \{\widehat{T_1 T_2}\}$.
(b) The curve Γ has one self-intersection, so there exists Bézier curve b_{AC_uB}, which has *double contact* with conic section K. Hence, the set $D_{in} = \{\widehat{T_1U_1} \cup \widehat{U_2T_2} \cup \{U_1, U_2\}\}$.

intersections with K. If $AB \cap K = \{X_1, X_2\}$, suitable middle control point of $b_{AC_{2T}B}$ is $C_{2T} = \frac{1}{2}A + \frac{1}{2}B$. If $AB \cap K = \{T\}$, there exists neighborhood $O(T)$ that suitable $C_{2T} \in O(T) \cap \overline{\rho}^{\,+}_{AB}$. If $AB \cap K = \emptyset$, then the set $D_{out} \neq \emptyset$. Let the point $T \in D_{out}$, then there exists neighborhood $O(C)$ of the point $C = \tau(A, B, T, \boldsymbol{\ell_T})$ that suitable $C_{2T} \in O(C)$. Finally, there exists neighborhood $O(C_u)$ that suitable $C_{4T} \in O(C_u)$.

We construct the set of Bézier curves $L(k) = (1-k)b_{AC_{2T}B} + kb_{AC_{4T}B}$, where $k \in [0, 1]$. According to the Hurwitz theorem (Th.(1,5) in [Mar66]), there exists

the point $C_3 \in \overline{\rho_+}$ that Bézier curve b_{AC_3B} has two transversal intersections and one common point of contact T_3 with the conic section K (see fig. 3.6(b)). According to the conditions on tangent line in the lemma 3.1(a), if $AB \cap K = \{X_1, X_2\}$ then the point $T_3 \in \overset{\frown}{T_1T_2}$. On the other hand, if $AB \cap K \neq \{X_1, X_2\}$ then $T_3 \in \overset{\frown}{T_1T_2}$ or $T_3 \in D_{out}$. But $T_3 \in D_{out}$ is a contradiction to the fact b_{AC_3B} has two transversal intersections with K. So, the point $T_3 \in \overset{\frown}{T_1T_2}$ in both cases and then $C_3 \in \Gamma$ for some parameter s_3. It holds $s_1 < s_3 < s_2$, because for $s \in (0, s_1] \cup [s_2, 1)$ the corresponding Bézier curves have not transversal intersections with K. Hence, the points of the arc $\overset{\frown}{U_1U_2}$ generate the Bézier curves with transversal intersections with K, because there is not other self-intersection of Γ except C_u.
We can divide the arc $\overset{\frown}{T_1T_2}$ into three arcs. For the points $T \in \overset{\frown}{T_1U_1} \cup \{U_1\}$ and $T \in \overset{\frown}{U_2T_2} \cup \{U_2\}$, the corresponding Bézier curves $b_{A\Gamma(T)B}$ have either only one common point with K, the point of contact T, or two points of contact with K, the points U_1, U_2. For the points $T \in \overset{\frown}{U_1U_2}$, the corresponding Bézier curves $b_{A\Gamma(T)B}$ have two transversal intersections with K except the common point of contact T. Hence, the set has form $D^+_{in} = \{X \in K \cap \rho_+ \colon A\boldsymbol{Q_K}X^\top < 0 \wedge B\boldsymbol{Q_K}X^\top < 0\} \setminus \{\overset{\frown}{U_1U_2}\}$. Note, that $U_1, U_2 \in D^+_{in}$.

Now, we prove that the curve Γ has at most one self-intersection. Let there exist another point $C_v \in \overline{\rho}^+_{AB}$ except C_u such that the Bézier curve b_{AC_vB} has double contact with K. The curve b_{AC_uB} divides the half-plane $\overline{\rho}^+_{AB}$ on two separating regions W_1, W_2. Let the region W_1 be enclosed and bounded by the curve b_{AC_uB} and the segment AB. Locally in the neighborhood of the point A (resp. B), the intersection of the curve b_{AC_vB} and W_1 must be an empty set, because b_{AC_vB} and K have not transversal intersection. But if the curve b_{AC_vB} lies in the neighborhood of the point A (resp. B) in the region W_2, then the whole curve lies in the region W_2 and it does not have common points with K. Hence, it is a contradiction to the assumption the Bézier curve b_{AC_vB} has a double contact with K.

If Γ does not have a self-intersection, for all the points $X \in \widehat{T_1T_2}$, the corresponding Bézier curves $b_{A\Gamma(X)B}$ have only one common point with K, the point of contact X (see fig. 3.6(a)). If there exists the point $X \in \widehat{T_1T_2}$ such that the corresponding Bézier curve $b_{A\Gamma(X)B}$ has a transversal intersection with K except the common point of contact X, there also exists the point $Y \in \widehat{T_1T_2}$ such that the corresponding Bézier curve $b_{A\Gamma(Y)B}$ has another common point of contact with the conic section K except the point Y. However, it is a contradiction to the assumption the curve Γ has no self-intersection. Hence, the set has the form $D^+_{in} = \{X \in K \cap \rho_+ \colon A\boldsymbol{Q_K}X^\top < 0 \wedge B\boldsymbol{Q_K}X^\top < 0\}$. $\square$

If $D_{in} = \{\widehat{T_1U_1} \cup \widehat{U_2T_2} \cup \{U_1, U_2\}\}$ consists of two half open arcs, the images of these arcs under the map Γ are interconnected at the point C_u (see fig. 3.8).

3.3 Set of admissible points of contact

As we said, the set of all points of order 2 contact $D = D_{ext} \cup D_{in}$. The following theorem describes the set D for various regular types of the conic section K.

Theorem 3.3 (Set of points of contact)**.**

1. Let K be an ellipse. Then, the set of the points of contact D is either one arc of the exterior points of contact or one arc of exterior and one arc of interior points of contact or one or two arcs of interior points of contact.

2. Let K be a parabola. Then, the set of the points of contact D is either one arc of the exterior points of contact or one arc of interior points of contact.

3. Let K be a hyperbola. Then, the set of the points of contact D is either two arcs of the exterior points of contact or one arc of exterior and one arc of interior points of contact.

The set of interior points of contact may have a pair of half open arcs. The set of exterior points of contact may contains only one point T, when segment $AB \cap K = \{T\}$.

Proof. a) (Ellipse) Let $AB \cap K = \emptyset$. Then among all tangents passing through A or B to K, there are two in the set $T_{sep}(AB, K)$. They determine one arc D_{ext}. The other two tangents are not in the set $T_{sep}(AB, K)$. If they converge, there is also one arc D_{in}. If they diverge, then $D_{in} = \emptyset$. If $AB \cap K = \{T\}$, the only difference is that the separating pair of tangent lines becomes one line $\overleftrightarrow{AB}$ and $D_{ext} = \{T\}$.
Let $AB \cap K = \{X_1, X_2\}$. Then, we consider two pairs of tangent lines ℓ_1^+, ℓ_2^+ and ℓ_1^-, ℓ_2^-. One pair, without loss of generality the pair ℓ_1^+, ℓ_2^+, always converge so $D_{in}^+ \neq \emptyset$. The pair ℓ_1^-, ℓ_2^- may converge or diverge, so we can obtain D as one or two arcs of D_{in}.

b) (Parabola) Let $AB \cap K = \emptyset$. Then among all tangents passing through A or B to K, there are two in the set $T_{sep}(AB, K)$. They determine one arc D_{ext}. The other two tangents are not in the set $T_{sep}(AB, K)$, but they always diverge so $D_{in} = \emptyset$. Hence, we obtain D as one arc D_{ext} (see fig. 3.7(a)). If $AB \cap K = \{T\}$, then $D = D_{ext} = \{T\}$.
Let $AB \cap K = \{X_1, X_2\}$. Without loss of generality, the pair ℓ_1^+, ℓ_2^+ always converge so $D_{in}^+ \neq \emptyset$ and the pair ℓ_1^-, ℓ_2^- always diverge so $D_{in}^- = \emptyset$. Hence, we obtain D as one arc D_{in} (see fig. 3.7(b)).

c) (Hyperbola) Each component K_1, K_2 of a hyperbola K separately behaves similarly to the parabola case. There are two cases of configuration AB and K_1, K_2. The first, $AB \cap K_1 = \emptyset$ and also $AB \cap K_2 = \emptyset$. Then, we obtain D as two arcs of D_{ext}. If $AB \cap K_1 = \{T\}$, the only difference is that $D_{ext}^1 = \{T\}$ (similarly for K_2 if $AB \cap K_2 = \{T\}$).
The second case, $AB \cap K_1 = \emptyset$ and $AB \cap K_2 = \{X_1, X_2\}$. Then, we obtain

	$\{V_Q\}$		p		$p \cup r$	
	D_{ext}	D_{in}	D_{ext}	D_{in}	D_{ext}	D_{in}
$AB \cap K = \emptyset \wedge \overleftrightarrow{AB} \cap K \neq \{T\}$	$\{V_Q\}$	$\emptyset$	p	$\emptyset$	$\overrightarrow{S_pP} \cup \overrightarrow{S_rR}$	$\emptyset$
$AB \cap K = \emptyset \wedge \overleftrightarrow{AB} \cap K = \{T\}$	$\{V_Q\}$	$\emptyset$	–	–	–	–
$AB \cap K = \{X_1, X_2\}$	–	–	–	–	–	–
$AB \cap K = \{T_0\}$	$\{V_Q\}$	$\emptyset$	–	–	–	–
$A = B$	$\{V_Q\}$	$\emptyset$	p	$\emptyset$	$\overrightarrow{V_QP} \cup \overrightarrow{V_QR}$	$\emptyset$

Table 3.1: The set D for singular types of conic section K.

D as one arc of $D_{ext} \subset K_1$ and one arc of $D_{in} \subset K_2$. There are no other configurations. □

Now, let K be a singular conic section. In the case of $K = \{V_Q\}$ (see fig. 3.1(b)), where V_Q is the top of the isotropic cone Q, we have $D = \{V_Q\}$ (see fig. 3.9(a)).
If $K = p$, where p is an isotropic double line (see fig. 3.1(c)), we must distinguish two cases. If A, B lie in the opposite half-planes generated by the line p, we have $D = \emptyset$. If A, B lie in the same half-plane, the set of points of contact $D = p$.
The last singular case is $K = p \cup r$, where p, r are a pair of distinct isotropic lines (see fig. 3.1(d)). Then, there are two regions of points lying out of K in the plane ρ. If A, B lie in the different regions, there is no collision-free Bézier curve b_{ACB}. Let A, B lie in the same region, which is determined by two half-lines $\overrightarrow{V_QP} \subset p$ and $\overrightarrow{V_QR} \subset r$ (see fig. 3.9(b)). Let $S_p \in p$ and $S_r \in r$ are the points of contact of the Bézier curve b_{AC_uB}, i.e. $b_{AC_uB} \cap K = \{S_p, S_r\}$ is double contact. Then, $D = \overrightarrow{S_pP} \cup \overrightarrow{S_rR}$. The special case is $S_p = S_r = V_Q$.

In the tables 3.1 and 3.2, we see the structure of the set D for various types of conic sections. The numbers in the table 3.2 represent the number of maximum connected arcs in the set D.

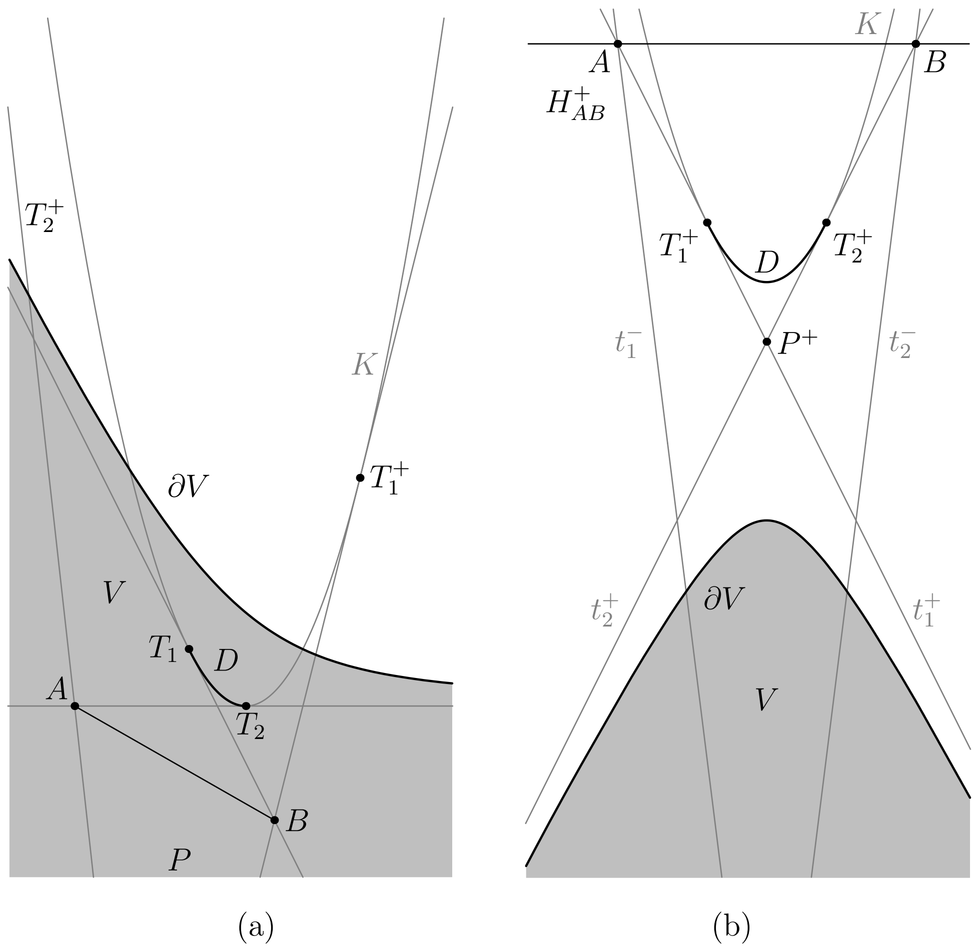

Figure 3.7: (a) Because $AB \cap K = \emptyset$, the set of exterior points of contact $D_{ext} = \widehat{T_1 T_2}$ is determined by the pair of tangent lines $t_1, t_2 \in T_{sep}(AB, K)$. The pair of non separating tangent lines t_1^+, t_2^+ diverge (the points T_1^+, T_2^+ and the point P lying in the opposite half-planes due to the line $\overleftrightarrow{AB}$). Therefore, the set of interior points of contact $D_{in} = \emptyset$. The set of points of contact $D = D_{ext}$ generates the boundary of admissible solutions $\partial V_\rho(A, B)$. The set of admissible solutions $V_\rho(A, B)$ consists of one region. (b) If $AB \cap K = \{X_1, X_2\}$, one pair of non separating tangent lines always diverge and the rest pair always converge. Without loss of generality, the set of points of contact $D = D_{in}^+ = \widehat{T_1^+ T_2^+}$. The set of admissible solutions $V_\rho(A, B)$ consists of one region.

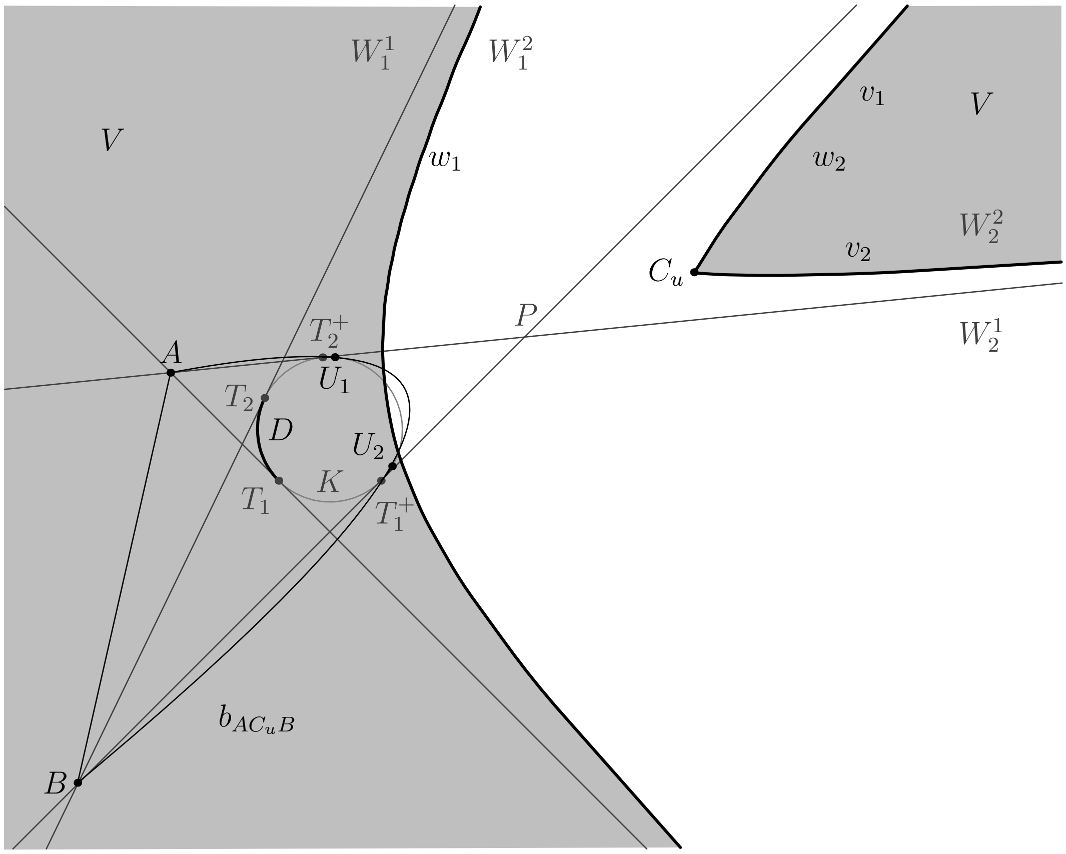

Figure 3.8: The set $D_{ext} = \{X \in K \colon A\boldsymbol{Q_K}X^\top > 0 \wedge B\boldsymbol{Q_K}X^\top > 0\} = \overset{\frown}{T_1T_2}$. The set $D_{in} \neq \emptyset$, because the point P lies in the same half-plane generated by $\overleftrightarrow{AB}$ as the points T_1^+, T_2^+. The set $D_{in} = \{X \in K \colon A\boldsymbol{Q_K}X^\top < 0 \wedge B\boldsymbol{Q_K}X^\top < 0\} \setminus \{\overset{\frown}{U_1U_2}\}$ consists of two half open arcs $\overset{\frown}{T_2^+U_1} \cup \overset{\frown}{U_2T_1^+} \cup \{U_1, U_2\}$. The split of the arc $\overset{\frown}{T_1^+T_2^+}$ is caused by the existence of the curve b_{AC_uB}, which has double contact with the conic section K. As one can see, $b_{AC_uB} \cap K = \{U_1, U_2\}$. Therefore, the set of points of contact $D = D_{ext} \cup D_{in}$ generates the curves w_1, $w_2 = v_1 \cup v_2$ such that $w_1 \cup w_2 = \partial V_\rho(A, B)$. Because the curve w_1 is generated by the exterior points of contact, the region W_1^1 containing the points A, B is subset $W_1^1 \subset V_\rho(A, B)$. The curve w_2 is generated by the interior points of contact. It bounds region W_2^2 not containing the points A, B and $W_2^2 \subset V_\rho(A, B)$ according to theorem 3.6. The set of admissible solutions $V_\rho(A, B) = W_1^1 \cup W_2^2$ consists of two regions.

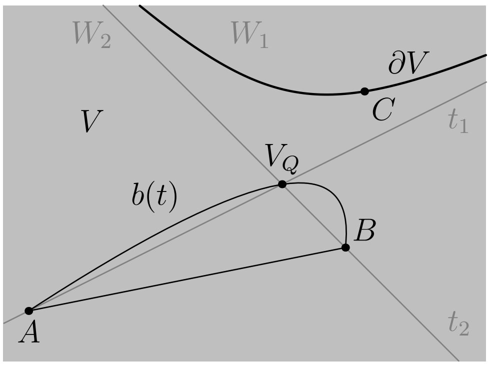

(a)

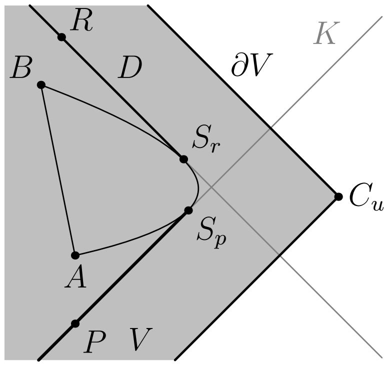

(b)

Figure 3.9: (a) Let the conic section $K = \{V_Q\}$. There is only one possible point of contact, so $D = \{V_Q\}$. The corresponding boundary of admissible solutions $\partial V_\rho(A, B)$ divides the plane ρ into two regions $W_1, W_2 \subset V_\rho(A, B)$, due to $b_{ACB} \cap K \neq \emptyset$ holds only for $C \in \partial V_\rho(A, B)$. So, the set of admissible solutions $V_\rho(A, B) = \rho \setminus \partial V_\rho(A, B)$. (b) Let the conic section $K = p \cup r$. The points A, B have to lie in the same quadrant with respect to K. Let the quadrant be determined by two half-lines $\overrightarrow{V_QP} \subset p$ and $\overrightarrow{V_QR} \subset r$. If there exists a Bézier curve b_{AC_uB} having double contact $M = \{S_p, S_r\}$ with K, the set of exterior points of contact $D_{ext} = \overrightarrow{S_pP} \cup \overrightarrow{S_rR}$. Otherwise, we get $S_p = S_r = V_Q$ and $D_{ext} = \overrightarrow{V_QP} \cup \overrightarrow{V_QR}$. The set of interior points of contact is always $D_{in} = \emptyset$. The boundaries generated by the half-lines $\overrightarrow{S_pP}, \overrightarrow{S_rR}$ are connected due to the fact that $\sigma(S_p) = \sigma(S_r) = C_u$. Hence, the set of admissible solution $V_\rho(A, B)$ consist of one region. Because the boundary is generated by the exterior points of contact, $A, B \in V_\rho(A, B)$.

	ellipse		parabola		hyperbola	
	D_{ext}	D_{in}	D_{ext}	D_{in}	D_{ext}	D_{in}
$AB \cap K = \emptyset \wedge \overleftrightarrow{AB} \cap K \neq \{T\}$	1	$\emptyset$,1	1	$\emptyset$	2	$\emptyset$
$AB \cap K = \emptyset \wedge \overleftrightarrow{AB} \cap K = \{T\}$	1	$\emptyset$	1	$\emptyset$	2	$\emptyset$
$AB \cap K = \{X_1, X_2\}$	$\emptyset$	1,2	$\emptyset$	1	1	1
$AB \cap K = \{T_0\}$	$\{T_0\}$	$\emptyset$,1	$\{T_0\}$	$\emptyset$	2	$\emptyset$
$A = B$	1	$\emptyset$	1	$\emptyset$	2	$\emptyset$

Table 3.2: The set D for regular conic sections. The numbers $1, 2$ in the table cells indicate the possible number of connected arc components in the set D. The symbol $\emptyset$ indicates that the corresponding set D might be empty. In the special cases, the set D consists of one point $\{T_0\}$.

3.4 Boundary map

For the given points A, B, $X \in D \setminus D_{AB} \subseteq K$ (see note 1 for the definition of D_{AB}) and the tangent line ℓ_X at X to K, the Bézier curve b_{ACB} touching the conic section K is clearly identified. In order to find the middle control vertex C, we use the following map σ. This map is very similar to the map τ from the section 1, only the direction vector of the line ℓ_X is expressed by the coefficients of the conic section K.

Definition 3.6 (Boundary map)**.** Let D be the set of points of contact for the given points A, B and K. The map $\sigma\colon D \setminus D_{AB} \to \rho$ is called *boundary map* if for every $X \in D \setminus D_{AB}$ the equality $\sigma(X) = C$ holds, for C from the definition 3.3 (see fig. 3.10).

Note 2. It is not possible to define the map σ on the points in D_{AB}. If $T_1 \in D_{AB} \subset K$ then the points A, B, T_1 are collinear on the tangent line t_1 to K.

Hence, there is an infinite number of points C such that the Bézier curve b_{ACB} touches K in T_1. All suitable C form a half-line, therefore we are interested in the end point of the half-line, the point C_1 (see fig. 3.11).

Theorem 3.4. Let the conic section $K \neq \{V_Q\}$ and $X \in D \setminus D_{AB}$. Then, the corresponding boundary map $\sigma\colon D \setminus D_{AB} \to \rho$ has the form

$$\sigma(X) = \frac{b(t_0) - B_0^2(t_0)A - B_2^2(t_0)B}{B_1^2(t_0)}, \tag{3.3}$$

where $t_0 \in [0, 1]$ is a solution of the equation

$$0 = \alpha t^2 + 2\beta t + \gamma \tag{3.4}$$

and for $A = [a_x, a_y, 1],\ B = [b_x, b_y, 1],\ X = [x_0, y_0, 1]$ are

$$\begin{aligned} \alpha &= (A - B)\boldsymbol{Q_K}X^\top, \\ \beta &= -A\boldsymbol{Q_K}X^\top, \\ \gamma &= -\beta. \end{aligned}$$

Proof. Since the point of contact $X \in b_{ACB}(t)$, there exists $t_0 \in [0, 1]$ such that $X = b_{ACB}(t_0) = B_0^2(t_0)A + B_1^2(t_0)C + B_2^2(t_0)B$. For the point $X \in K$, the equality $X\boldsymbol{Q_K}X^\top = 0$ holds, so $X \notin \{A, B\}$ and $t_0 \notin \{0, 1\}$. Because $X = [x_0, y_0] \in D \setminus D_{AB}$, the equality $\left\langle \nabla f(x_0, y_0), \frac{d}{dt} b_{ACB}(t_0) \right\rangle = 0$ holds. The equation (3.4) has a real solution, if the discriminant $\Delta = (A\boldsymbol{Q_K}X^\top)(B\boldsymbol{Q_K}X^\top) \geq 0$. It is satisfied due to $X \in D_{ext}$ provides that both brackets are positive. On the other hand, if $X \in D_{in}$ then both brackets are negative and their product is positive. From this quadratic equation, we obtain two roots t_1, t_2. The question is, whether they are both within $\langle 0, 1\rangle$. We use the theorem 1.1. The table 3.3 shows the values of the sequences $\{f(t), f'(t), f''(t)\}$ in the end points of the interval $\langle 0, 1\rangle$ for $f(t) = \alpha t^2 + 2\beta t + \gamma$. From the previous, the expressions $A\boldsymbol{Q_K}X^\top$ and $B\boldsymbol{Q_K}X^\top$ have the same sign. Hence, the table 3.4 shows the number of sign changes of the

	$t=0$	$t=1$
$f(t)$	$A\boldsymbol{Q_K}X^\top$	$-B\boldsymbol{Q_K}X^\top$
$f'(t)$	$-2A\boldsymbol{Q_K}X^\top$	$-B\boldsymbol{Q_K}X^\top$
$f''(t)$	$2(A-B)\boldsymbol{Q_K}X^\top$	

Table 3.3: The values of derivatives of the function $f(t) = \alpha t^2 + 2\beta t + \gamma$ at the end points of the interval $\langle 0, 1\rangle$.

	$A\boldsymbol{Q_K}X^\top > 0 \wedge B\boldsymbol{Q_K}X^\top > 0$		$A\boldsymbol{Q_K}X^\top < 0 \wedge B\boldsymbol{Q_K}X^\top < 0$	
	$t=0$	$t=1$	$t=0$	$t=1$
$f(t)$	$+$	$-$	$-$	$+$
$f'(t)$	$-$	$-$	$+$	$+$
$f''(t)$	$+$ $-$	$+$ $-$	$+$ $-$	$+$ $-$
# of sign changes	2 1	1 0	1 2	0 1

Table 3.4: Looking at the numbers of sign changes, the differences $2-1$ and $1-0$ are all equal to 1. So, the function $f(t)$ has one real solution within the interval $\langle 0, 1\rangle$.

sequences $\{f(t), f'(t), f''(t)\}$ with respect to the signs of $A\boldsymbol{Q_K}X^\top$ and $B\boldsymbol{Q_K}X^\top$. According to theorem 1.1 applied to the function $f(t)$, only one root is in $\langle 0, 1\rangle$. If both $t_1, t_2 \in (0, 1)$ and $t_1 \neq t_2$, then $X \in D_{AB}$. Let $t_1 \in (0, 1)$. Then, we substitute $t_0 = t_1$ into the Bézier curve equation and obtain the relevant point C from the definition 3.3 for the point of contact X. Hence, $C = \sigma(X)$. □

The only difference between the lemma 3.1 and the theorem 3.4 is that the tangent line ℓ_T is arbitrary in the lemma, but $\ell_T \in T_K$ and the vector $\boldsymbol{n_\ell} = \nabla K$ in the theorem.

Lemma 3.3. For each $X \in D \setminus D_{AB}$, there exists exactly one point C such that the Bézier curve $b_{ACB}(t) \cap K = \{X\}$.

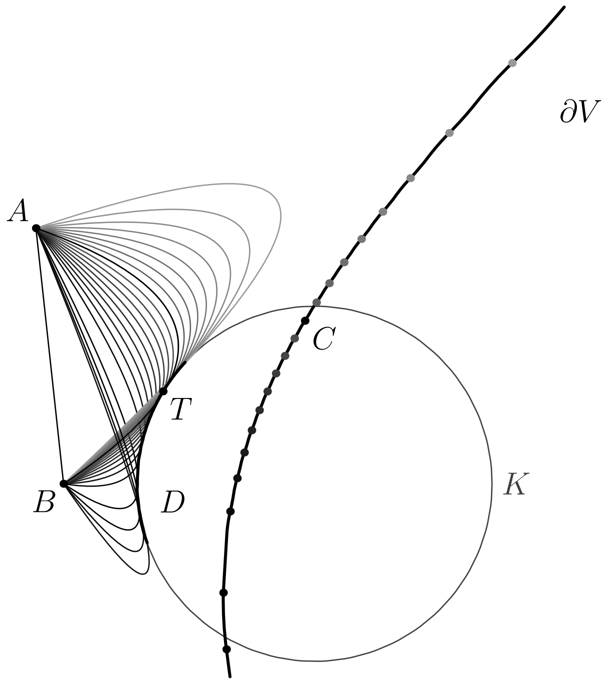

Figure 3.10: The boundary map σ maps the points of the arc D to the points on ∂V, see that $\sigma(T) = C$.

Proof. Let $\ell_X \in T_K$ touches the conic section in the point $X \in K$. We know the Bézier curve b_{ACB} has the points A, B as the end points, it contains the point X and it has the tangent line ℓ_X at X. Using the lemma 3.1, the quadratic b_{ACB} is uniquely determined up to the case $A, B, X \in \ell_X$, when they are collinear. However, $X \in D_{AB}$ in this case. □

Lemma 3.4. The boundary map σ is injective for the set $D \setminus \{D_{AB}, U_1, U_2\}$.

Proof. Let $X_1, X_2 \in D \setminus \{D_{AB}, U_1, U_2\} \subset K$, $X_1 \neq X_2$ and $\sigma(X_1) = \sigma(X_2) = C$. Then, there exists a double contact Bézier curve b_{ACB} such that X_1, X_2 are the points of contact. Then, $\{X_1, X_2\} = \{U_1, U_2\}$, which is a contradiction. □

Note 3. Let the two half open arcs $\{\overset{\frown}{T_1U_1} \cup \overset{\frown}{U_2T_2} \cup \{U_1, U_2\}\} \subset D_{in}$. The image $\sigma(\overset{\frown}{T_1U_1} \cup \{U_1\})$ is a connected curve v_1, because the boundary map σ is a continuous map. Also, the image $\sigma(\overset{\frown}{U_2T_2} \cup \{U_2\})$ is a connected curve v_2. There exists a point C_u such that the intersection $b_{AC_uB} \cap K = \{U_1, U_2\}$, hence, $C_u \in v_1$ and $C_u \in v_2$. Simultaneously, the points U_1, U_2 are the end points of the continuous arcs $\overset{\frown}{T_1U_1}$ and $\overset{\frown}{U_2T_2}$. Hence, the image of the two half open arcs under the boundary map σ is the connected curve $w_2 = v_1 \cup v_2$ (see fig. 3.8).

Now, we can find the corresponding point C for the points of contact from the set $D \setminus D_{AB}$. The question is, how can we find the point C corresponding to a given point of contact $T \in D_{AB} \subset D$.

Lemma 3.5. Let the points A, B and $T \in D_{AB} \subset K$ be collinear.
(a) Let $AB \cap K = \{T\}$. The Bézier curve $b_{ACB} \cap K = \{T\}$ iff $C \in \overleftrightarrow{AB}$.
(b) Let $AB \cap K = \emptyset$. The Bézier curve $b_{ACB} \cap K = \{T\}$ if and only if $C \in \overrightarrow{C_SX} \subset \overleftrightarrow{AB}$, where $A, B \notin \overrightarrow{C_SX}$ and C_S is such that the derivative $\frac{d}{dt} b_{AC_SB}(t_0) = 0$ for $T = b_{AC_SB}(t_0)$. For the special case $A = B$, the point $C_S = A + 2(T - A)$.

Proof. See the proof of the lemma 3.1, cases (d), (e). □

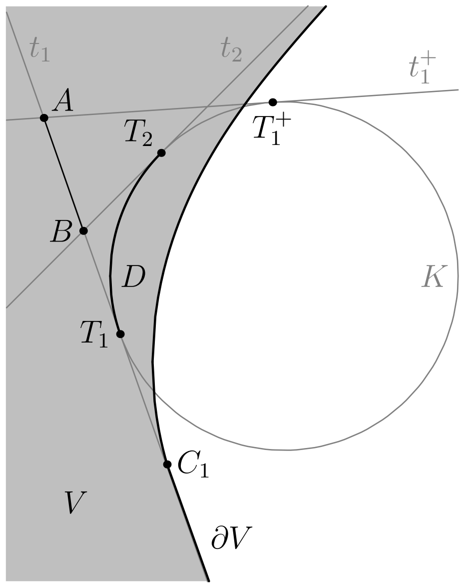

Figure 3.11: The points A, B, T_1 are collinear on the tangent line t_1 to K. The point $C_1 \in t_1$ determines the Bézier curve $b_{ACB}(t)$, which is equivalent to the segment AT_1. There is an infinite number of points C such that the Bézier curve b_{ACB} touches K in T_1. It causes that part of the boundary ∂V is the half-line from the point C_1.

Note 4. In the equation (3.3) of the boundary map σ, the inequality $B_1^2(t_0) > 0$ holds for $t_0 \in (0, 1)$, so the map σ is continuous. The σ maps the connected set $D_{ext} \setminus D_{AB}$ onto one connected curve w. If the point $T \in D_{AB} \neq \emptyset$, then $\lim_{X \to T} \sigma(X) = C_S$ and the union $w \cup \overrightarrow{C_S X}$ is a connected curve (see fig. 3.11).

3.5 Set of admissible solutions

Theorem 3.5 (Boundary of the set $V_\rho(A, B)$)**.** The set of all such points C that Bézier curve $b_{ACB} \cap K \subset D$ yields, is the boundary of the set of admissible solutions $V_\rho(A, B)$. We denote it $\partial V_\rho(A, B)$.

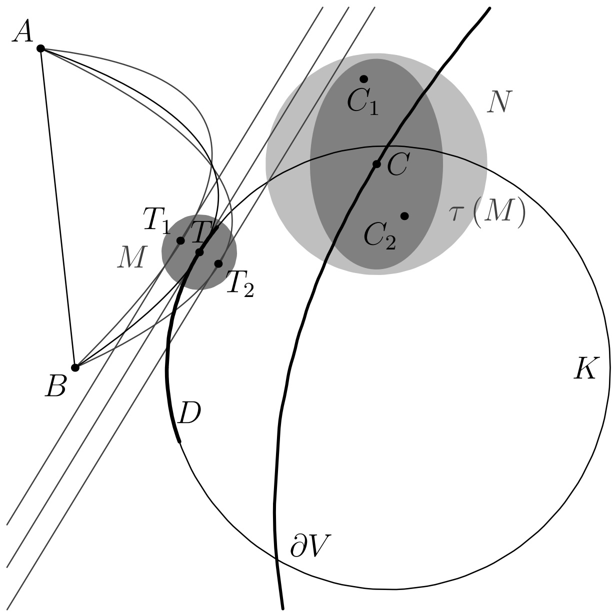

Figure 3.12: Let C be such that $b_{ACB} \cap K \subset D$ and $T \in b_{ACB} \cap K$. For arbitrary neighborhood N of the point C, there exists a neighborhood M of the point T such that for $T_1, T_2 \in M$ the corresponding $C_1 = \tau(T_1), C_2 = \tau(T_2) \in N$. Moreover, $b_{AC_1B} \cap K = \emptyset$ and $b_{AC_2B} \cap K = \{X_1, X_2\}$ with transversal intersection. Hence, $C \in \partial V_\rho(A, B)$.

Proof. The point C belongs to the boundary of the set $V_\rho(A, B)$, if each neighborhood N of the point C contains both the point $C_1 \in V_\rho(A, B)$ and the point $C_2 \in \rho \setminus V_\rho(A, B)$. So, we prove the existence of points $C_1, C_2 \in N$ such that $b_{AC_1B} \cap K = \emptyset$ and $b_{AC_2B} \cap K = \{X_1, X_2\}$ with transversal intersection (see fig. 3.12).

Let $A, B, \boldsymbol{u}$ be given as in the lemma 3.1. Let C be such that $b_{ACB} \cap K \subset D$ and $T \in b_{ACB} \cap K$. Let the line ℓ_T with the direction vector $\boldsymbol{u}$ is the tangent line to K in T. Since $B_1^2(t_0) > 0$ for $t_0 \in (0, 1)$, the map τ assigning to each point T its corresponding point C is continuous. It means, there exists a neighborhood M of the point T for each neighborhood N of the point C such that $\tau(M) \subset N$. For an arbitrary neighborhood N of the point C, the neighborhood M of the point

T exists such that $\tau(M) \subset N$. Let $T_1 = T + k\nabla f(T)$ and $T_2 = T - k\nabla f(T)$, where $k > 0$ is such that $T_1, T_2 \in M$ and they satisfy the conditions of the lemma 3.1. Let the lines ℓ_1, ℓ_2 be parallel to the line ℓ_T (i.e. the vector $\boldsymbol{u}$ is their direction vector) and $T_1 \in \ell_1, T_2 \in \ell_2$. Then, the points $C_1 = \tau(A, B, T_1, \boldsymbol{u})$ and $C_2 = \tau(A, B, T_2, \boldsymbol{u})$ are $C_1, C_2 \in N$. We obtain the Bézier curves b_{AC_1B}, b_{AC_2B}. Since each tangent line ℓ_1, ℓ_2 defines the supporting half-plane to the convex quadratic Bézier curve and the points A, B lie out of K, it holds $b_{AC_1B} \cap K = \emptyset$ and $b_{AC_2B} \cap K = \{X_1, X_2\}$ with transversal intersection. $\square$

We say that the boundary of the set of admissible solutions $\partial V_\rho(A, B)$ *is generated* by the set D mapped by the boundary map σ.

Lemma 3.6. If the conic section $K = p$, then the boundary of the set of admissible solutions ∂V is the parallel line with the line p.

Proof. Without loss of generality, let us consider the conic section K represented by

$$\boldsymbol{Q_K} = \begin{pmatrix} 0 & 0 & -\frac{1}{2} \\ 0 & 0 & \frac{1}{2} \\ -\frac{1}{2} & \frac{1}{2} & 0 \end{pmatrix}.$$

The set of points of contact $D = p$ (see the table 3.1). We compute the coefficients α, β, γ from the theorem 3.4, which are

$$\alpha = -a_x + a_y + b_x + b_y,$$
$$\beta = -2x_0 + 2y_0 + 2a_x - 2a_y,$$
$$\gamma = x_0 - y_0 - a_x + a_y,$$

in order to find the corresponding point C to the point of contact $[x_0, y_0] \in D$. Since $[x_0, y_0] \in p$, $x_0 = y_0$ holds and the coefficient α, β, γ depend on the points A, B. So the parameter t_0 does not depend on the point $[x_0, y_0]$ and it is the same for all points of contact from D. Let $T_0 \in D$ be arbitrary fixed point of contact and let C_0 be the corresponding middle control point. Let $T \in D$ be arbitrary point of contact different from T_0. We express $T = T_0 + u\boldsymbol{s_p}$, where $0 \neq u \in \mathbb{R}$ and $\boldsymbol{s_p}$ is direction vector of the line p. The corresponding point C is obtained from formula (3.1) and $B_1^2(t_0) > 0$ by the theorem 3.4. If we substitute T by $T_0 + u\boldsymbol{s_p}$ and T_0 by $B_0^2(t_0)A + B_1^2(t_0)C_0 + B_2^2(t_0)B$, we obtain $C = C_0 + \frac{u}{B_1^2(t_0)}\boldsymbol{s_p}$. Hence, the boundary of the set of admissible solutions ∂V is the line with the same direction vector as the line p. □

Note 5. Let $K = p \cup r$. According to the table 3.1, the set of points of contact $D = \overrightarrow{S_pP} \cup \overrightarrow{S_rR}$ (in special case $S_p = S_r = V_Q$). From the previous lemma, the set ∂V consists from two half-lines parallel with p, resp. r, connected in the point C_u (see fig. 3.9(b)).

Lemma 3.7. The boundary of admissible solutions $\partial V_\rho(A, B)$ consists of one or two continuous unbounded curves with degree at most four.

Proof. The set D contains one or two arcs of the type D_{ext} or D_{in}. Due to the notes 3, 4, the boundary of admissible solutions consists of one or two continuous curves. They are unbounded, because the arcs in D are either unbounded or the point $T \in D_{AB}$ generates the half-line. The degree of the curves is determined by the formula (3.3) of the map σ. □

The curve $w \subset \partial V_\rho(A, B)$ divides the plane ρ into two regions W_1, W_2 and one of them is the component of set of acceptable solution $V_\rho(A, B)$. The following theorem says which one.

Theorem 3.6 (Set of admissible solutions)**.**

(a) Let K be a connected component of the regular conic section. Let $w \subset \partial V_\rho(A, B)$ be a connected curve, which divides the plane into two regions W_1, W_2. If w is generated by D_{ext}, then $W_i \subseteq V_\rho(A, B)$ when $A, B \in W_i$. If

	$\{V_Q\}$	p	$p \cup r$	ellipse	parabola	hyperbola
$AB \cap K = \emptyset \wedge$ $\overleftrightarrow{AB} \cap K \neq \{T\}$	2	1	1	1,2	1	1
$AB \cap K = \emptyset \wedge$ $\overleftrightarrow{AB} \cap K = \{T\}$	1	–	–	1	1	1
$AB \cap K = \{X_1, X_2\}$	–	–	–	1,2	1	1
$AB \cap K = \{T_0\}$	2	–	–	1,2	1	1
$A = B$	1	1	1	1	1	1

Table 3.5: The possible number of regions in the set of acceptable solutions $V_\rho(A, B)$.

w is generated by D_{ext} and $AB \subset w$, then $W_i \subseteq V_\rho(A, B)$ when $K \notin W_i$. If w is generated by D_{in}, then $W_i \subseteq V_\rho(A, B)$ when $A, B \notin W_i$.

(b) In the case of $K = \{V_Q\}$, both $W_1, W_2 \subset V_\rho(A, B)$. If $K = p$ or $K = p \cup r$, then $W_i \subseteq V_\rho(A, B)$ when $A, B \in W_i$.

Proof. (a) The intersection $AB \cap w \neq \emptyset$ iff $AB \cap K = \{T\}$. Then, the curve w is generated by exterior points of contact. The connected component K is a convex curve and the line $\overleftrightarrow{AB}$ determine the supporting half-plane to K. Hence, $W_i \subseteq V_\rho(A, B)$ if $K \notin W_i$.

If there exists only one curve $w = \partial V_\rho(A, B)$, we decide about W_i according to the point $C = \frac{1}{2}A + \frac{1}{2}B$.

Suppose that w_1 and w_2 exist such that $w_1 \cup w_2 = \partial V_\rho(A, B)$. According to the table 3.2, the conic section K is an ellipse. If both w_1, w_2 are generated by the sets of interior points of contact, in both cases we can decide about W_i according to the point $C = \frac{1}{2}A + \frac{1}{2}B$. The segment AB lies between the curves w_1, w_2 and the set $V_\rho(A, B)$ consists of two regions. Now, let the curve w_1 be generated by the set

of exterior points of contact and the curve w_2 be generated by the set of interior points of contact (see fig. 3.8). The intersection $w_1 \cap w_2 = \emptyset$, because the Bézier curve with one exterior and one interior point of contact with K simultaneously does not exist. Let the curve w_1 divide the plane ρ into two components W_1, W_2 and $A, B \in W_1$. The curve $w_2 \subset W_2$, because for $C = \frac{1}{2}A + \frac{1}{2}B$ is $b_{ACB} \cap K = \emptyset$ and the set $W_1 \subset \partial V_\rho(A, B)$. Let the curve w_2 divide the region W_2 into two components W_3, W_4 and w_1 be the boundary between W_1, W_3. According to the theorem 3.5, the region W_3 consists of such points C that b_{ACB} and K have only transversal intersections and the region $W_4 \subset \partial V_\rho(A, B)$.
(b) For $C \in \partial V_\rho(A, B)$ only, $b_{ACB} \cap K \neq \emptyset$, so $V_\rho(A, B) = \rho \setminus \partial V_\rho(A, B)$. The other propositions are consequences of the lemma 3.6 and note 5. $\square$

In the case of hyperbola, each component generates one set of admissible solutions. Hence, we obtain the regions $V_1(A, B), V_2(A, B)$ for the K_1, K_2. For every point $C \in V_1(A, B)$, the Bézier curve $b_{ACB} \cap K_1 = \emptyset$. We are looking for the set of points C, such that $b_{ACB} \cap (K_1 \cup K_2) = \emptyset$. It holds for every point $C \in V_1(A, B) \cap V_2(A, B)$, see fig. 3.13 and 3.14.

Finally, for the two given points A, B and the conic K, the set of acceptable solutions $V_\rho(A, B)$ consists of one or two regions, see the table 3.5. It depends on the number of arcs in the set D and on the type of the conic section K.

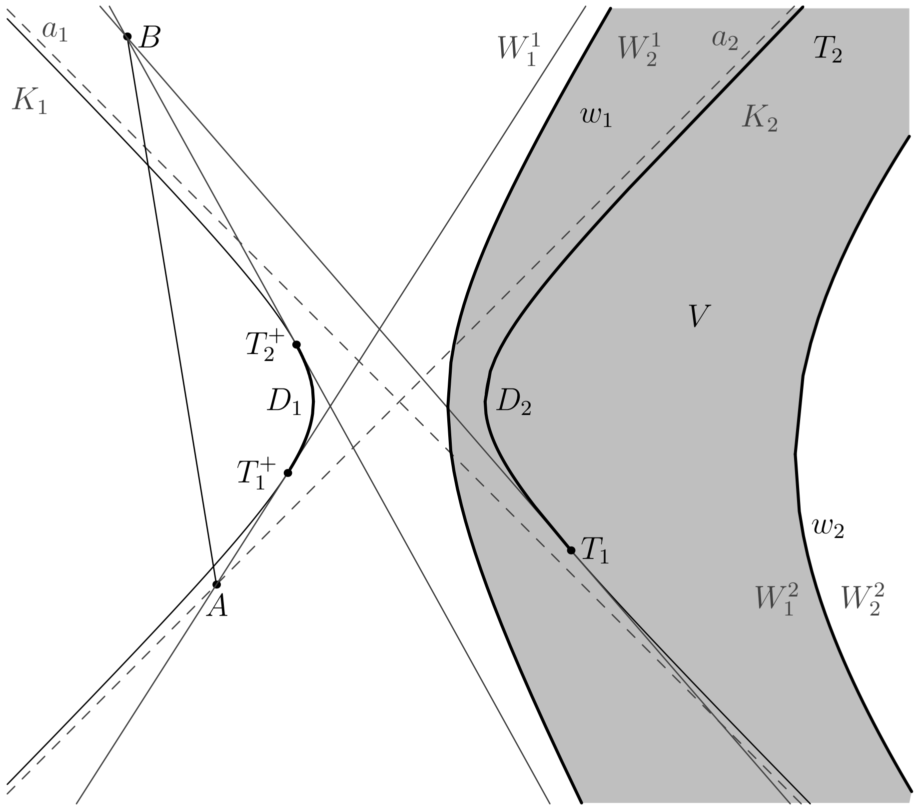

Figure 3.13: For the component K_1, the set of exterior points of contact $D^1_{ext} = \emptyset$ and the set of interior points of contact $D^1_{in} = \overset{\frown}{T_1^+ T_2^+}$. The set of points of contact $D^1 = D^1_{in}$ generates the curve $w_1 \subset \partial V_\rho(A,B)$. The curve w_1 divides the plane ρ into two regions W_1^1, W_2^1. Let the points $A, B \in W_1^1$. According to the theorem 3.6, the set of admissible solutions for the component K_1 is $V^1(A,B) = W_2^1$. For the component K_2, since $T_2 = a_2^\infty$, the set of exterior points of contact $D^2_{ext} = \overset{\frown}{T_1 a_2^\infty}$ and the set of interior points of contact $D^2_{in} = \emptyset$. The set of points of contact $D^2 = D^2_{ext}$ generates the curve $w_2 \subset \partial V_\rho(A,B)$ and if the points $A, B \in W_1^2$, then $V^2(A,B) = W_1^2$. Finally, the set of admissible solutions for the conic section K is $V_\rho(A,B) = V^1(A,B) \cap V^2(A,B)$.

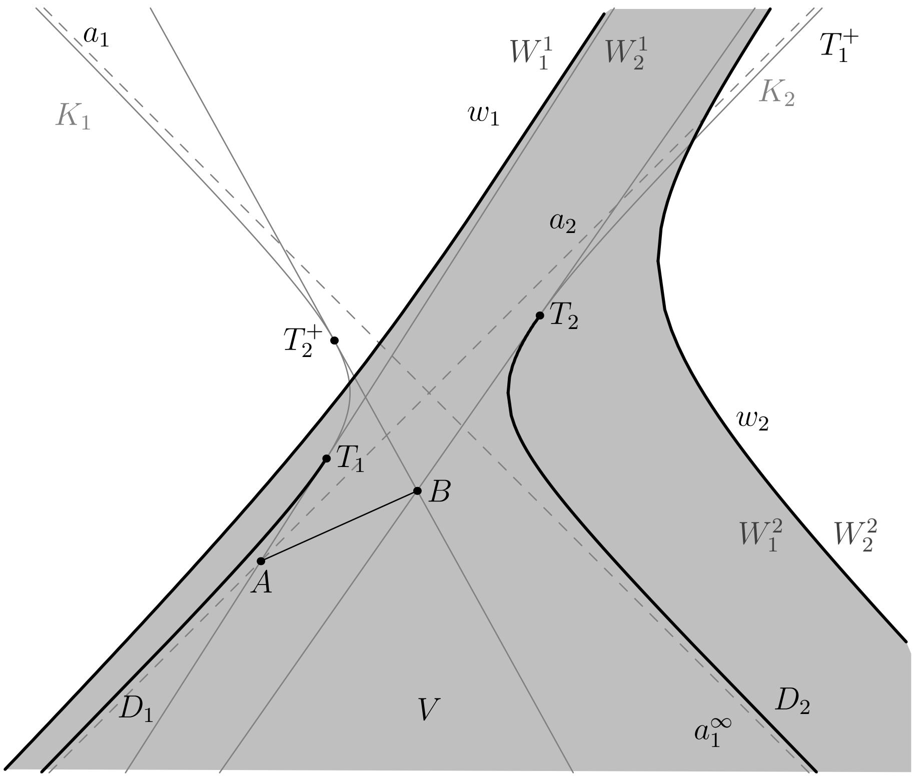

Figure 3.14: Let us analyse the component K_1. Since $T_1^+ = a_2^\infty$, the set $S(A, K_1) = \overset{\frown}{T_1 a_2^\infty}$. The set $S(B, K_1) = \overset{\frown}{a_2^\infty T_2^+}$. According to the theorem 3.1, the set $D_{ext}^1 = \overset{\frown}{T_1 a_2^\infty} \cap \overset{\frown}{a_2^\infty T_2^+}$. The set $D_{in}^1 = \emptyset$. The set of points of contact $D^1 = D_{ext}^1$ generates the curve $w_1 \subset \partial V_\rho(A, B)$. The curve w_1 divides the plane ρ into two regions W_1^1, W_2^1. Let the points $A, B \in W_2^1$. According to the theorem 3.6, the set of admissible solutions for the component K_1 is $V^1(A, B) = W_2^1$. Now, let us analyse the component K_2. The set $S(A, K_2) = \overset{\frown}{a_1^\infty T_1^+} = K_2$ and the set $S(B, K_2) = \overset{\frown}{a_1^\infty T_2}$. Hence, the set $D_{ext}^2 = \overset{\frown}{T_2 a_1^\infty}$. The set $D_{in}^2 = \emptyset$. The set of points of contact $D^2 = D_{ext}^2$ generates the curve $w_2 \subset \partial V_\rho(A, B)$ and $V^2(A, B) = W_1^2$. Finally, the set of admissible solutions for the conic section K is $V_\rho(A, B) = V^1(A, B) \cap V^2(A, B)$.

4

Collision-free piecewise quadratic spline

In applications, a frequent task is to find a path from the starting point to the ending point while passing through the given set of points avoiding obstacles. Also, there may be more than one obstacle in the scene. Let $\mathcal{P} = \{P_1, \ldots, P_n\}$ be the given set of points in $\mathbb{R}^2$. Let $\mathcal{O} = \{O_1, \ldots, O_m\}$ be the given set of obstacles represented by conic sections as their bounding objects. We search the collision-free path avoiding the set of obstacles $\mathcal{O}$ starting at the point P_1, ending at the point P_n and passing through the points $P_2, \ldots, P_{n-1}$. The achieved results allow construction of the collision-free path as piecewise quadratic spline. As we mention in the introduction, some applications may request C^1 continuity of the path because in mobile robotics a non smooth motions can cause slippage of the wheels. In this chapter, we describe how to avoid several obstacles simultaneously. Then, we show the step by step creation of C^0- and C^1-continuous spline.

4.1 Evading several obstacles simultaneously

Let the starting point P_1 and ending point P_2 be given. Let $\mathcal{O} = \{O_1, \ldots, O_m\}$ be given set of obstacles. We find the set V containing such points C, that the Bézier curve $b_{P_1CP_2}$ is a collision-free path with respect to the set of obstacles $\mathcal{O}$.

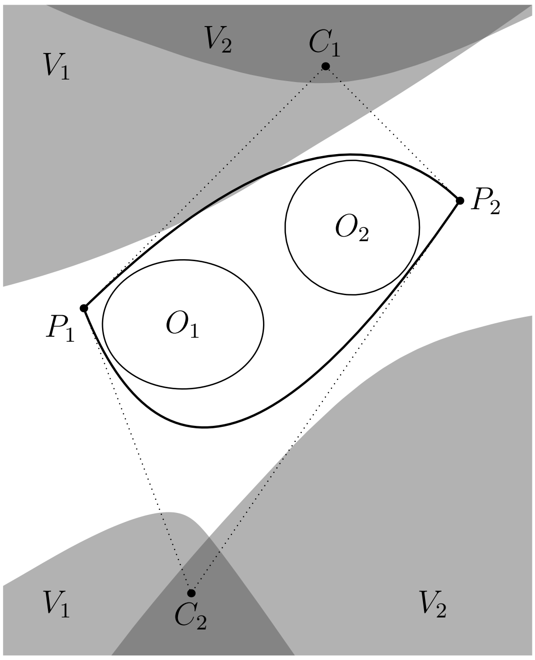

Figure 4.1: First, we find the set of admissible middle control points V_1 for the obstacle O_1. This set represents all such points C, that the Bézier curve $b_{P_1CP_2}$ is collision-free path due to the obstacle O_1. Similarly, we find the set of admissible middle control points for the obstacle O_2. If we want to avoid both obstacles simultaneously, we need middle control point $C \in V_1 \cap V_2$. In the figure, one can see the points $C_1, C_2 \in V_1 \cap V_2$ determining two collision-free paths.

Using the results in previous chapter, we find the set $V_j(P_1, P_2)$ containing the admissible points C for collision-free path with respect to one obstacle O_j. Now, we need to avoid all obstacles simultaneously. So, the point $C \in V_j(P_1, P_2)$ for all $j = 1, \dots, m$ in order to secure avoiding of each O_j. For searching the set $V = \bigcap_{j=1}^{m} V_j(P_1, P_2)$, the algorithm 1 can be used. The intersection can be computed using some of the standard algorithms for computing intersection of algebraic areas in CAD, e. g. cylindrical algebraic decomposition or vertical decomposition [BPR06, BT07].

Algorithm 1 Avoiding several objects simultaneously

function FINDV($P_1, P_2, O_1, \dots, O_m$)
    for $j = 1$ **to** m **do**
        find the set $V_j(P_1, P_2)$
        if $j = 1$ **then**
            $V \leftarrow V_1(P_1, P_2)$
        else
            $V \leftarrow V \cap V_j(P_1, P_2)$
        end if
    end for
    return V
end function

Now, we may choose an arbitrary point $C \in V$ for obtaining collision-free path $b = b_{P_1CP_2}(t)$. An example for two obstacles is shown in fig. 4.1.

4.2 Creation of C^0-continuous spline

Let $\mathcal{P} = \{P_1, \dots, P_n\}$ be the given set of points and $\mathcal{O} = \{O_1, \dots, O_m\}$ be the given set of obstacles. The path have the start point at P_1 and the end point at P_n. We need to find the system of sets $\mathcal{V} = \{V_1, \dots, V_{n-1}\}$ such that each Bézier curve $b_{P_i C_i P_{i+1}}$ with $C_i \in V_i$ represent collision-free path between the points P_i and P_{i+1} with respect to all obstacles from $\mathcal{O}$.

The path is constructed sequentially, so that the algorithm 1 for each segment $P_i P_{i+1}$ can be used. The algorithm 2 shows the whole process.

Algorithm 2 Finding C^0-continuous path

function $\textsc{FindSpline}(P_1, \dots, P_n, O_1, \dots, O_m)$
    for $i = 1$ **to** $n - 1$ **do**
        $V_i \leftarrow \textsc{FindV}(P_i, P_{i+1}, O_1, \dots, O_m)$
    end for
    $V \leftarrow \{V_1, \dots, V_{n-1}\}$
    return V
end function

Now, we choose the set of points $\{C_1, \dots, C_{n-1}\}$ such that C_i is an arbitrary point from V_i. Then, the C^0-continuous collision-free path $b = \bigcup_{i=1}^{n-1} b_{P_i C_i P_{i+1}}(t)$. Computing of b for the set of three points $\{P_1, P_2, P_3\}$ and two obstacles $\{O_1, O_2\}$ is illustrated in the fig. 4.2 (a), (b).

4.3 Creation of C^1-continuous spline

Let $\mathcal{P} = \{P_1, \dots, P_n\}$ be the given set of points and $\mathcal{O} = \{O_1, \dots, O_m\}$ be the given set of obstacles. Let the set $\mathcal{V} = \{V_1, \dots, V_{n-1}\}$, where each set V_i contains all C_i representing collision-free path between the points P_i and P_{i+1}.

Now, we pick the points $C_1, \dots, C_{n-1}$ for obtaining the C^1-continuous spline. The decision must be compatible with the conditions of C^1 continuity of quadratic Bézier curves

$$2(P_i - C_{i-1}) = 2(C_i - P_i) \text{ for } i = 2, \dots, n-1.$$

Hence, one can see that the points C_{i-1} and C_i are centrally symmetric with respect to the point P_i for $i = 2, \dots, n-1$. We denote by $\mathrm{Ref}_P(X)$ the reflection of a point X with respect to a point P. Note that by choosing C_1, we determine all remaining middle control points, because $C_2 = \mathrm{Ref}_{P_2}(C_1), \ldots, C_{n-1} = \mathrm{Ref}_{P_{n-1}}\mathrm{Ref}_{P_{n-2}} \ldots \mathrm{Ref}_{P_2}(C_1)$. So, we find the subset $W \subset V_1$ of such points C_1, that all reflected $C_i \in V_i$ for $i = 2, \ldots, n-1$. This ensures that the final spline is collision-free. The following algorithm 3 is based on these facts.

Algorithm 3 Finding C^1-continuous path

function FindSmoothSpline($P_1, \ldots, P_n, O_1, \ldots, O_m$)
  $V \leftarrow$ FindSpline($P_1, \ldots, P_n, O_1, \ldots, O_m$)
  $W \leftarrow V.V_{n-1}$
  for $i = n-2$ **to** 1 **do**
    $W \leftarrow V.V_i \cap \mathrm{Ref}_{P_{i+1}}(W)$
  end for
  return W
end function

Theorem 4.1. Let $\mathcal{P} = \{P_1, \ldots, P_n\}$ be the given set of points and $\mathcal{O}$ be the given set of obstacles. Let the sets $V_1, \ldots, V_{n-1}$ represent the admissible points C_i for collision-free paths over every P_iP_{i+1}. Let the set $W = V_1 \cap \mathrm{Ref}_{P_2}(\mathrm{Ref}_{P_3}(\ldots(\mathrm{Ref}_{P_{n-1}}(V_{n-1}) \cap V_{n-2}) \cap \cdots \cap V_3) \cap V_2)$ is obtained by the algorithm 3. For each point $C \in W$ the path $b = \bigcup_{i=1}^{n-1} b_{P_iC_iP_{i+1}}(t)$, where $C_1 = C$, $C_2 = \mathrm{Ref}_{P_2}(C), \ldots, C_{n-1} = \mathrm{Ref}_{P_{n-1}}\mathrm{Ref}_{P_{n-2}} \ldots \mathrm{Ref}_{P_2}(C)$, is collision-free with respect to obstacles $\mathcal{O}$ and C^1-continuous.

Proof. We use mathematical induction with respect to the number of points P for proving the theorem.

Basis: Let $\mathcal{P} = P_1, P_2, P_3$ be the given points. Let V_1, V_2 be the sets of admissible middle control points for the segments P_1, P_2, resp. P_2, P_3.

The set $W = V_1 \cap \mathrm{Ref}_{P_2}(V_2)$. Hence, the set $\mathrm{Ref}_{P_2}(W) \subset V_2$. If we choose

$C_1 \in W$, the point $C_2 = \mathrm{Ref}_{P_2}(C_1) \in V_2$. Thus, the obtained spline is collision-free, because $C_1 \in V_1$ and $C_2 \in V_2$, and it is also C^1-continuous, because C_1 and C_2 are centrally symmetric with respect to the point P_2. For illustration, see fig. 4.2 (c), (d).

Inductive step: Let $\mathcal{P} = P_1, \ldots, P_{n-1}$ be the set of points with $V_1, \ldots, V_{n-2}$ as above. Let $W = V_1 \cap \mathrm{Ref}_{P_2}(\mathrm{Ref}_{P_3}(\ldots(\mathrm{Ref}_{P_{n-2}}(V_{n-2}) \cap V_{n-3}) \cap \cdots \cap V_3) \cap V_2)$ be the set of admissible middle control points C_1 such that the final spline over $\mathcal{P}$ is C^1-continuous.

Let P_n be the new end point and let V_{n-1} be the corresponding set of middle control points for the segment $P_{n-1}P_n$. For C^1-continuous connection of two segments $P_{n-2}P_{n-1}$ and $P_{n-1}P_n$, we have to substitute the set V_{n-2} by $V_{n-2} \cap \mathrm{Ref}_{P_{n-1}}(V_{n-1})$ according to induction assumption. Hence, the new $W = V_1 \cap \mathrm{Ref}_{P_2}(\mathrm{Ref}_{P_3}(\ldots(\mathrm{Ref}_{P_{n-1}}(V_{n-1}) \cap V_{n-2}) \cap \cdots \cap V_3) \cap V_2)$. $\square$

4.4 Existence of the quadratic spline

The spline existence is dependent on the existence of collision-free Bézier curve between two consecutive points P_i, P_{i+1} for $i = 1, \ldots, n-1$. If there are too many obstacles and the quadratic path does not exist for any pair P_i, P_{i+1}, it is necessary to add another point P between P_i, P_{i+1}. We can use e.g. sample-based planning algorithms.

Moreover, the existence of C^1-continuous path requires $W \neq \emptyset$. It may be problematic for complicated environments, because the quadratic curves are not so flexible. That is the reason why we also study the cubic curves.

4.5 Example

We apply this study to the following example. Let the virtual agent starts at the point P_1 and needs to get to the point P_3 while passing through the point P_2.

Moreover, it is supposed to avoid two obstacles O_1, O_2 represented by an ellipse and a hyperbola respectively. Conic sections as bounding objects well represent a wide range of obstacles. For example, ellipses are suitable for buildings, trees and things and hyperbolas and parabolas for coast or areas with special features.

The C^0-continuous collision-free path is sought sequentially. At first, we find the set V_1 consisting of such points C that the Bézier curve $b_{P_1CP_2}$ is collision-free path between P_1, P_2 due to ellipse O_1. Then, we find the set V_2 consisting of such points C that the Bézier curve $b_{P_1CP_2}$ is collision-free path between P_1, P_2 due to hyperbola O_2. Since we need to avoid both obstacles simultaneously, it is necessary to choose the final point $C_1 \in W = V_1(P_1, P_2) \cap V_2(P_2, P_3)$. The collision-free path between the points P_2, P_3 and $C_2 \in W'$ is found similarly as shown in fig. 4.2(b). The final path $b = b_{P_1C_1P_2} \cup b_{P_2C_2P_3}$ is C^0-continuous, because we choose the point C_2 irrespective to C_1.

If we want the C^1-continuous collision-free path, the condition for choosing the point C_1 is more complicated. We must map the set $W' = V_1(P_2, P_3) \cap V_2(P_2, P_3)$ by point reflection with respect to a point P_2 to the set $\mathrm{Ref}_{P_2}(W')$. If we choose the point $C_1 \in W \cap \mathrm{Ref}_{P_2}(W')$, the final path b is C^1-continuous, see fig. 4.2 (c), (d).

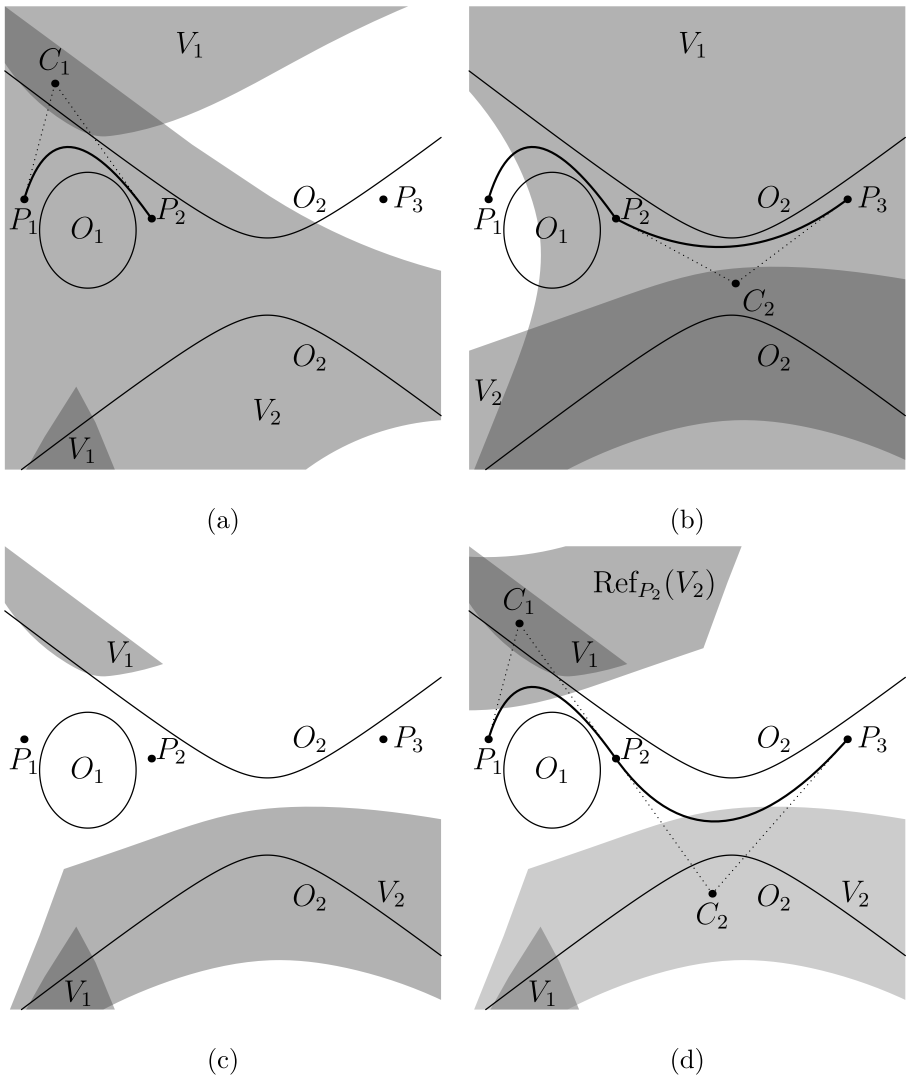

Figure 4.2: (a) First, we search the collision-free path between the points P_1, P_2. After finding the sets of admissible solutions V_1, V_2 for each obstacle separately, we pick a point $C_1 \in V_1 \cap V_2$. (b) Then, we find the sets V_1, V_2 for the points P_2, P_3 and choose the point $C_2 \in V_1 \cap V_2$. The final spline is C^0-continuous. (c) The set V_1 contains all such points C_1, that the curve $b_{P_1C_1P_2}$ is a collision-free segment. Similarly, the set V_2 contains all such points C_2 for the segment P_2P_3. (d) We have to pick the points C_1, C_2. Taking the point $C_1 \in V_1 \cap \mathrm{Ref}_{P_2}(V_2)$ and $C_2 = \mathrm{Ref}_{P_2}(C_1)$, the finial spline is C^1-continuous.

5

Cubic collision-free Bézier path

We look for the collision-free condition of the Bézier curves of higher degree than two. They provide more natural-looking path and they are more flexible while avoiding obstacles including non-planar curves. The important reason is written in section 4.3. The quadratic C^1-continuous spline is globally defined by $P_1, \ldots, P_n$ and by picking C_1. Cubic splines are more flexible.

We start to study a conditions for planar cubic curves, using the knowledge and methods from the quadratic case. Let $A, C, F, B \in \rho$ be the control points of the Bézier curve b_{ACFB}. Let the conic section $K \in \rho$. Let A, B lie outside of the conic section K, i.e. $q(\boldsymbol{a}) > 0, q(\boldsymbol{b}) > 0$. Let the point F be arbitrary, but fixed. We need to find the *set of admissible solutions* $V_\rho(A, F, B)$ of such points $C \in \rho$, that the curve b_{ACFB} is collision-free with respect to K. By $V_\rho^v(A, F, B)$, we denote the set of points $C \in \rho$ such that $b_{ACFB} \cap K$ contains only the points of contact of order 2 between the Bézier curve and the conic section.

Definition 5.1 (Set of points of contact)**.** We say that the set $D \subset K$ is the *set of points of contact* between K and the set of all b_{ACFB} if for any point $X \in D$, there is a point C such that $C \in V_\rho^v(A, F, B)$ and $X \in b_{ACB} \cap K$.

The exact shape of the set D is shown later.

5.1 Boundary map

We need to obtain the points C corresponding to the set D forming the boundary of the set $V_\rho(A, F, B)$. In order to find the control point C, we use the following map σ.

Definition 5.2 (Boundary map)**.** Let D be the set of points of contact for the given points A, F, B and K and let $\mathcal{P}(\rho)$ be the power set of the plane ρ. The map $\sigma : D \to \mathcal{P}(\rho)$ is called *boundary map* if for every $X \in D$ holds $\sigma(X) = \{C \in \rho \mid C \in V_\rho^v(A, F, B)$ and $X \in b_{ACFB} \cap K$ is the point of contact$\}$.

Theorem 5.1. *Let the point $X \in D \subset K$ whereas the conic section K be represented with matrix $\boldsymbol{Q_K}$. Let the real numbers*

$$\alpha = (A - 3F + 2B)\boldsymbol{Q_K}X^\top,$$
$$\beta = (F - A)\boldsymbol{Q_K}X^\top,$$
$$\gamma = A\boldsymbol{Q_K}X^\top,$$
$$\delta = -\gamma$$

be the coefficients of the cubic function

$$R(t) = \alpha t^3 + 3\beta t^2 + 3\gamma t + \delta \tag{5.1}$$

for $A = [a_x, a_y, 1]$, $F = [f_x, f_y, 1]$, $B = [b_x, b_y, 1]$, $X = [x_0, y_0, 1]$. Then, the corresponding boundary map $\sigma : D \to \mathcal{P}(\rho)$ has the form

$$\sigma(X) = \left\{ \frac{b(t_0) - B_0^3(t_0)A - B_2^3(t_0)F - B_3^3(t_0)B}{B_1^3(t_0)},\ t_0 \in (0, 1) \wedge R(t_0) = 0 \right\}. \tag{5.2}$$

Proof. Since the point of the contact $X \in b_{ACFB}(t)$, there exists $t_0 \in [0, 1]$ such that $X = b_{ACFB}(t_0) = B_0^3(t_0)A + B_1^3(t_0)C + B_2^3(t_0)F + B_3^3(t_0)B$. The point $X \in K$ so $X \notin \{A, B\}$ and $t_0 \notin \{0, 1\}$. The equality $\left\langle \nabla f(x_0, y_0), \frac{d}{dt} b_{ACFB}(t_0) \right\rangle = 0$ holds, because $X \in D$. The point X belongs to the conic section, so $X\boldsymbol{Q_K}X^\top = 0$. From the cubic equation (5.1), we obtain three roots $t_{1,2,3} \in \mathbb{C}$. The line ℓ_X is feasible, so at least one (at most three) $t_i \in (0,1)$, $i \in \{1,2,3\}$. For each $t_i \in (0,1)$, we obtain the corresponding point C_i using the equation (5.2). Each point C_i satisfies the definition 5.1 for the point of the contact X. Hence, $\sigma(X) = \{C_i \mid t_0 = t_i \in (0,1)\} \neq \emptyset$. $\square$

For the discriminant Δ of cubic equation with real coefficients $a_3x^3 + a_2x^2 + a_1x + a_0 = 0$ holds $\Delta = 18a_3a_2a_1a_0 - 4a_2^3a_0 + a_2^2a_1^2 - 4a_3a_1^3 - 27a_3^2a_0^2$. Using the notation of polar lines equation we can rewrite the coefficient of equation (5.1)

$$\begin{aligned}
a_3 &= \alpha = P(A,X) - 3P(F,X) + 2P(B,X),\\
a_2 &= 3\beta = 3P(F,X) - 3P(A,X),\\
a_1 &= 3\gamma = 3P(A,X),\\
a_0 &= \delta = -P(A,X).
\end{aligned}$$

Then, the discriminant of the equation $R(t) = a_3t^3 + 3a_2t^2 + 3a_1t + a_0$ is

$$\Delta = 108P(A,X)(P^3(F,X) - P(A,X)P^2(B,X)). \tag{5.3}$$

Using this discriminant one computes the number of real roots of the function given by (5.1) over an interval. Combining with theorem 1.1 applied on interval $\langle 0,1\rangle$, we are able to determine the number of roots lying in $(0,1)$. In other words, we know how many points C_i exist for given $X \in K$.

5.2 Singular conic sections

Now, we find the set of admissible points of the contact D for cubic Bézier curves. At first, we find it for singular conic sections, then we consider regular conic sections.

Lemma 5.1. If the conic section $K = p$, the set of admissible points of the contact $D = K$. Moreover, the boundary of the set of admissible solutions ∂V is a parallel line to the line p (see fig. 5.1).

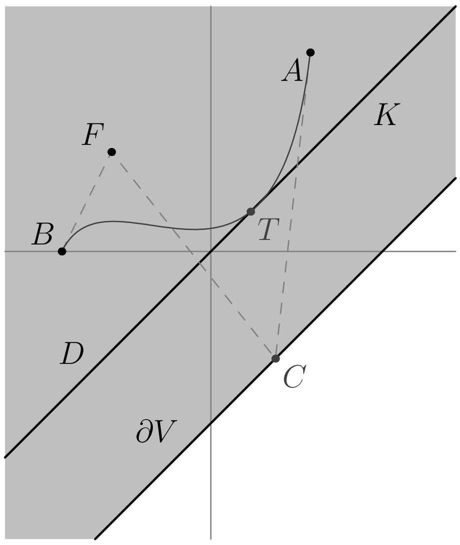

Figure 5.1: The boundary ∂V of the set of admissible solutions is a parallel line to the line p for $K = p$.

Proof. Without loss of generality, let us consider the conic section K is represented by

$$\boldsymbol{Q_K} = \begin{pmatrix} 0 & 0 & -\frac{1}{2} \\ 0 & 0 & \frac{1}{2} \\ -\frac{1}{2} & \frac{1}{2} & 0 \end{pmatrix}.$$

We compute $P(A, X) = A\boldsymbol{Q_K}X^\top$ for $X = (x, y, 1) \in K$ and $A = (a_x, a_y, 1)$. We obtain $P(A, X) = \frac{1}{2}(-a_x + a_y) + \frac{1}{2}(-x + y)$. But $-x + y = 0$, because $X\boldsymbol{Q_K}X^\top = 0$ for $X \in K$. So, we have $P(A, X) = \frac{1}{2}(-a_x + a_y)$ which is the constant independent on the choice of X. Similarly, the expressions $P(B, X)$ and $P(F, X)$ are constants. Hence, the coefficients $\alpha, \beta, \gamma, \delta$ in (5.2) are constants independent on the point $X \in D$. Hence, the solutions t_1, t_2, t_3 of the equation (5.1) are constants for all $X \in D \subset K$.

Now, we need to prove that $D = p$ and for every $X \in D$ exists exactly one $i \in 1, 2, 3$ such that root $t_i \in (0, 1)$. Let us count the number of roots of the equation (5.1) belonging to $(0, 1)$. We use the theorem 1.1. Let us denote $P_A =$

	$t=0$	$t=1$
$f(t)$	$-P_A$	$2P_B$
$f'(t)$	$3P_A$	$-3P_F+6P_B$
$f''(t)$	$-6P_A+6P_F$	$-12P_F+12P_B$
$f'''(t)$	$6P_A-18P_F+12P_B$	
Δ	$108P_A(P_F^3-P_AP_B^2)$	

Table 5.1: The values of derivatives of the function $f(t)=R(t)$ at the end points of the interval $\langle 0,1\rangle$ and the value of the discriminant.

$P(A,X), P_B=P(B,X), P_F=(F,X)$. Computing the derivatives of $f(t)=R(t)$, we obtain

$$\begin{aligned}
f(t) &= (P_A-3P_F+2P_B)t_0^3+3(P_F-P_A)t_0^2+3P_At_0-P_A,\\
f'(t) &= 3(P_A-3P_F+2P_B)t_0^2+6(P_F-P_A)t_0+3P_A,\\
f''(t) &= 6(P_A-3P_F+2P_B)t_0+6(P_F-P_A),\\
f'''(t) &= 6(P_A-3P_F+2P_B). \qquad (5.4)
\end{aligned}$$

The table 5.1 summarizes the values of derivatives in the end points of the interval $\langle 0,1\rangle$ and the value of the discriminant. As we compute above, in the case of singular conic sections all the values are constants independent on the point $X\in D$.

The assumption of the theorem 1.1 reads that the product $f(0)f(1)\neq 0$. It holds iff $P_A\neq 0\wedge P_B\neq 0$. This is accomplished, because the points $A,B\notin K$.

Now, we consider some configurations of the points A,F,B with respect to K and check the corresponding number of roots of the equation (5.1) in the interval $\langle 0,1\rangle$. For the obtaining of the collision-free path, the points A,B must lie in the same half plane with respect to K, so we assume $P_AP_B>0$.

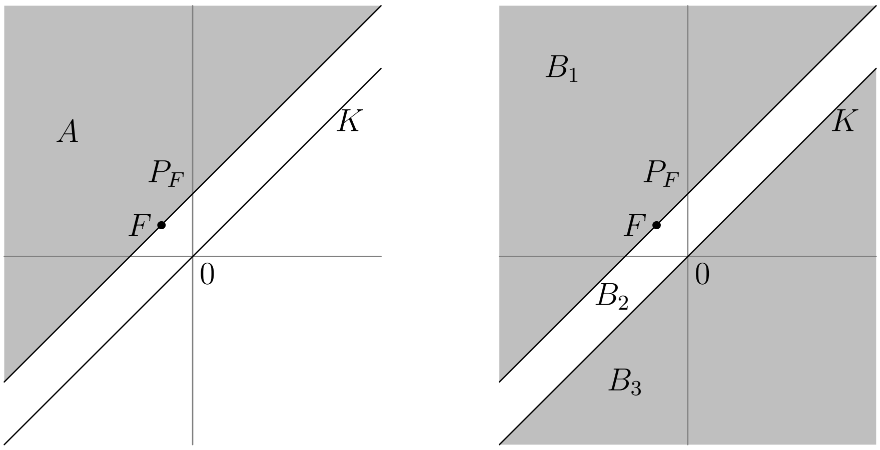

Figure 5.2: (a) We can see the situation of the case $P_F > 0$. If for the coordinates of the point A holds $0 < P_F < P_A$, the point A must lie in the gray area.
(b) The area B_1 represents the condition $0 < P_F < P_B$, the area B_2 represents the condition $0 < P_B < P_F$. The area B_3 represents the condition $P_B < 0$, but we do not consider this case, because we need $P_A P_B > 0$.

For $P_F = 0$, we obtain the table 6.9. As we can see, the number of sign changes is equal to 3 and the discriminant $\Delta < 0$. According to the table 1.1(fig. 1.6(d)) there is exactly one real root t_0 within the interval $\langle 0, 1\rangle$. So, the Bézier curve always exists and is uniquely defined.

Let $P_F \neq 0$ and without loss of generality let $P_F > 0$. If $0 < P_F < P_A$, we distinguish these two possible positions of the point B (see fig. 5.2). The table 6.10 shows that is exactly one real root t_0. If $0 < P_A < P_F$, we distinguish two possible positions of the point B elaborated in the table 6.11. The number of sign changes is either 3 or 1, but in the case of 3 the discriminant $\Delta < 0$. It restrict the number of roots to 1. If $P_A < 0 < P_F$, the point B must be in the same half-plane, so $P_B < 0$. According to the table 6.12, there is only one real root within $\langle 0, 1\rangle$.

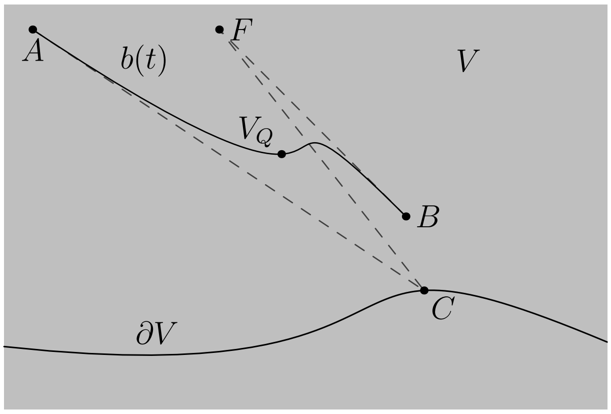

Figure 5.3: Let the conic section $K = \{V_Q\}$. There is only one possible point of contact, so $D = \{V_Q\}$. The equality $b(t) \cap K \neq \emptyset$ holds only for $C \in \partial V_\rho(A, F, B)$. So, the set of admissible solutions $V_\rho(A, F, B) = \rho \setminus \partial V_\rho(A, F, B)$.

The conclusion of all the cases is, that the set of points of contact $D = p$ and for every $X \in D$ exists exactly one Bézier curve b_{ACFB}, where $C = \sigma(X)$.

At the end, we determine the shape of the curve ∂V. Let $T_0 \in D$ be an arbitrary fixed point of contact and let C_0 be the corresponding middle control point. Let $T \in D$ be arbitrary point of contact different from T_0. We express $T = T_0 + u\boldsymbol{s_p}$, where $0 \neq u \in \mathbb{R}$ and $\boldsymbol{s_p}$ is direction vector of the line p. The corresponding point C is obtained from formula (5.2) and for $t_0 \in (0, 1)$ is $B_1^3(t_0) > 0$. If we substitute T by $T_0 + u\boldsymbol{s_p}$ and T_0 by $B_0^3(t_0)A + B_1^3(t_0)C_0 + B_2^3(t_0)F + B_3^3(t_0)B$, we obtain $C = C_0 + \frac{u}{B_1^3(t_0)}\boldsymbol{s_p}$. Hence, the boundary of the set of admissible solutions ∂V is the line with the same direction vector as the line p. □

Note 6. Let $K = p \cup r$. The set of points of contact $D = \overrightarrow{S_pP} \cup \overrightarrow{S_rR}$ (in special case $S_p = S_r = V_Q$). From the previous lemma, the set ∂V consists of two half-lines parallel with p, resp. r, connected in the point C_u.

Lemma 5.2. If the conic section $K = \{V_Q\}$, then the set $D = \{V_Q\}$ and the boundary of the set of admissible solutions ∂V is one continuous curve (see fig. 5.3).

Proof. Without loss of generality, let us consider the conic section K is represented by

$$\boldsymbol{Q_K} = \begin{pmatrix} 1 & 0 & 0 \\ 0 & 1 & 0 \\ 0 & 0 & 0 \end{pmatrix}.$$

Then, we obtain the coefficients in (5.1) $\alpha, \beta, \gamma, \delta = 0$. So each $t_0 \in (0, 1)$ is the root of the equation and the corresponding point $C_0 = \sigma([0, 0])$. □

5.3 Regular conic sections

Now, we need to find the set $D \subset K$ for regular conic sections. Let us focus on the necessary algebraic conditions for $X \in K$ to be $X \in D$. We denote $P_A = P(A, X) = A\boldsymbol{Q_K}X^\top, P_B = P(B, X) = B\boldsymbol{Q_K}X^\top, P_F = P(F, X) = F\boldsymbol{Q_K}X^\top$. Then,

$$\begin{aligned}
\alpha &= P_A - 3P_F + 2P_B, \\
\beta &= P_F - P_A, \\
\gamma &= P_A, \\
\delta &= -P_A.
\end{aligned}$$

If we compute the derivatives of the expression (5.1), we obtain the same expression (5.4) as in the case of singular conic sections. But now, the polar forms P_A, P_B, P_F are not constants and they depend on the choice of $X \in D$.

Similarly, we use the table 5.1 for determination of sign changes of derivatives of the function $f(t) = R(t)$ in the end points of the interval $\langle 0, 1\rangle$. In the case of regular conic sections, the derivatives are dependent on the choice of $X \in K$.

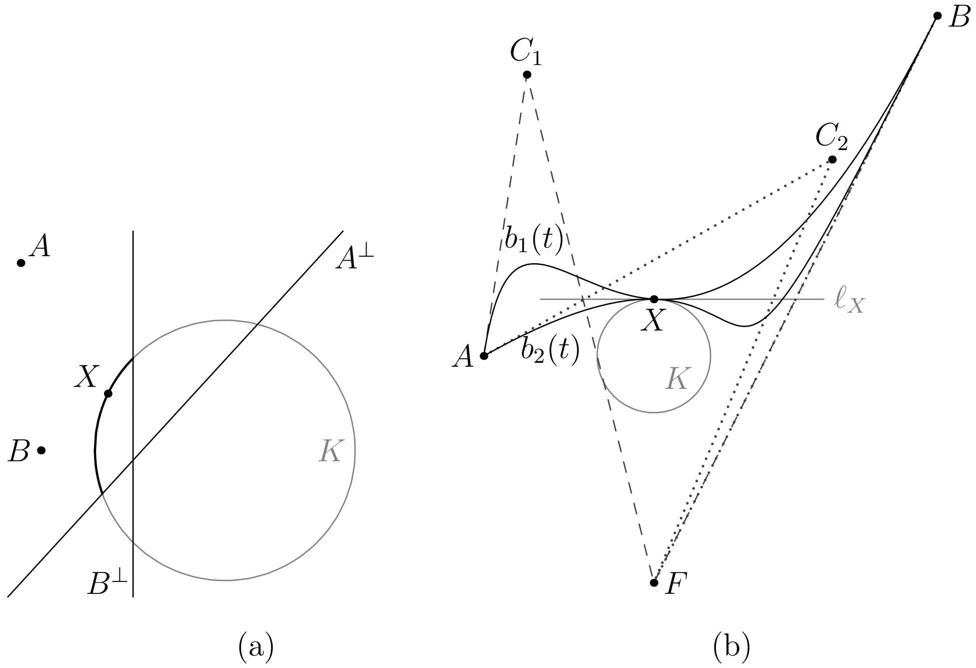

Figure 5.4: (a) The polar lines $A^{\perp}, B^{\perp}$ of the points A, B such that $P(A, A) > 0, P(B, B) > 0$ divide the conic section K into four arcs in generic case. Each arc is determined by algebraic inequalities, for example for X holds $P_A = P(A, X) > 0$ and $P_B = P(B, X) > 0$. (b) For some $X \in K$ exist even two different Bézier curves $b_1(t), b_2(t)$ having with K the common point of contact X. Note that they lie locally in different half-planes with respect to the tangent line ℓ_X.

Hence, we must distinguish several cases with respect to the mutual position of the point $X \in K$ and the polar lines $A^{\perp}, B^{\perp}$.

The polar lines $A^{\perp}, B^{\perp}$ divide the conic section K into several arcs, see fig. 5.4(a). Now, we need to find suitable candidates for the set D between them or their subset. We create the tables showing the number of real roots of the equation (5.1) for X from each arc.

In the first case, we consider the arc of $X \in K$ such that $P_A > 0, P_B > 0$, see the tables 6.1, 6.2. The second case, we consider the arc of $X \in K$ such that $P_A < 0, P_B < 0$, see the tables 6.3, 6.4.

As we can see, the difference of numbers of sign changes in $t = 0$ and $t = 1$ is almost everywhere equal to 1. In two cases, the difference is equal to 3, but there is $\Delta < 0$. According to the table 1.1, the cubic equation (5.1) has exactly one real root. We conclude that if for $X \in K$ either $P_A > 0, P_B > 0$ or $P_A < 0, P_B < 0$ hold, then there exist exactly one Bézier curve b_{ACFB} having the common point of contact X with K.

Now, let P_A and P_B have the different signs. We have $X \in K$ such that $P_A > 0, P_B < 0$, see the tables 6.5, 6.6. For $X \in K$ such that $P_A < 0, P_B > 0$, see the tables 6.7, 6.8.

Let us focus on the difference of numbers of sign changes in $t = 0$ and $t = 1$ and compare them with the table 1.1. If the difference is equal to 0, regardless of the sign of Δ, the equation (5.1) has no real root within the interval $\langle 0, 1 \rangle$. The same conclusion is for the case that the difference is equal to 2 and $\Delta < 0$. The interesting situation for us is the last case, when difference is equal to 2 and $\Delta > 0$. It indicates that there exist two real roots or no real root, see the table 1.1 and the fig. 1.6(c), (h). The example of the situation where for one $X \in K$ there exist two admissible points C is shown on the fig. 5.4(b).

The $\Delta = 108P_A(P_F^3 - P_A P_B^2)$. So, the conclusion for these arcs is as follows. If for $X \in K$ the inequalities $P_A > 0, P_B < 0$ hold, then the Bézier curve b_{ACFB} having with K the common point of contact X may exist only if $P_F^3 - P_A P_B^2 > 0$. The statement for the second arc is similar. If for $X \in K$ the inequalities $P_A < 0, P_B > 0$ hold, then the Bézier curve b_{ACFB} having the common point of contact X with K may exist only if $P_F^3 - P_A P_B^2 < 0$.

Based on these inequalities, the following statement holds.

Theorem 5.2 (Necessary condition for the set D)**.** The set of admissible points of the contact D is the subset of the union of the arcs $K_i \subset K$ for $i = 1, \ldots, 4$, where

$$\begin{aligned}
K_1 &= \{X \in K\colon P_A \geq 0 \wedge P_B \geq 0\},\\
K_2 &= \{X \in K\colon P_A \leq 0 \wedge P_B \leq 0\},\\
K_3 &= \{X \in K\colon P_A \geq 0 \wedge P_B \leq 0 \wedge P_F^3 - P_A P_B^2 \geq 0\},\\
K_4 &= \{X \in K\colon P_A \leq 0 \wedge P_B \geq 0 \wedge P_F^3 - P_A P_B^2 \leq 0\}. \quad \square
\end{aligned}$$

We use not sharp inequalities, because the end points of the arcs may belong to the set D. Depending on the positions of the points A, B, F, some of these sets may be empty. For example, the set K_1 is empty iff the segment AB is a secant of K.

5.4 Sufficient condition for the set of admissible points of contact

The necessary condition for the set D is not the sufficient condition simultaneously. It may happened, that the Bézier curve determined by the point $X \in \bigcup_{i=1}^{4} K_i$ has some transversal intersection with K, see fig. 5.5(a).

We solved a similar problem in the quadratic case. We found the geometrical conditions for removing some points from the arc determined by $P_A < 0, P_B < 0$. The first was the existence of the Bézier curve with double contact with K. Using the quadratic case, we formulate the following hypotheses.

Hypothesis 5.1. If there exists the point C_u, such that the Bézier curve $b_{AC_uFB} \cap K = \{U_1, U_2\}$, where U_1, U_2 are points of the contact, then for the arc $\overset{\frown}{U_1U_2} \subset K_2$ holds $\overset{\frown}{U_1U_2} \not\subset D$. See fig. 5.5(b,c).

The second geometrical condition in quadratic case, which remove some points from the arc determined by $P_A < 0, P_B < 0$, was the divergence of non-separating

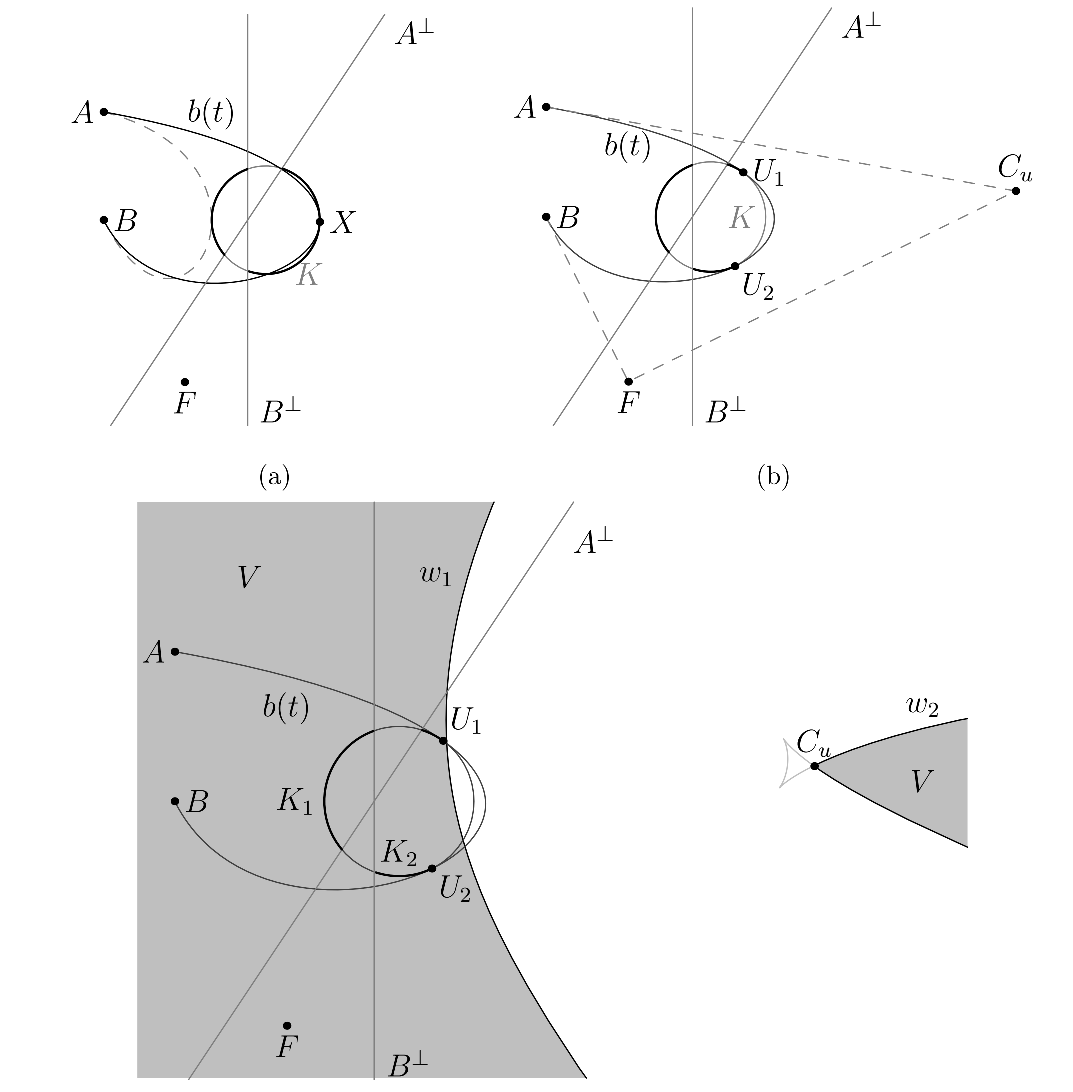

(c)

Figure 5.5: (a) From the necessary condition we obtain $D \subset K_1 \cup K_2$, because in this case $K_3 = K_4 = \emptyset$. But we need to use some additional conditions for determine D, because not all $K_2 \subset D$. (b) The existence of the point C_u cause split of the arc K_2. The arc $\widehat{U_1U_2} \not\subset D$. (c) The set of admissible points of contact $D = K_1 \cup K_2 \setminus \{\widehat{U_1U_2}\}$. We obtain $\sigma(K_1) = w_1$ and $\sigma(K_2 \setminus \{\widehat{U_1U_2}) = w_2$. The set of admissible solutions V consist of two components.

tangent lines from the points A and B. In other words, the degree 2 of the path was too low to be able enclose the conic section. We show, that the degree 3 is much more flexible, but still not enough in all cases.

Lemma 5.3. Let the triangle $\triangle ABF \cap K = \emptyset$. Let the lines t_1, t_2 be the supporting lines to triangle and conic section simultaneously and $T_1 = t_1 \cap K$, $T_2 = t_2 \cap K$. Moreover, the triangle and the conic section lie in the same half-planes with respect to the lines, i.e. $\triangle ABF, K \subset H^+_{t_1}$ and $\triangle ABF, K \subset H^+_{t_2}$. If $X \in \{X \in K \colon P_A < 0 \wedge P_B < 0\} \subset D$, then the point $P = t_1 \cap t_2$ lie in the same half-plane determined by the line $\overleftrightarrow{T_1T_2}$ as the point X (see fig. 5.6(b)).

Proof. The proof is based on the fact that the whole Bézier curve lie in the convex hull of their control points. The point X is out of the convex hull of the points A, B, F, because $\triangle ABF \cap K = \emptyset$. The first request for the point C is X belongs to the convex hull of A, C, F, B. The Bézier curve connect the point A with the point X and the point B with the point X also. Hence, there exist the points Y_1, Y_2 in Bézier curve such that $Y_1 \in H^-_{t_1}$ and $Y_2 \in H^-_{t_2}$ (see fig. 5.6). We have another requests for the point C, the points Y_1, Y_2 belongs to the convex hull of A, C, F, B. If the point $P = t_1 \cap t_2$ lie in the different half-plane determined by the line $\overleftrightarrow{T_1T_2}$ as the point X, the point C satisfying all the required conditions does not exist. $\square$

Hypothesis 5.2. The lemma 5.3 can be extended for each $\triangle AFB$ with suitable supporting lines.

Hypothesis 5.3. The hypotheses 5.1, 5.2 are the only geometrical conditions removing the points from $\bigcup_{i=1}^{4} K_i$. So, the set of admissible solutions $V_\rho(A, F, B)$ consist of one or two regions determined by curves generated by the map σ.

The proving of hypotheses will be the subject of further research. An interesting observation comparing to quadratic case is that the boundary ∂V may

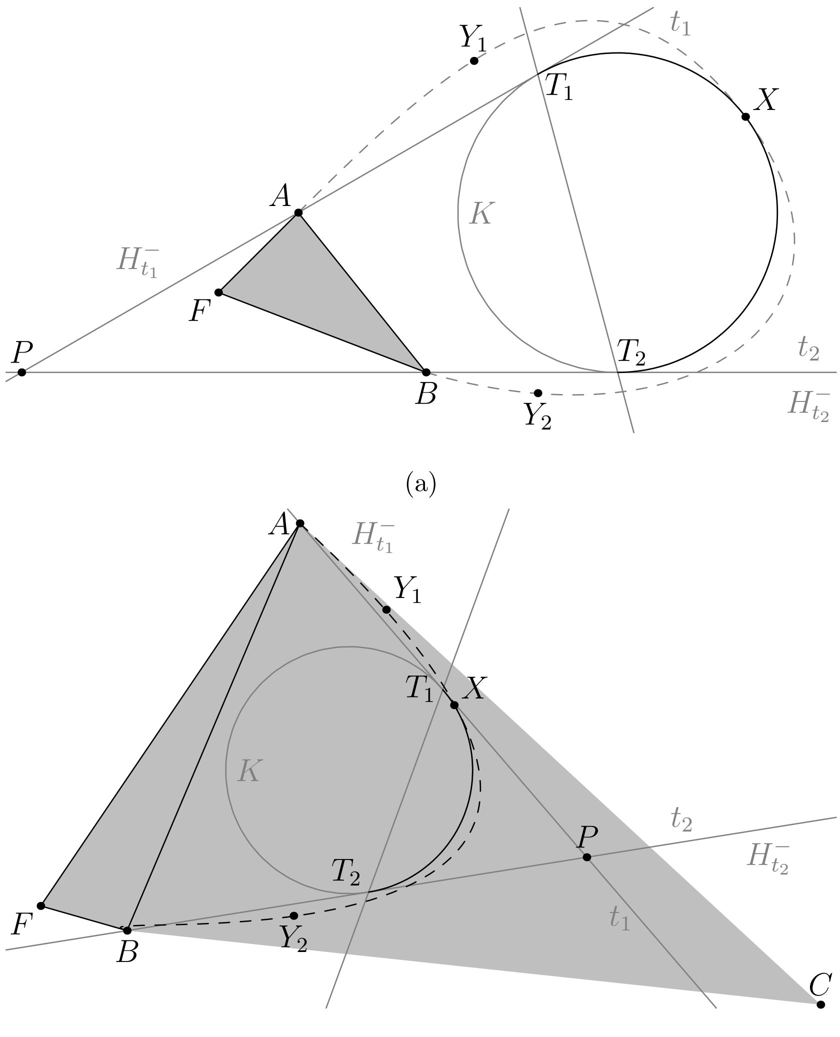

(b)

Figure 5.6: (a) If the point P lies in the different half-plane as the point X with respect to the line T_1T_2, the point C such that all the points Y_1, Y_2, X lie within the convex hull of the points A, C, F, B does not exist. (b) The point P lies in the same half-plane as the point X with respect to the line T_1T_2. Hence, the set D may contain some points from $K_2 = \{X \in K : P_A < 0 \wedge P_B < 0\}$. For example, the point $X \in D$ and the point C is corresponding control point of Bézier curve. We can see that all the points Y_1, Y_2, X are within the convex hull of the points A, C, F, B.

contains an inflection point. The fig. 5.7 shows the interconnections between a sign of discriminant, a number of sign changes of derivatives of the function $R(t)$ and a number of roots within $\langle 0, 1\rangle$. Also, the geometrical consequence of the fact that for some $X \in D$ may exist two different points $C_1, C_2 \in \sigma(X)$.

For cubic Bézier curves, we have to take into account that they could have a self-intersection. This can be easily controlled, because it happens when the control polygon has a self-intersection. If we use our method for path planning, we can either omit the loop of such path or omit the whole such path for corresponding C.

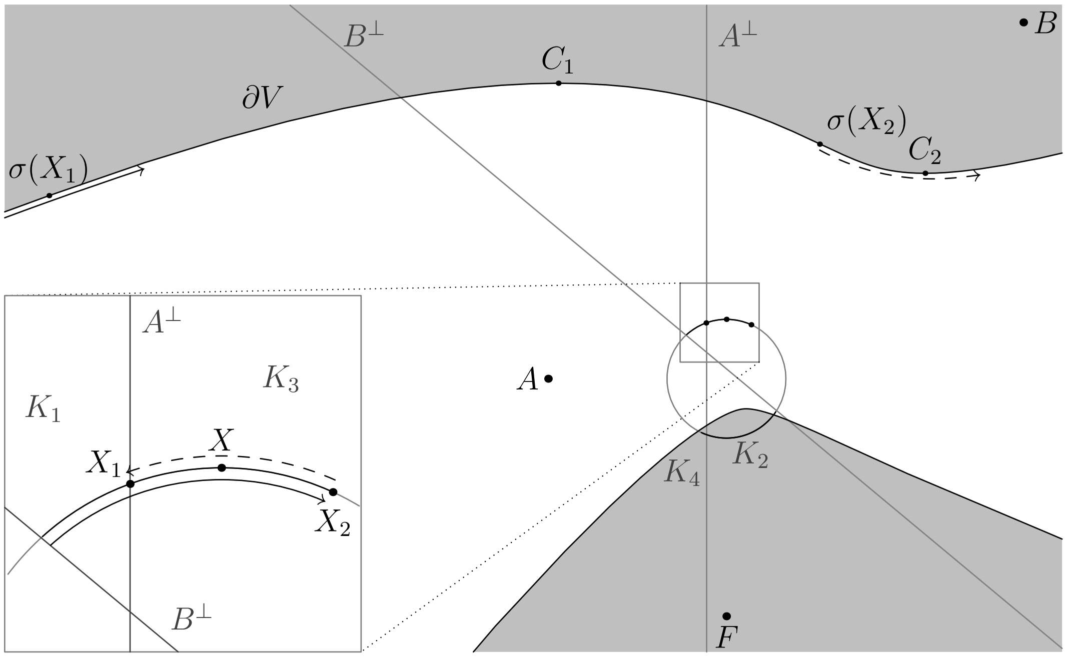

Figure 5.7: Let all the sets K_1, K_2, K_3, K_4 be non-empty. For K_1, we have difference of numbers of sign changes equals 3 and the negative discriminant. Combination of these two facts gives us one real solution of $R(t)$ within $\langle 0, 1\rangle$. Hence, for $X \in K_1$ exists only one $C \in \sigma(X)$. For K_3, there is difference of numbers of sign changes equals 2 and the positive discriminant. It implies existence of two different real solutions of $R(t)$ within $\langle 0, 1\rangle$. So for $X \in K_3$, we have $C_1, C_2 \in \sigma(X)$. If we orient the boundary ∂V in directions of arrows, the corresponding orientation of domain is more complicated as in quadratic case. A new phenomenon comparing to the quadratic case is the inflection point $\sigma(X_2)$ of the boundary ∂V. At the endpoint X_2 of the arc K_3 we have difference equals 2, but the discriminant $\Delta = 0$. It indicates one multiple root within $\langle 0, 1\rangle$ generates $\sigma(X_2)$. The arcs K_2, K_4 behave very similarly. For the arc K_2 we have difference 3 and negative discriminant, it means one real solution of $R(t)$ within $\langle 0, 1\rangle$. For the arc K_4 with difference 2 and positive discriminant, we have two real solutions.

6

Results and Discussion

In this chapter, we summarize the main results and show some areas of application. Then, we present the topics suitable for future work.

6.1 Results and applications

We worked in three dimensional space with the given start and end position. This space contains the set of obstacles represented by regular quadrics. The goal was to find the collision-free path from the start to the end. In the chapter 3, we consider with one quadric. The spatial problem was reduced into planar problem and the quadratic collision-free path was found for each type of conic section. These knowledges was generalised in order to avoid more obstacles simultaneously and for constructing C^0 or C^1-continuous spline in the chapter 4. We present some facts about collision-free planar cubic paths in the chapter 5.

Our results solved the path planning problem for point-size robot in two or three dimensional space, because its configuration space can be identified with our working space for obstacles represented by regular quadrics. It can be also used for translational robots and all robots with two or three dimensional configuration space, when we describe a space C_{obs} by conic sections. The main benefit of the work is a mathematical model of path finding with proofs about existence and uniqueness, which involves a complete solution (we find all possible collision-free quadratic paths).

In most algorithms, the finding of collision-free path consists of two main steps. The first one is acquisition of linear spline path generated by sample-based planning algorithms. The second step is smoothing of the path because in mobile robotics a non smooth motions can cause slippage of wheels. The finding of smooth collision-free path using Bézier curves was mentioned in 1.3. But the algorithms working with polynomials or Bézier curves are used as post processing, because they assume some linear collision-free path and they only smooth the path. Moreover, the algorithms provide only a numerical solution. The proposed method offers a direct analytical computation of all possible collision-free smooth paths without using sample-based planning algorithms. We assume an obstacle represented by a regular quadric and given start and end position of robot. We find all quadratic Bézier curves constituting the set of collision-free paths. One can use such a set for optimization of the sought path.

Sometimes the scene with the given obstacles is too complicated and the smooth collision-free path cannot be found directly. Then, the use of sample-based planning algorithms is necessary. But the obtained linear path is jerky, because it contains many redundant nodes which was generated randomly. In order to remove these nodes the path pruning techniques as in [GO07] are used. Our results can also form a path pruning algorithm, where the node v_i can be removed if there is a quadratic Bézier collision-free path between nodes v_{i-1} and v_{i+1}. Such an algorithm is more flexible comparing with a piecewise linear approach.

There is another use for the affine three dimensional Minkowski space typically determined by a light cone. In the section 1.4, we mention the work [Geo08] about conditions for Bézier curve to be space-like. The set of all pointwise space-like curves is determined by the set V. The light cone represents a quadric. If we take two space-like points as a first and a last control point, we can find all quadratic pointwise space-like Bézier curves.

6.2 Topics for future research

We would like to proof the hypotheses 5.1, 5.2, 5.3 on the set of admissible points of contact. Then, the case of cubic planar Bézier curves will be entirely completed.

In order to prove the hypothesis 5.1, we study the image Γ of the sets K_1, K_2, K_3, K_4 under the continuous map τ. We focus on the self-intersections of the image Γ similarly as in the proof of the theorem 3.2. The Plücker formula [Hil20, Kle77] can be useful for finding the singularities. Regarding the hypothesis 5.2, we consider a mutual position of the convex hull of the $\triangle AFB$ and the conic section K and the tangent lines from the points A, F, B to the conic section.

After closure of the planar cubic case, we want to study a conditions for spatial cubic case. We will use the knowledge and methods from planar case as much as possible, additional methods will be applied too. The main goal is to find the condition for C^2-continuous spatial cubic Bézier splines.

Conclusion

We conclude that the goals proposed in the chapter 2 were reached and the following results were achieved. For better understanding, the notions and procedures were illustrated via lot of figures and examples.

At first, we defined a working space. The three dimensional Euclidean space with regular quadric κ as obstacle and two given points A, B. The first goal was to find all quadratic Bézier paths starting at A and ending at B representing collision-free path with respect to an obstacle κ. This set of Bézier curves we represent by the set of corresponding middle control points $V(A, B)$. Because a quadratic curve lies in a plane (denote by ρ), we studied the set $V_\rho(A, B) = V(A, B) \cap \rho$ for each type of conic section $K = \kappa \cap \rho$. We determine the set of admissible points of contact $D \subset K$ between Bézier curves b_{ACB} and K, where $C \in \rho$. The set D consist of some arcs on K, where the polars of the points A, B play the key role. The number of the arcs for each type of conic section K show the tables 3.1, 3.2. For the points A, B and contact point $X \in D$ is the Bézier curve uniquely defined. Using the map sigma $\sigma\colon D \to \rho$ the corresponding middle control point $C = \sigma(X)$ was obtained. The equations for σ are listed in the theorem 3.4. We proved also that thus obtained points C create the boundary $\partial V_\rho(A, B)$. The boundary consists of one ore two continuous curves, which divide the plane ρ in some areas. The set of admissible middle control points $V_\rho(A, B)$ consist of one or two areas depending on type of conic section (see table 3.5).

The second goal was to find the quadratic spline representing collision-free path with respect to set of obstacles $O = \{O_1, \ldots, O_m\}$ and passing through the points $P = \{P_1, \ldots, P_n\}$. The avoiding more obstacles simultaneously for $P = \{P_1, P_2\}$ is described in algorithm 1. At first, we determine the set $V_j(P_1, P_2)$

containing the admissible points C for collision-free path due to one obstacle O_j separately for $j = 1, \dots, m$. The set of admissible middle control points $V_\rho(P_1, P_2)$ is obtained as intersection of all the sets $V_j(P_1, P_2)$. If the set P contains more then two points, we create the spline as connection of quadratic Bézier paths between each pair P_iP_{i+1} for $i = 1, \dots, n-1$. For the creation of C^0-continuous spline it is necessary to find the sets $V_\rho(P_iP_{i+1})$ for each i. The algorithm 2 describes such a procedure in detail. The existence of such spline is dependent on the existence of all the sets $V_\rho(P_iP_{i+1})$. For ensuring the C^1-continuity of the spline, we used the properties of the first derivative at the points of connection P_i for $i = 2, \dots, n-1$. Validity of the equalities $C_i = 2P_i - C_{i-1}$ for $i = 2, \dots, n-1$ is necessary for C^1-continuity of the spline. We used the fact that the points C_i, C_{i-1} are centrally symmetric with respect to the point P_i. So, if we choose the first $C_1 \in V\rho(P_1, P_2)$ then all remaining $C_2, \dots, C_{n-1}$ are uniquely determined. We showed that if the point C_1 is chosen from the set $W = V_1 \cap \mathrm{Ref}_{P_2}(\mathrm{Ref}_{P_3}(\dots(\mathrm{Ref}_{P_{n-1}}(V_{n-1}) \cap V_{n-2}) \cap \dots \cap V_3) \cap V_2)$ where $V_i = V_\rho(P_i, P_{i+1})$, then the spline is collision-free with respect to set of obstacles O. Finding of C^1-continuous spline is described in algorithm 3. The existence of such spline is dependent on the $W \neq \emptyset$.

The third goal was to apply the observations from quadratic paths on the collision-free paths represented by planar cubic Bézier curves and to formulate some theorems and hypothesis about them. We focus on planar cubic Bézier paths with fixed control point F. We solve the situation in the plane ρ with respect to $K = \kappa \cap \rho$. We determine the map $\sigma\colon D \to \rho$ for cubic Bézier curves in theorem 5.1. From the equations of this map, we derive the necessary conditions for the set D as arcs $K_1, \dots, K_4$ on K. Again, the key role is played by polars from the points A, B and the points where discriminant of equation (5.1) vanishes. For singular K, the set $V_\rho(A, F, B)$ of admissible points C consist of one or two areas similarly as in quadratic case. For regular K, we formulate sufficient geometrical conditions for the set D in some special cases. For other cases, we formulate some hypothesis. While searching for the conditions, the property of Bézier curves that they lie in the convex hull of their control points was very helpful. We formulate the hypothesis 5.3 that the set $V_\rho(A, F, B)$ consists of one or two areas, because the hypotheses 5.1, 5.2 work very well in a lot of examples.

References

[BBB87] R. H. Bartels, J. C. Beatty, and B. A. Barsky. *An Introduction to Splines for Use in Computer Graphics & Geometric Modeling.* Morgan Kaufmann Publishers Inc., San Francisco, CA, USA, 1987.

[Ber87a] M. Berger. *Geometry I.* Universitext. Springer-Verlag, Berlin, 1987. Translated from the French by M. Cole and S. Levy.

[Ber87b] M. Berger. *Geometry II.* Universitext. Springer-Verlag, Berlin, 1987. Translated from the French by M. Cole and S. Levy.

[BG88] M. Berger and B. Gostiaux. *Differential geometry: manifolds, curves, and surfaces*, volume 115 of *Graduate Texts in Mathematics.* Springer-Verlag, New York, 1988. Translated from the French by S. Levy.

[Bix06] R. Bix. *Conics and cubics.* Undergraduate Texts in Mathematics. Springer, New York, second edition, 2006. A concrete introduction to algebraic curves.

[BL91] J. Barraquand and J.-C. Latombe. Robot Motion Planning: A Distributed Representation Approach. *International Journal of Robotics Research*, 10(6):628–649, December 1991.

[BM11] C. B. Boyer and U. C. Merzbach. *A History of Mathematics.* Wiley, third edition, 2011.

[BPR06] S. Basu, R. Pollack, and M.-F. Roy. *Algorithms in real algebraic geometry*, volume 10 of *Algorithms and Computation in Mathematics*. Springer-Verlag, Berlin, second edition, 2006.

[BT07] J.-D. Boissonnat and M. Teillaud, editors. *Effective computational geometry for curves and surfaces*. Mathematics and Visualization. Springer-Verlag, Berlin, 2007.

[dC76] M. P. do Carmo. *Differential geometry of curves and surfaces*. Prentice-Hall, Inc., Englewood Cliffs, N.J., 1976. Translated from the Portuguese.

[ES14] M. Elbanhawi and M. Simic. Sampling-based robot motion planning: A Review. *IEEE Access*, 2:56–77, 2014.

[Far99] G. E. Farin. *NURBS*. A K Peters, Ltd., Natick, MA, second edition, 1999. From projective geometry to practical use.

[Far08] R. T. Farouki. *Pythagorean-hodograph curves: algebra and geometry inseparable*, volume 1 of *Geometry and Computing*. Springer, Berlin, 2008.

[FHK02] G. Farin, J. Hoschek, and M.-S. Kim, editors. *Handbook of computer aided geometric design*. North-Holland, Amsterdam, 2002.

[For72] A. R. Forrest. Interactive interpolation and approximation by Bézier polynomials. *Comput. J.*, 15(1):71–79, 1972. reprinted in Computer-Aided Design 22(9):527-537,1990.

[FS04] T. Fraichard and A. Scheuer. From Reeds and Shepp's to continuous-curvature paths. *IEEE Transactions on Robotics*, 20(6):1025–1035, 2004.

[Geo08] G. H. Georgiev. Space-like Bézier curves in the three-dimensional Minkowski space. In *Applications of mathematics in engineering and economics (AMEE'34)*, volume 1067 of *AIP Conf. Proc.*, pages 373–380. Amer. Inst. Phys., Melville, NY, 2008.

[Geo09] G. H. Georgiev. Constructions of spacelike Bézier surfaces in the three-dimensional Minkowski space. In *Applications of mathematics in engineering and economics (AMEE'09)*, volume 1184 of *AIP Conf. Proc.*, pages 201–208. Amer. Inst. Phys., Melville, NY, 2009.

[GO07] R. Geraerts and M. H. Overmars. Creating High-quality Paths for Motion Planning. *The International Journal of Robotics Research*, 26(8):845–863, 2007.

[GVRLR98] L. González-Vega, T. Recio, H. Lombardi, and M.-F. Roy. Sturm-Habicht sequences, determinants and real roots of univariate polynomials. In *Quantifier elimination and cylindrical algebraic decomposition (Linz, 1993)*, Texts Monogr. Symbol. Comput., pages 300–316. Springer, Vienna, 1998.

[GVT97] L. González-Vega and G. Trujillo. Multivariate Sturm-Habicht sequences: real root counting on n-rectangles and triangles. *Rev. Mat. Univ. Complut. Madrid*, 10(Special Issue, suppl.):119–130, 1997. Real algebraic and analytic geometry (Segovia, 1995).

[Hil20] H. Hilton. *Plane Algebraic Curves.* Clarendon Press, 1920.

[HL93] J. Hoschek and D. Lasser. *Fundamentals of computer aided geometric design.* A K Peters Ltd., Wellesley, MA, 1993. Translated from the 1992 German edition by L. L. Schumaker.

[JKV09] K. G. Jolly, R. Sreerama Kumar, and R. Vijayakumar. A Bézier curve based path planning in a multi-agent robot soccer system without violating the acceleration limits. *Robotics and Autonomous Systems*, 57(1):23–33, 2009.

[KH97] Y. J. Kanayama and B. I. Hartman. Smooth Local-Path Planning for Autonomous Vehicles. *I. J. Robotic Res.*, 16(3):263–284, 1997.

[KL94] L. E. Kavraki and J.-C. Latombe. Randomized preprocessing of configuration space for path planning: articulated robots. In *Proceedings of IEEE/RSJ International Conference on Intelligent Robots* *and Systems, IROS 1994, September 12 - 16, 1994, Munich, Germany*, pages 1764–1771, 1994.

[Kle77] S. L. Kleiman. The enumerative theory of singularities. In *Real and complex singularities (Proc. Ninth Nordic Summer School/NAVF Sympos. Math., Oslo, 1976)*, pages 297–396. Sijthoff and Noordhoff, Alphen aan den Rijn, 1977.

[KSLO96] L. E. Kavraki, P. Svestka, J.-C. Latombe, and M. H. Overmars. Probabilistic roadmaps for path planning in high-dimensional configuration spaces. *IEEE T. Robotics and Automation*, 12(4):566–580, 1996.

[Küh06] W. Kühnel. *Differential geometry*. Student Mathematical Library. American Mathematical Society, Providence, RI, second edition, 2006. Curves—surfaces—manifolds, Translated by B. Hunt.

[Kun05] E. Kunz. *Introduction to plane algebraic curves*. Birkhäuser Boston Inc., Boston, MA, 2005. Translated from the 1991 German edition by R. G. Belshoff.

[Lat91] J.-C. Latombe. *Robot Motion Planning*. Kluwer, Boston, MA, 1991.

[LaV98] S. M. LaValle. Rapidly-Exploring Random Trees: A New Tool for Path Planning. Technical Report 98-11, Computer Science Dept., Iowa State University, October 1998.

[LaV06] S. M. LaValle. *Planning Algorithms*. Cambridge University Press, Cambridge, U.K., 2006. Available at http://planning.cs.uiuc.edu/.

[LP83] T. Lozano-Pérez. Spatial planning: A configuration space approach. *IEEE Transactions on Computing*, C-32(2):108–120, 1983.

[Mar66] M. Marden. *Geometry of polynomials*. Second edition. Mathematical Surveys, No. 3. American Mathematical Society, Providence, R. I., 1966.

[Mar05] D. Marsh. *Applied geometry for computer graphics and CAD*. Springer Undergraduate Mathematics Series. Springer-Verlag London, Ltd., London, second edition, 2005.

[Nab12] G. L. Naber. *The geometry of Minkowski spacetime*, volume 92 of *Applied Mathematical Sciences*. Springer, New York, 2012. An introduction to the mathematics of the special theory of relativity, Second edition.

[Nil69] N. J. Nilsson. A mobile automaton: An application of artificial intelligence techniques. In *1st International Conference on Artificial Intelligence*, pages 509–520, 1969.

[PBP02] H. Prautzsch, W. Boehm, and M. Paluszny. *Bézier and B-spline techniques*. Mathematics and Visualization. Springer-Verlag, Berlin, 2002.

[PPP02] E. Papadopoulos, I. Poulakakis, and I. Papadimitriou. On Path Planning and Obstacle Avoidance for Nonholonomic Platforms with Manipulators. *I. J. Robotic Res.*, 21(4):367–386, 2002.

[PZM11] J. Pan, L. Zhang, and D. Manocha. Collision-Free and Curvature-Continuous Path Smoothing in Cluttered Environments. In *Robotics: Science and Systems VII, University of Southern California, Los Angeles, CA, USA, June 27-30, 2011*, 2011.

[PZM12] J. Pan, L. Zhang, and D. Manocha. Collision-free and smooth trajectory computation in cluttered environments. *I. J. Robotic Res.*, 31(10):1155–1175, 2012.

[SB11] D. Stanovský and L. Barto. *Počítačová algebra*. MATFYZPRESS, 2011.

[Sch88] I. J. Schoenberg. Contributions to the problem of approximation of equidistant data by analytic functions. In C. de Boor, editor, *I. J. Schoenberg Selected Papers*, Contemporary Mathematicians, pages 3–57. Birkhäuser Boston, 1988.

[TMea06] S. Thrun, M. Montemerlo, and H. Dahlkamp et al. Stanley: The robot that won the DARPA Grand Challenge. *J. Field Robotics*, 23(9):661–692, 2006.

[UAea09] C. Urmson, J. Anhalt, and D. Bagnell et al. Autonomous Driving in Urban Environments: Boss and the Urban Challenge. In *The DARPA Urban Challenge: Autonomous Vehicles in City Traffic, George Air Force Base, Victorville, California, USA*, pages 1–59, 2009.

[UMY11] H. Ugail, M. C. Márquez, and A. Yılmaz. On Bézier surfaces in three-dimensional Minkowski space. *Comput. Math. Appl.*, 62(8):2899–2912, 2011.

[YJS13] K. Yang, D. Jung, and S. Sukkarieh. Continuous curvature path-smoothing algorithm using cubic Bézier spiral curves for non-holonomic robots. *Advanced Robotics*, 27(4):247–258, 2013.

[YÖT09] S. Yılmaz, E. Özyılmaz, and M. Turgut. On the differential geometry of the curves in Minkowski space-time. II. *Int. J. Comput. Math. Sci.*, 3(2):53–55, 2009.

[YS08] K. Yang and S. Sukkarieh. 3D Smooth Path Planning for a UAV in Cluttered Natural Environments. *Proc. IEEE/RSJ International Conference on Intelligent Robots and Systems*, pages 794–800, 2008.

[YS10] K. Yang and S. Sukkarieh. An Analytical Continuous-Curvature Path-Smoothing Algorithm. *IEEE Transactions on Robotics*, 26(3):561–568, 2010.

[YT08] S. Yilmaz and M. Turgut. On the differential geometry of the curves in Minkowski space-time. I. *Int. J. Contemp. Math. Sci.*, 3(25-28):1343–1349, 2008.

Appendix

In this part, we embed some supplementary tables to the chapter 5, which we do not insert directly into the text because of their extensiveness. We list the tables for regular and singular conic sections gradually.

Each table contains the signs of derivatives of the function $f(t) = R(t)$ in the end points of the interval $\langle 0, 1\rangle$. Since f is cubic function, the first three derivatives are given there. The decisive data for determining the number of real roots within $\langle 0, 1\rangle$ of the function f are the number of sign changes of the derivatives and the discriminant of the function. While the discriminant says about simple and multiple roots, the difference between the number of sign changes in the sequences $\{f(0), f'(0), f''(0), f'''(0)\}$ and $\{f(1), f'(1), f''(1), f'''(1)\}$ says about the number of roots unless the even number. The combination of these two indicators seems useful for our purpose.

	$P_A < P_F$ $P_F < P_B$		$P_A < P_F$ $\frac{1}{2}P_F < P_B < P_F$		$P_A < P_F$ $P_B < \frac{1}{2}P_F$	
	$t = 0$	$t = 1$	$t = 0$	$t = 1$	$t = 0$	$t = 1$
$f(t)$	$-$	$+$	$-$	$+$	$-$	$+$
$f'(t)$	$+$	$+$	$+$	$+$	$+$	$-$
$f''(t)$	$+$	$+$	$+$	$-$	$+$	$-$
$f'''(t)$	$+$ $-$	$+$ $-$	$-$	$-$	$-$	$-$
# of sign changes	1 2	0 1	2	1	2	1

Table 6.1: We consider the arc of regular conic section K such that $P_A > 0$, $P_B > 0$. The signs of derivatives depend on the value of P_F with respect to P_A, P_B. Here, the first three configurations of the six possibilities are discussed (for the rest see the table 6.2).

	$P_F < P_A$ $P_F < P_B$		$P_F < P_A$ $\frac{1}{2}P_F < P_B < P_F$		$P_F < P_A$ $P_B < \frac{1}{2}P_F$	
	$t = 0$	$t = 1$	$t = 0$	$t = 1$	$t = 0$	$t = 1$
$f(t)$	$-$	$+$	$-$	$+$	$-$	$+$
$f'(t)$	$+$	$+$	$+$	$+$	$+$	$-$
$f''(t)$	$-$	$+$	$-$	$-$	$-$	$-$
$f'''(t)$	$+$	$+$	$+$ $-$	$+$ $-$	$+$ $-$	$+$ $-$
# of sign changes	3	0	3 2	2 1	3 2	2 1
sign of Δ	$-$		no influence		no influence	

Table 6.2: We consider the arc of regular K such that $P_A > 0$, $P_B > 0$. Here, three remaining configurations of P_A, P_B, P_F of the six possibilities are discussed (for the rest see the table 6.1).

	$P_A < P_F$ $P_F < \frac{1}{2}P_F < P_B$		$P_A < P_F$ $P_F < P_B < \frac{1}{2}P_F$		$P_A < P_F$ $P_B < P_F$	
	$t = 0$	$t = 1$	$t = 0$	$t = 1$	$t = 0$	$t = 1$
$f(t)$	$+$	$-$	$+$	$-$	$+$	$-$
$f'(t)$	$-$	$+$	$-$	$-$	$-$	$-$
$f''(t)$	$+$	$+$	$+$	$+$	$+$	$-$
$f'''(t)$	$+$ $-$	$+$ $-$	$+$ $-$	$+$ $-$	$-$	$-$
# of sign changes	2 3	1 2	2 3	1 2	3	0
sign of Δ	no influence		no influence		$-$	

Table 6.3: We consider the arc of regular K such that $P_A < 0, P_B < 0$. The signs of derivatives depend on the value of P_F with respect to P_A, P_B. Here, the first three configurations of the six possibilities are discussed (for the rest see the table 6.4).

	$P_F < P_A$ $P_F < \frac{1}{2}P_F < P_B$		$P_F < P_A$ $P_F < P_B < \frac{1}{2}P_F$		$P_F < P_A$ $P_B < P_F$	
	$t = 0$	$t = 1$	$t = 0$	$t = 1$	$t = 0$	$t = 1$
$f(t)$	$+$	$-$	$+$	$-$	$+$	$-$
$f'(t)$	$-$	$+$	$-$	$-$	$-$	$-$
$f''(t)$	$-$	$+$	$-$	$+$	$-$	$-$
$f'''(t)$	$+$	$+$	$+$	$+$	$+$ $-$	$+$ $-$
# of sign changes	2	1	2	1	2 1	1 0

Table 6.4: We consider the arc of regular K such that $P_A < 0, P_B < 0$. Here, three remaining configurations of P_A, P_B, P_F of the six possibilities are discussed (for the rest see the table 6.3).

	$P_A < P_F$ $\frac{1}{2}P_F < P_B$		$P_A < P_F$ $P_F < P_B < \frac{1}{2}P_F$		$P_A < P_F$ $P_B < P_F$	
	$t = 0$	$t = 1$	$t = 0$	$t = 1$	$t = 0$	$t = 1$
$f(t)$	$-$	$-$	$-$	$-$	$-$	$-$
$f'(t)$	$+$	$+$	$+$	$-$	$+$	$-$
$f''(t)$	$+$	$+$	$+$	$+$	$+$	$-$
$f'''(t)$	$+$ $-$	$+$ $-$	$+$ $-$	$+$ $-$	$-$	$-$
# of sign changes	1 2	1 2	1 2	1 2	2	0
sign of Δ	no influence		no influence		$\pm$	

Table 6.5: We consider the arc of regular K such that $P_A > 0, P_B < 0$. The signs of derivatives depend on the value of P_F with respect to P_A, P_B. Here, the first three configurations of the six possibilities are discussed (for the rest see the table 6.6).

	$P_F < P_A$ $\frac{1}{2}P_F < P_B$		$P_F < P_A$ $P_F < P_B < \frac{1}{2}P_F$		$P_F < P_A$ $P_B < P_F$	
	$t = 0$	$t = 1$	$t = 0$	$t = 1$	$t = 0$	$t = 1$
$f(t)$	$-$	$-$	$-$	$-$	$-$	$-$
$f'(t)$	$+$	$+$	$+$	$-$	$+$	$-$
$f''(t)$	$-$	$+$	$-$	$+$	$-$	$-$
$f'''(t)$	$+$	$+$	$+$	$+$	$+$ $-$	$+$ $-$
# of sign changes	3	1	3	1	3 2	1 0
sign of Δ	$-$		$-$		$\pm$	

Table 6.6: We consider the arc of regular K such that $P_A > 0, P_B < 0$. Here, three remaining configurations of P_A, P_B, P_F of the six possibilities are discussed (for the rest see the table 6.5).

	$P_A < P_F$ $\frac{1}{2}P_F < P_B$		$P_A < P_F$ $\frac{1}{2}P_F < P_B < P_F$		$P_A < P_F$ $P_B < \frac{1}{2}P_F$	
	$t = 0$	$t = 1$	$t = 0$	$t = 1$	$t = 0$	$t = 1$
$f(t)$	$+$	$+$	$+$	$+$	$+$	$+$
$f'(t)$	$-$	$+$	$-$	$+$	$-$	$-$
$f''(t)$	$+$	$+$	$+$	$-$	$+$	$-$
$f'''(t)$	$+$ $-$	$+$ $-$	$-$	$-$	$-$	$-$
# of sign changes	2 3	0 1	3	1	3	1
sign of Δ	$\pm$		$-$		$-$	

Table 6.7: We consider the arc of regular K such that $P_A < 0, P_B > 0$. The signs of derivatives depend on the value of P_F with respect to P_A, P_B. Here, the first three configurations of the six possibilities are discussed (for the rest see the table 6.8).

	$P_F < P_A$ $\frac{1}{2}P_F < P_B$		$P_F < P_A$ $\frac{1}{2}P_F < P_B < P_F$		$P_F < P_A$ $P_B < \frac{1}{2}P_F$	
	$t = 0$	$t = 1$	$t = 0$	$t = 1$	$t = 0$	$t = 1$
$f(t)$	$+$	$+$	$+$	$+$	$+$	$+$
$f'(t)$	$-$	$+$	$-$	$+$	$-$	$-$
$f''(t)$	$-$	$+$	$-$	$-$	$-$	$-$
$f'''(t)$	$+$	$+$	$+$ $-$	$+$ $-$	$+$ $-$	$+$ $-$
# of sign changes	2	0	2 1	2 1	2 1	2 1
sign of Δ	$\pm$		no influence		no influence	

Table 6.8: We consider the arc of regular K such that $P_A < 0, P_B > 0$. Here, three remaining configurations of P_A, P_B, P_F of the six possibilities are discussed (for the rest see the table 6.7).

	$P_A > 0 \wedge P_B > 0$		$P_A < 0 \wedge P_B < 0$	
	$t = 0$	$t = 1$	$t = 0$	$t = 1$
$f(t)$	$-$	$+$	$+$	$-$
$f'(t)$	$+$	$+$	$-$	$-$
$f''(t)$	$-$	$+$	$+$	$-$
$f'''(t)$	$+$	$+$	$-$	$-$
$\#$ of sign changes	3	0	3	0
sign of Δ	$-$		$-$	

Table 6.9: Let $K = p$ be the singular conic section and $P_F = 0$. We require $P_A P_B > 0$, so either $P_A > 0 \wedge P_B > 0$ or $P_A < 0 \wedge P_B < 0$. Because $P_F = 0$, the discriminant $D = -108 P_A^2 P_B^2 < 0$. Combining with the difference $3 - 0$, the function $f(t)$ have one real solution within the interval $\langle 0, 1 \rangle$.

	$0 < P_F < P_A$ $0 < P_F < P_B$		$0 < P_F < P_A$ $0 < P_B < P_F$	
	$t = 0$	$t = 1$	$t = 0$	$t = 1$
$f(t)$	$-$	$+$	$-$	$+$
$f'(t)$	$+$	$+$	$+$	$+$ $-$
$f''(t)$	$-$	$+$	$-$	$-$
$f'''(t)$	$+$	$+$	$+$ $-$	$+$ $-$
$\#$ of sign changes	3	0	3 2	2 1
sign of Δ	$-$		no influence	

Table 6.10: Let $K = p$ be the singular conic section and $P_F > 0$ and $P_A, P_B > 0$. If $0 < P_F < P_A$, there are either the difference $3 - 0$ with negative Δ or the difference equal to 1. In both cases, the function $f(t)$ have one real solution within $\langle 0, 1 \rangle$.

	$0 < P_A < P_F$ $0 < P_F < P_B$		$0 < P_A < P_F$ $0 < P_B < P_F$	
	$t = 0$	$t = 1$	$t = 0$	$t = 1$
$f(t)$	$-$	$+$	$-$	$+$
$f'(t)$	$+$	$+$	$+$	$\pm$
$f''(t)$	$+$	$+$	$+$	$-$
$f'''(t)$	$\pm$	$\pm$	$-$	$-$
# of sign changes	1 / 2	0 / 1	2	1
sign of Δ	no influence		no influence	

Table 6.11: Let $K = p$ be the singular conic section and $P_F > 0$ and $P_A, P_B > 0$. If $0 < P_A < P_F$, there are the difference $1 - 0$ or $2 - 1$. In both cases it is equal to 1, so the function $f(t)$ have one real solution within $\langle 0, 1 \rangle$.

	$P_A < 0 \wedge P_B < 0$	
	$t = 0$	$t = 1$
$f(t)$	$+$	$-$
$f'(t)$	$-$	$-$
$f''(t)$	$+$	$-$
$f'''(t)$	$-$	$-$
# of sign changes	3	0
sign of Δ	$-$	

Table 6.12: Let $K = p$ be the singular conic section and $P_F > 0$. The combination of $P_A, P_B < 0$ causes the difference $3 - 0$ with negative Δ. The function $f(t)$ have one real solution within $\langle 0, 1 \rangle$.